A novel approach for large-scale flood risk assessments: continuous and long-term simulation of the full flood risk chain

Daniela Falter

Institute of Earth- and Environmental Sciences

A novel approach for large-scale flood risk assessments: continuous and long-term simulation of the full flood risk chain

Cumulative Dissertation

for the degree of
Doctor of Natural Sciences (Dr. rer. nat.)
in Hydrology

submitted to the
Faculty of Mathematics and Natural Sciences
at the University of Potsdam, Germany

by
Daniela Falter

Submitted: November 2015

Referees:
Prof. Dr. Bruno Merz, University of Potsdam
Prof. Dr. Axel Bronstert, University of Potsdam
Prof. Dr. Bernd Diekkrüger, University of Bonn

Submitted: November 2015
Defended: April 2016
Published: May 2016

Published online at the
Institutional Repository of the University of Potsdam:
URN urn:nbn:de:kobv:517-opus4-90239
http://nbn-resolving.de/urn:nbn:de:kobv:517-opus4-90239

Contents

List of Figures

List of Tables

Abstract

In the past, floods were basically managed by flood control mechanisms. The focus was set on the reduction of flood hazard. The potential consequences were of minor interest. Nowadays river flooding is increasingly seen from the risk perspective, including possible consequences. Moreover, the large-scale picture of flood risk became increasingly important for disaster management planning, national risk developments and the (re-) insurance industry. Therefore, it is widely accepted that risk-orientated flood management approaches at the basin-scale are needed. However, large-scale flood risk assessment methods for areas of several 10,000 km² are still in early stages. Traditional flood risk assessments are performed reach wise, assuming constant probabilities for the entire reach or basin. This might be helpful on a local basis, but where large-scale patterns are important this approach is of limited use. Assuming a T-year flood (e.g. 100 years) for the entire river network is unrealistic and would lead to an overestimation of flood risk at the large scale. Due to the lack of damage data, additionally, the probability of peak discharge or rainfall is usually used as proxy for damage probability to derive flood risk. With a continuous and long term simulation of the entire flood risk chain, the spatial variability of probabilities could be consider and flood risk could be directly derived from damage data in a consistent way.

The objective of this study is the development and application of a full flood risk chain, appropriate for the large scale and based on long term and continuous simulation. The novel approach of 'derived flood risk based on continuous simulations' is introduced, where the synthetic discharge time series is used as input into flood impact models and flood risk is directly derived from the resulting synthetic damage time series.

The bottleneck at this scale is the hydrodynamic simulation. To find suitable hydrodynamic approaches for the large-scale a benchmark study with simplified 2D hydrodynamic models was performed. A raster-based approach with inertia formulation and a relatively high resolution of 100 m in combination with a fast 1D channel routing model was chosen.

To investigate the suitability of the continuous simulation of a full flood risk chain for the large scale, all model parts were integrated into a new framework, the Regional Flood Model (RFM). RFM consists of the hydrological model SWIM, a 1D hydrodynamic river network model, a 2D raster based inundation model and the flood loss model FELMOps+r. Subsequently, the model chain was applied to the Elbe catchment, one of the largest catchments in Germany. For the proof-of-concept, a continuous simulation was performed for the period of 1990-2003. Results were evaluated / validated as far as possible with available observed data in this period. Although each model part introduced its own uncertainties, results and runtime were generally found to be adequate for the purpose of continuous simulation at the large catchment scale.

Finally, RFM was applied to a meso-scale catchment in the east of Germany to firstly perform a flood risk assessment with the novel approach of 'derived flood risk assessment based on continuous simulations'. Therefore, RFM was driven by long term synthetic meteorological input data generated by a weather generator. Thereby, a virtual time series of climate data of 100 x 100 years was generated and served as input to RFM providing subsequent 100 x 100 years of spatially consistent river discharge series, inundation patterns and damage values. On this basis, flood risk curves and expected annual damage could be derived directly from damage data, providing a large-scale picture of flood risk. In contrast to traditional flood risk analysis, where homogenous return periods are assumed for the entire basin, the presented approach provides a coherent large-scale picture of flood risk. The spatial variability of occurrence probability is respected. Additionally, data and methods are consistent. Catchment and floodplain processes are represented in a holistic way. Antecedent catchment conditions are implicitly taken into account, as well as physical processes like storage effects, flood attenuation or channel–floodplain interactions and related damage influencing effects. Finally, the simulation of a virtual period of 100 x 100 years and consequently large data set on flood loss events enabled the calculation of flood risk directly from damage distributions. Problems associated with the transfer of probabilities

in rainfall or peak runoff to probabilities in damage, as often used in traditional approaches, are bypassed.

RFM and the ‘derived flood risk approach based on continuous simulations’ has the potential to provide flood risk statements for national planning, re-insurance aspects or other questions where spatially consistent, large-scale assessments are required.

Zusammenfassung

In der Vergangenheit standen bei der Betrachtung von Hochwasser insbesondere technische Schutzmaßnahmen und die Reduzierung der Hochwassergefahr im Mittelpunkt. Inzwischen wird Hochwasser zunehmend aus der Risikoperspektive betrachtet, d.h. neben der Gefährdung werden auch die Auswirkungen berücksichtigt. In diesem Zuge wurde auch die Notwendigkeit von großräumigen Hochwasserrisikoanalysen für das Management von Naturgefahren und als Planungsgrundlage auf nationaler Ebene sowie für die Rückversicherungsindustrie erkannt. Insbesondere durch die Einführung der Europäischen Hochwasserrisikomanagement Richtlinie sind risikoorientierte Managementpläne auf Einzugsgebietsebene obligatorisch. Allerdings befinden sich großräumige Hochwasserrisikoanalysen von mehreren 10.000 km², noch in den Anfängen. Traditionell werden Hochwasserrisikoanalysen für Gewässerabschnitte durchgeführt, wobei homogene Wiederkehrintervalle für das ganze Untersuchungsgebiet angenommen werden. Für lokale Fragestellungen ist diese Vorgehensweise sinnvoll, dies gilt allerdings nicht für die großräumige Analyse des Hochwasserrisikos. Die Annahme eines beispielsweise 100-jährigen Hochwassers im gesamten Gebiet ist unrealistisch und das Hochwasserrisiko würde dabei stark überschätzt werden. Aufgrund unzureichender Schadensdaten werden bei der Berechnung des Risikos oftmals die Wahrscheinlichkeiten des Niederschlags oder der Hochwasserscheitelabflüsse als Annäherung für die Wahrscheinlichkeit des Schadens angenommen. Durch eine kontinuierliche Langzeit-Simulation der gesamten Hochwasserrisikokette könnte sowohl die räumliche Verteilung der Wiederkehrintervalle berücksichtig werden, als auch das Hochwasserrisiko direkt aus Schadenszeitreihen abgeleitet werden.

Die Zielsetzung dieser Arbeit ist die Entwicklung und Anwendung einer, für großräumige Gebiete geeigneten, kontinuierlichen Hochwasserrisikomodellkette. Damit wird ein neuartiger Ansatz des ‚abgeleiteten Hochwasserrisikos basierend auf kontinuierlichen Simulationen' eingeführt, der das Hochwasserrisiko direkt aus den simulierten Abflusszeitreichen und den daraus resultierenden Schadenzeitreihen ableitet. Die größte Herausforderung der Hochwasserrisikokette liegt bei den sehr rechenintensiven, detaillierten hydraulischen Simulationen. Um geeignete hydraulische Modelle für die großräumige Anwendung zu identifizieren, wurde eine Benchmark-Studie mit 2D Modellen unterschiedlicher Komplexität durchgeführt. Auf dieser Grundlage wurde für die Hochwasserrisikomodellkette ein raster-basierter Ansatz mit einer relativ hohen Auflösung von 100 m in Kombination mit einem schnellen 1D Fließgewässermodell ausgewählt.

Um die Eignung einer kontinuierlichen Simulation der gesamten Hochwasserrisikokette für großräumige Anwendungen zu prüfen, wurden zunächst alle Komponenten der Modellkette im ‚Regional Flood Model' (RFM) zusammengeführt. RFM besteht aus dem hydrologischen Modell SWIM, 1D und 2D hydraulischen Modellen, sowie dem Schadensmodell FELMOps+r. Nachfolgend wurde die Modellkette für das Elbe-Einzugsgebiet (>60.000 km²) angewendet. Es wurde eine kontinuierliche Simulation für den Zeitraum 1990-2003 durchgeführt. Die Ergebnisse wurden nach Möglichkeit mit vorhandenen Messdaten validiert/evaluiert. Auch wenn jede Komponente zu Unsicherheiten in den Ergebnissen der Modellkette beiträgt, sind die Ergebnisse und Rechenzeiten für die Anwendung auf großskaliger Einzugsgebietsebene als adäquat anzusehen.

Schließlich wurde RFM in einem meso-skaligen Einzugsgebiet (6.000 km²) im Osten von Deutschland angewendet, um erstmals eine Hochwasserrisikoanalyse mit dem neuartigen Ansatz des ‚abgeleiteten Hochwasserrisikos basierend auf kontinuierlichen Simulationen' durchzuführen. Als Input wurde eine 100 x 100-jährige Zeitreihe meteorologischer Daten von einem Wettergenerator erzeugt. Die somit erzeugte 100 x 100-jährige konsistente Abflusszeitreihe, Überschwemmungsmuster und Schadenswerte dienten als Basis für die nachfolgende Erstellung von Hochwasserrisikokurven und Schadenserwartungswerten für das Untersuchungsgebiet. Diese ermöglichen eine großräumige Analyse des Hochwasserrisikos. Dabei wurde die räumliche Variation der Wahrscheinlichkeiten berücksichtigt. Die verwendeten Daten und Methoden waren außerdem im gesamten Untersu-

chungsgebiet einheitlich. Einzugsgebietsprozesse und Prozesse der Überschwemmungsflächen werden holistisch dargestellt. Die Vorbedingungen im Einzugsgebiet sowie physikalische Prozesse, wie Rückhalteeffekte, Überlagerungseffekte im Gewässernetz oder Interaktionen zwischen Fluss und Überschwemmungsflächen, werden implizit berücksichtigt. Die Simulation von 100 x 100 Jahren und die daraus resultierende große Anzahl an Schadensdaten ermöglichen die direkte Berechnung des Hochwasserrisikos aus Schadenswahrscheinlichkeiten. Die Probleme, die durch die Übertragung von Wahrscheinlichkeiten von Niederschlag oder Scheitelabfluss auf die Wahrscheinlichkeiten im Schaden resultieren, werden umgangen.

RFM und der Ansatz des ‚abgeleiteten Hochwasserrisikos basierend auf kontinuierlichen Simulationen' haben das Potential Hochwasserrisikoaussagen für nationale Planungen, Rückversicherungsaspekte oder andere Fragestellungen, bei denen räumlich konsistente und großräumige Analysen nötig sind, zu treffen.

1 Introduction

Introduction

1.1 Background

During the last decades several extreme river floods affected Germany and Central Europe and caused enormous damage, for example in the Rhine catchment (in 1993 and 1995), the river Odra (in 1997), the Danube catchment (in 1999, 2002, 2005 and 2013) and the river Elbe (in 2002, 2006 and 2013). The prominent August flood in 2002, mainly affecting the Elbe and Danube catchments, caused damage of around €15 billion in Germany alone (in values of 2013, (Merz et al. 2014)) and thus was the most expensive natural hazard that occurred in Germany to date. Less damaging but even more exceptional in a hydrological sense, the flood in June 2013 (again affecting mainly Elbe and Danube) caused damage of about €8.8 billion in Germany (Bundestag 2013; GDV 2013).

These recent extreme events have raised the public and scientific attention on flood management strategies and pushed forward actions and discussions. New strategies in treatment of river flooding have to be developed. In the past, floods were basically managed by flood control mechanisms or flood protection. Such actions include e.g. river training, dike and dam building. The focus was set on the reduction of flood hazard, indicated by inundation extents and discharge dimensions. The potential consequences were of minor interest. Damage however is caused by an entire chain of processes, starting with the triggering rainfall, leading to floodplain inundation and finally affecting elements at risk as buildings, infrastructure or people.

Nowadays river flooding is increasingly seen from the risk perspective or risk analysis is even demanded, e.g. by the European Union Flood Directive (European Commision, 2007). Flood risk is defined as the product of occurrence probability and damage. Moreover, the large-scale picture of flood risk became increasingly important for disaster management planning, national risk developments and the (re-) insurance industry. Therefore, it is widely accepted that risk-orientated flood management approaches on a basin-scale are needed. However, large-scale flood risk assessment methods for areas of several 10,000 km² are still in early stages, several challenges have to be met at that scale.

On a large scale, an apparent challenge is to keep the **spatial consistency of data and methods**, especially, where borders of federal states or countries cross catchment boarders. Driven by the European Flood Directive, flood risk maps were developed all over Europe. De Moel et al., 2009 has summarized the attempts on a European scale and found large variety of methods. The results are therefore not comparable and for large-scale assessments not very useful. Even on a national scale methods and approaches might not be consistent. In Germany, where responsibilities lie with federal states, flood risk approaches vary from state to state. Some approaches on a basin scale try to solve this problem. One example in Germany is the Rheinatlas (http://www.rheinatlas.de/), providing inundation extent and associated damage along the river Rhine for several return periods. On an European scale Alfieri et al. (2014) proposed the development of a pan-European flood hazard map with a spatial consistent methodology based on the assessment of uniform 100-year flood flows for all river stretches and piece-wise hydraulic modelling of corresponding flood areas.

The approaches that were developed over the last years in Europe are an important step forward to improve risk communication and integrated flood risk management and are indeed helpful on a local basis. However, even if spatially consistent methods and data are used, they are of limited use where large-scale patterns of flood risk are important, because of the traditional approach that derives flood risk reach wise and assumes constant return periods in the entire basin. Assuming a T-year flood (e.g. 100 years) for the entire river network gives an unrealistic picture of flood risk on the large scale. The probability of a single flood reaching a 100-year recurrence interval in the entire large-scale river network is very small and much smaller than the probability of such a flood at a single site. This can lead to an over-estimation of flood risk. This effect was shown e.g. by Thieken et al. (2014) for the river Rhine.

For the large-scale picture of flood risk, approaches are necessary that **consider the spatial variability of occurrence probability** at the catchment scale. It is not feasible to asses flood risk directly from historic events, due to the low occurrence of such events and few flood loss data. Alternatively, flood events can be generated synthetically. The possibilities to generate a flood event set are numerous. Most methods are based on a combination of statistical analysis of available meteorological or hydrological data and physical models. One approach that has recently gained attention is the application of multivariate distribution functions. Stochastic flood event sets (flood peaks) are generated with multivariate statistical models from gauging station data, while the spatial dependence between gauging stations was considered (Lamb et al. 2010; Keef et al. 2013). These event sets can be combined with inundation and flood loss models (impact models) to predict flood risk.

Alternatively to the generation of event sets, it is possible to simulate floods continuously. Therefore, long term meteorological time series are generated and used as input into continuous hydrological models. From the simulated synthetic discharge time series, flood probabilities can be calculated. For flood frequency assessments, this approach is increasingly popular (e.g. Boughton and Droop, 2003; Viviroli et al., 2009; Grimaldi et al., 2013; Haberlandt and Radtke, 2014). This, so called, 'derived flood frequency approach based on continuous simulation' has the advantage that the complete flood event, including antecedent processes is modelled throughout the entire catchment in a consistent way. The importance of initial catchment conditions for the flood development could recently be observed by the disastrous flood event in 2013 in Central Europe, where the interplay of event precipitation and very wet initial catchments played a dominant role for the exceptional event severity (Schröter et al. 2015).

For flood risk assessments, the most holistic way would be to complement the continuous hydrological simulation by continuous hydrodynamic simulations of water levels and inundation processes and continuous simulation of damage. This would extent the 'derived flood frequency approach based on continuous simulation' to a novel 'derived flood risk approach based on continuous simulation'.

On a large scale, detailed hydrodynamic simulations are mainly avoided due to computational constraints and data limitations. Discharge is often transformed to water levels and inundation extent using simple approaches that are based on rating curves and water surface intersection with topographic data or simulated only one-dimensional. Additionally, representation of dikes and channel–floodplain interactions are often disregarded. Although the channel and its banks might be represented adequately by one-dimensional (1D) hydrodynamic models, inundation processes on extended floodplains need a two-dimensional (2D) representation.

Two-dimensional inundation simulations on a large scale are only rarely applied. Research on simplification of fully hydrodynamic equations and on reduction of model run-time (e.g. parallelising) have only recently encouraged detailed 2D hydrodynamic simulations on a large scale. However, simulating the entire flood risk chain continuously would be a novel and holistic approach of flood risk assessments. In that way also, physical processes like storage effects, flood attenuation or channel–floodplain interactions can be accounted for and it would allow to consider the effects of floodplain processes on flood damage patterns.

A further advantage of the 'derived flood risk approach based on continuous simulation' would be that flood risk can be derived directly from the synthetic damage time series. Flood risk was defined as the product of (occurrence) probability and damage. However, probability was not discussed much so far here. Ideally, the probability is the **occurrence probability of damage.** However, practically probability is introduced at all stages of the risk chain. One can start from generation of stochastic rainfall events used by hydrological models to simulate the corresponding T-year discharge as, e.g. Rodda (2001) presented for the United Kingdom. Subsequent calculation of inundation depth and extents as well as associated damage enable an entire flood risk assessment as, e.g. performed by Wicks et al. (2013) for the Taihu Basin in China. Thereby the probability of flood loss events is estimated from the probability of rainfall. Even more commonly, the probability of peak discharge, derived from gauging station data, is used as proxy for damage probability. However, the probability of rainfall or

peak discharges does not necessary equal the probability of damage, probabilities may change along the flood risk chain. For instance, two events with the same flood peak discharge may lead to very different inundation and damage patterns. A rare exception to derive flood risk directly from damage probability was undertaken by Thieken et al. (2014). In this study an event set was statistically generated from gauging station data and combined with a flood impact model. Afterwards, flood risk was estimated directly from the damage probability. The 'derived flood risk approach based on continuous simulation' would allow deriving flood risk easily and directly from the long term damage simulations. Problems related to the transformation of rainfall or peak runoff probabilities to damage probabilities could be bypassed.

1.2 Objective and research questions

The objective of this study is the development and application of a framework for large-scale flood risk assessments that overcome the three described problems of (large-scale) flood risk estimations - method and data inconsistency, spatial variability of occurrence probability and transformation of probability - by continuous simulation of the entire model chain on a large scale. The novel approach of derived flood risk based on long term continuous simulations is introduced. For the realization of this aims several steps are needed. The objective is summarized by three research questions. Thereby, each objective builds upon the other.

1. The continuous simulation of the entire flood risk chain requires a vast number of data and computational resources. The bottleneck at this scale, however, is the hydrodynamic model. Detailed hydrodynamic simulations that are necessary for detailed damage simulations are usually avoided at this scale, due to computational restrictions. Research on simplified and fast hydrodynamic models is still in the beginning. As a first step, the assessment of simplified and fast hydraulic models and methods is needed. **What kind of hydraulic model is suitable for the large-scale and long term application?**

2. The application of a model framework for flood risk assessments on a large scale, including detailed and continuous hydrodynamic and damage simulations is new. It requires the set-up and linkage of several models, data of different sources and adequate computational capacities. Furthermore, each model part will introduce its own uncertainties into the chain. A detailed investigation of the suitability of the approach is required. **Is the continuous simulation of the entire flood risk chain a suitable approach on the large-scale?**

3. The long-term application of a full and continuous flood risk chain will provide a unique data base of damaging flood events. This would allow flood risk assessments directly on the damage distribution and provide a large scale picture of flood risk. This 'derived flood risk approach based on continuous simulation' is novel and needs investigation. **What are the advantages of flood risk assessments with the 'derived flood risk approach based on continuous and long-term simulations'? What are the differences to traditional flood risk approaches?**

1.3 Task, structure and author contribution

In line with the research questions, the tasks to realize the objectives are divided in three steps. Each part is addressed in a separate chapter where each can stand for itself. However, all tasks are strongly related and each task builds up on the previous.

Firstly, it is necessary to focus on the, so far, most challenging part of the flood risk chain, the detailed hydrodynamic simulations. To identify suitable hydrodynamic approaches for the large-scale a benchmark study with simplified 2D hydrodynamic models

has to be performed. The results will be used to investigate how useful the approaches are for the large scale purpose with respect to runtime and prediction of inundation depth and extents. This task is addressed in Chapter 2.

Secondly, all parts of the flood risk chain are to be set-up and brought together into a new flood risk framework. This includes a hydrological model for runoff simulation, hydrodynamic models for simulation of inundation depth and extent and a flood loss model. For the proof-of-concept on a large scale the model chain is to be set-up and run in a continuous simulation mode for the Elbe catchment in Germany. Results are to be investigated in terms of uncertainty, feasibility of the model chain approach and evaluated as far as possible with observed data. This task is address in Chapter 3.

Thirdly, the flood risk chain has to be driven by long term meteorological input data to perform firstly a flood risk assessment based on continuous simulations. The synthetic long term meteorological input data to drive the model chain will be provided by an available weather generator. As example study area, the Mulde catchment is selected, a meso-scale catchment in east of Germany. On basis of continuous damage simulations, a flood risk analysis will be presented directly on damage values providing a large scale picture of flood risk. Additionally, derived damage probabilities will be compared to corresponding flood peak probabilities to discuss problems that may arise from transformations of flood peak probabilities to damage probabilities as they are used in more traditional flood risk assessments. This task is addressed in Chapter 4.

Finally, the main results and achievements of the tasks will be summarized in the concluding Chapter 5. Answers to the research questions, further research questions and an outlook are also presented there.

The comprehensive work of setting up and running the full flood risk chain was realized by an entire team of scientists. The author's contribution mainly relies with hydrodynamic model development and application, linkage of model parts and analysis of final results. Hydrological simulations and simulations of the weather generator were performed by Yeshewatesfa Hundecha. Damage simulations were undertaken by Kai Schröter with support of Heidi Kreibich. Viet-Dung Nguyen, Sergiy Vorogushyn and Heiko Apel substantially contributed to the development and application of the hydrodynamic models. As indicated in Chapter 2-4, the listed co-authors contributed to the conceptual design of the papers, discussion of results as well as final formulations of the manuscript.

2 Hydraulic model evaluation for large-scale flood risk assessments

Hydraulic model evaluation for large-scale flood risk assessments

Abstract

For a nationwide flood risk assessment in Germany, simulations of inundation depth and extent for all major catchments are required. Therefore, a fast two-dimensional hydraulic model is needed. From the range of existing methods, two storage cell models are evaluated to find an appropriate method for large-scale applications. The Dynamic Rapid Flood Spreading Model (Dynamic RFSM) based on irregular storage cells, and a raster-based model with inertia formulation of momentum equation are compared. Simulation performed with the fully dynamic shallow water model InfoWorks RS 2D served as a reference. The hydraulic models are applied to a test area having a very flat topography adjacent to the river Elbe. As a benchmark scenario, the outflow through a hypothetical dike breach was chosen. To investigate the impact of the grid resolution on run time and model performance, the simulation with the raster model is carried out with different grid sizes. Furthermore, the sensitivity of the Dynamic RFSM to the choice of time step was analysed. Both models were able to simulate the final inundation extent and depths with a reasonable accuracy. However, the Dynamic RFSM showed some weakness in simulating inundation extent over the flat test area. Coarsening the grid resolution reduced the run time of the raster-based model considerably and can be regarded as a promising strategy to constrain the computational efforts for a large-scale application, although the model accuracy gradually deteriorated. With similar run time, the raster-based model performed better than the Dynamic RFSM in terms of inundation extent and comparable regarding maximum inundation depth. Generally, an application at national scale appears feasible with both hydraulic modelling schemes.

Published as:

Falter, D., Vorogushyn, S., Lhomme, J., Apel, H., Gouldby, B., & Merz, B. (2013). Hydraulic model evaluation for large-scale flood risk assessments. *Hydrological Processes*, *27*(9), 1331 – 1340. doi:10.1002/hyp.9553

2.1 Introduction

During the last decades, a series of heavy flood events affected Europe and raised the public and scientific interest in flood risk related issues. The assessment of current and future risk and the causes driving the change of risk became important research questions. There is controversy regarding the nature of the trends in flood discharges and their climate drivers (Wilby et al., 2008; Petrow and Merz, 2009; Villarini et al., 2011). Current research on socio-economic factors indicates that a major contribution to the increase of flood damages in the last decades in Europe seems to be caused by changes in vulnerability (Barredo, 2009).

The European Member States are obliged to carry out flood hazard and risk assessments of each river basin by 2013 as required by the European Directive on Assessment and Management of Flood Risks (EU, 2007). Currently, there appears to be no common strategy or methodological approach among European countries (de Moel et al., 2009). Until recently, relatively few projects have addressed national scale flood risk, e.g. the RASP-project in England and Wales (Hall et al., 2003; Hall et al., 2005) as well as FLORIS-project in the Netherlands (FLORIS, 2005). In Germany, the responsibility of risk assessments is distributed to authorities at the level of federal states (Bundesländer). In most cases, this does not allow a consistent catchment-wide analysis of flood risk. The methodologies used for large-scale flood risk assessments suffer from a number of drawbacks that may constrain the reliability of the results. Risk assessments are typically carried out reach-wise, meaning that an assumption of e.g. a 100-year flood is consecutively applied to each reach based on the extreme value statistics for an upstream gauging station. However, a uniform 100-year event at all gauges is an unrealistic assumption. Such a scenario would lead to the overestimation of flood risk. Another drawback of the reach-wise approach is that the attenuation of a flood wave passing a long and ramified reach is not considered. Floodplain storage, dike overtopping and breaches are therefore not taken into account on a catchment scale, but only considered locally for a particular reach. Wide and flat floodplains in the lowland river parts possess considerable storage capacities that would capture flood peaks and reduce the risk farther downstream. Therefore, continuous unsteady simulations of flow in the whole river network including inundation areas are required.

For a nationwide flood risk assessment in Germany, a complete model chain, starting from rainfall-runoff to damage evaluation is currently being set up. Within this model chain, hydraulic simulations of flood depths and inundation areas will be carried out countrywide for all major river basins including not only main river channels but also tributaries of higher orders. In contrast to other projects, unsteady hydraulic simulations will be performed over long-term periods to investigate the response of flood risk to global changes. Therefore, a fast and efficient hydraulic model for channel flow and floodplain inundation is needed.

For the purposes of hazard assessment, it is widely accepted that river channel flow processes are adequately captured by one-dimensional models. However, inundation processes on a floodplain clearly have a two-dimensional character. Especially in the northern parts of Germany where floodplains are wide and flat, the flood can spread over large areas. For such large-scale applications, usually two-dimensional (2D) models with simplified shallow water equations are applied. The use of the reduced complexity models is often motivated by the intention to reduce computation time, as fully-dynamic 2D models can be very demanding in terms of computational effort. However, the intention to reduce run time by simplification of equations cannot be assumed to be generally valid. This can be concluded from a recent benchmark study of the Environment Agency for England and Wales (UK) (Néelz and Pender, 2010). In that study, the performance of various two-dimensional models from fully-dynamic to very simplified models was investigated. The reduced complexity models were not always found to be faster than fully-dynamic models. However, the variations between the hardware used to run different codes made it difficult to draw definitive conclusions. On the other hand, Neal et al. (2011a) benchmarked two simplified and one fully-dynamic model within a single code and on a uniform computing platform. They concluded that a simplified diffusive wave model was much slower compared to the recently developed and more complex inertia and the

full-dynamic models because of the smaller time steps needed to retain model stability. The straightforward implementations of simplified approaches have the advantage of relatively easy code handling, as opposed to the 2D shallow water equations that need complex numerical solutions and pre-processing steps. Furthermore, reduced complexity approaches are often sufficient to provide the necessary results in terms of accuracy, when compared to the more complex schemes with respect to inundation extent (Horritt and Bates 2001b; Horritt and Bates 2002) and flood risk estimates (Apel et al., 2009).

Among the 2D reduced complexity inundation models, one can further distinguish between models based on continuity and simplified momentum equations, and those based solely on the continuity or floodplain connectivity. Particularly, models based on discretisation of the diffusive wave equation over the 2D Cartesian grids were extensively used in recent years (Bates and de Roo, 2000; Bradbrook et al., 2005; Hunter et al., 2005; Vorogushyn et al., 2010). Their success can be attributed to the relatively simple model structure based on a regular grid and straightforward explicit numerical solutions. The reliance on a regular grid allows a direct use of widely available digital elevation and land-use data for model parameterisation, as well as remote sensing flood extent data for model calibration and validation.

Particularly, the widely used LISFLOOD-FP model (Bates and de Roo, 2000) was successfully applied to a number of catchments, among others to the large-scale basins such as Amazon (Trigg et al., 2009; Wilson et al., 2007) and Ob (Biancamaria et al., 2009). In these studies, the model was applied with a coarse grid resolution to overcome the still high CPU time required. The early LISFLOOD-FP scheme, applied also to the mentioned large scale applications, used a so-called flow limiter approach to counteract numerical instabilities emerging during the computation of flows across cells with deep water and small free surface gradients (Hunter et al., 2005). However, the flow limiter approach suffers from insensitivity of the model to floodplain roughness, which led to the development of an adaptive time step solution scheme for the explicit solver (Hunter et al., 2005). This approach improved the model sensitivity to the roughness parameter, however, at the expense of computational time. Accordingly, the advantage over a fully-dynamical hydraulic model decreased. Driven by this problem, the LISFLOOD-FP code was further developed to include the inertia term into the momentum equation (Bates et al., 2010). With the inclusion of the local acceleration term, the model gained numerical stability. The more stable solution allowed the usage of larger time steps, which positively influenced the computational performance.

Other reduced complexity inundation models are based on the application of the Manning's formula or weir overflow equations on irregular grids. These approaches have a long history, with the first applications dating back to the 1970s (Cunge, 1975) and have experienced a renaissance in the recent years (Moussa and Bocquillon, 2009; Castellarin et al., 2011). The floodplain is represented by interconnected storage cells of irregular shapes. Water volume fluxes between cells are typically computed by the Manning's equation or weir-type formulas, whereas water levels within the cells are derived from water stage-volume functions. A pre-processing algorithm is needed to define the storage cells and their topology. The definition of the irregular storage cells is often done manually based on distinct topographic features constraining the flood spreading. However, such a subjective delineation may result in an inadequate representation of inundation dynamics. This could especially cause problems in wide and flat areas, where topographic constrains are difficult to evaluate. In the Rapid Flood Spreading Model (RFSM) developed at HR Wallingford (Gouldby et al., 2008), an automatic approach to derive irregular storage cells from a digital elevation model of the floodplain is used. With a search algorithm, local depressions in the topography are located and the storage cells are delineated around them. Hence, this method defines the storage cells in the whole floodplain objectively.

Storage cell models, based on an irregular mesh and using stage-volume functions and simple flux approximations, were developed to perform faster computations when compared to more sophisticated shallow water models. In one respect, this is attributed to the use of very simple equations that do not need complex numerical solution algorithms. Additionally, the fewer number of computational cells reduces the number of calculation steps. Due to representation of

sub-grid topography, the water depth variability within the computational cells is retained. The popularity of this approach is probably explained by the need to perform large-scale hydraulic computations. However, these models may suffer from an oversimplified representation of inundation dynamics and may not capture the flood wave propagation properly (e.g. Aureli et al., 2005).

To assess the suitability of simplified hydraulic models for large scale inundation simulations, in this study two models are compared in a benchmarking analysis: the irregular storage cell model Dynamic RFSM (HR Wallingford), based on the diffusive wave approximation, and a raster-based storage cell model with the inertia formulation as proposed by Bates et al. (2010). The objective of this benchmark study is to examine the model efficiency in terms of computational effort as well as the model performance to reproduce the bulk inundation characteristics relevant for large-scale flood risk assessment such as maximum inundation extent and depth. Dynamic RFSM and the raster-based inertia model were part of recent benchmark studies by Néelz and Pender (2010) and Neal et al. (2011a) respectively. This study further complements the two mentioned benchmark studies as Dynamic RFSM and the raster-based inertia model are compared directly. With the intention to evaluate the model performance in lowland areas, where there are few distinct topographic features and flow paths are difficult to identify, a study area in north-eastern Germany was chosen. The area is adjacent to the river Elbe and covers around 2000 km² and was severely affected by flooding in summer 2002. During this event, vast areas of the Elbe floodplain were inundated as a consequence of multiple dike breaches. In the absence of reliable flood event data, such as dike breaches and breach outflows, no real scenario is chosen. Instead a hypothetical dike breach scenario was modelled. Additionally, a simulation with the fully-dynamic shallow water model InfoWorks RS 2D (MWH Soft / Innovyze) was performed and used as a reference for checking the accuracy of the above two model approaches.

In contrast to the regular raster model, the Dynamic RFSM does not have a time step stability constraint, hence the sensitivity of the Dynamic RFSM to time step is also analysed. The choice of time step obviously has a direct influence on the run time; a large time step is desirable as it will reduce the total number of iterations, but a too large time step will produce inaccurate results. Furthermore, the possibility to reduce run time in the raster-based inertia model by coarsening of the grid resolution is examined. Simulations on a raster size from 25 m to 500 m are performed. The accuracy of 2D raster models depending on the grid size were already extensively examined for some test sites, particularly in urban environments (Horritt and Bates, 2001a; Yu and Lane, 2006a; Fewtrell et al., 2008), with the general conclusion that the smoothening of the topography and poorer representation of blockage at coarse grid resolution adversely affects the surface routing processes. However, we particularly test the model performance in terms of run time and accuracy for lowland floodplains typical for eastern-central Germany.

In the following sections, detailed descriptions of the inertia model and the Dynamic RFSM are provided. After performing the comparative analysis, the paper concludes on the applicability of both model types to the countrywide flood risk assessment.

2.2 Methods

2.2.1 Raster-based inertia model

In this study a raster-based storage cell model with an implementation of the inertia formulation, as presented by Bates et al. (2010), is used. Thereby the diffusive flood wave formulation is extended by the local acceleration term, whereas the advective acceleration term is still disregarded.

The equation development will be described here briefly, a more detailed derivation is provided by Bates et al. (2010). The inertia model solves the continuity (Eq. 1) and momentum (Eq. 2) equations of the Saint-Venant equations with the latter one neglecting the advective inertial term only:

$$\frac{\partial h^{i,j}}{\partial t} = \frac{q_x^{i-1,j} - q_x^{i,j} + q_y^{i-1,j} - q_y^{i,j}}{\Delta x} \quad (1)$$

$$\frac{\partial v}{\partial t} + v\frac{\partial v}{\partial x} = -g\frac{\partial h}{\partial x} + gS_f - gS_0 \qquad (2)$$

local and advective acceleration term | pressure term | friction term | bed slope term

where, $h^{i,j}$ is the water free surface height, $q^{i,j}$ is the specific flow per unit width at the node (i, j), Δx is the cell dimension, v is velocity, g is gravity, S_f is the friction slope and S_0 is the bed slope.

Expressing the momentum in terms of specific flow per unit width and approximating the hydraulic radius with the flow depth between cells (h_{flow}), the explicit equation for q at time $t+\Delta t$ reads:

$$q_{t+\Delta t} = \frac{q_t - gh_{flow}\,\Delta t S_f}{(1 + gh_{flow}\,\Delta t + n^2 |q_t| / h_{flow}^{10/3})} \qquad (3)$$

where n is the Manning's roughness coefficient and Δt is the time step. The fluxes across cell boundaries in x and y directions are computed independently of each other and are used to update the water level using the continuity equation (Eq. 1).

However, the numerical scheme is not unconditionally stable. The time step for a stable numerical solution is constrained by the Courant-Friedrichs-Levy criterion:

$$\Delta t_{max} = \alpha \frac{\Delta x}{\sqrt{gh_{flow}}} \qquad (4)$$

where α was introduced by Bates et al. (2010), as a factor reducing Δt_{max} to enhance model stability. Bates et al. (2010) indicated a value ranging between 0.2 and 0.7 as sufficient for most floodplain flow situations.

The inclusion of the inertia term implies that the water mass can gradually accelerate and decelerate that precludes the flow overshooting and resulting instabilities known for this type of codes (Bates et al., 2010). However, previous studies (Bates et. al, 2010; Dottori and Todini, 2011; Neal et al., 2011b) indicated a small difference between the diffusive storage cell code and the inertia formulation regarding model accuracy. Nevertheless the inertia model requires by far less computational time because of the stabilizing effect of inertia on the numerical solution that allows using larger time steps compared to the diffusive wave approximation. In contrast to the diffusive storage cell code with an adaptive time stepping solution developed by Hunter et al. (2005), the maximum stable time step of the inertia model is 1-3 orders of magnitude larger (Bates et al., 2010). Moreover, with the decreasing cell size, the stable time step of the inertia model reduces linearly instead of quadratic dependence for the diffusive code. This leads to an increased computational performance, especially for fine grid resolutions. Speedups of 2.5 to 1125 times depending on the grid size of 200 m to 5 m were reported for inundation over horizontal planes and planar beaches (Bates et al., 2010).

2.2.2 Dynamic RFSM

The Dynamic Rapid Flood Spreading Model (Dynamic RFSM) is an irregular storage cell model developed by HR Wallingford in 2009. It is based on a previous developed steady-state model, the so-called Direct RFSM (Lhomme et al., 2008; Gouldby et al., 2008). The Direct RFSM determines the final inundation extent by distributing a given water volume over the storage cells. Conversely, the Dynamic RFSM is an unsteady model, which computes fluxes across cell boundaries as a function of time based on the weir formula or Manning's equation. Both Direct and Dynamic RFSM were applied in the model benchmarking exercise conducted by the UK Environment Agency (Néelz and Pender, 2010). That study however, did not include an inertia based model and did not cover a large scale site of regional extent as is presented here.

The computational mesh of irregular storage cells is established with a fully automated procedure presented in Gouldby et al. (2008). These so called impact zones do not follow a regular raster. Depending on the topography, the impact zones can be very different in size and shape. They are delineated around depressions in the topography. With an automated search algorithm, low points in the digital elevation model (DEM) are identified and denoted as accumulation points (see Fig. 2-1). Looking at the topography gradient, all DEM cells draining towards the same

accumulation point form a polygon called impact zone. All the interfaces between two neighbour impact zones are screened to identify the lowest communication level and the relationship between water level and flow width across the impact zone boundary. Flow between two impact zones is initiated when the water level in one or both impact zones is higher than the communication level. Furthermore, the relationship between water level and storage volume is also calculated for each impact zone. All the information described above characterising the impact zones is stored in a SQL database.

Within the Dynamic RFSM, at each time step, the discharge between the impact zones is calculated with the weir formula or with the Manning's equation using the water levels in the two neighbour impact zones. In this study only the weir formula was used, the model is able to switch automatically between free flow and drowned flow. Water levels are updated using the water depth-volume relationships.

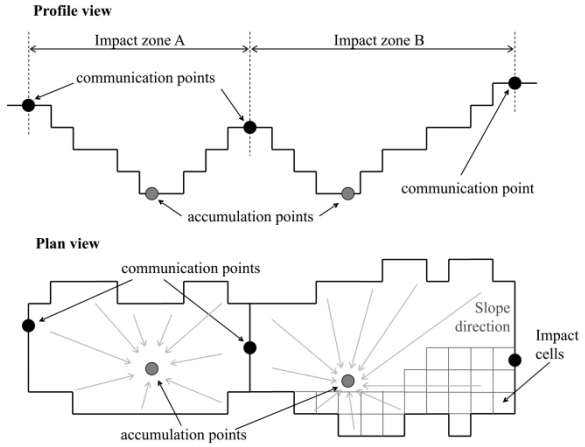

Figure 2-1: Example structure of impact zones (Lhomme et al., 2008)

The constant time step at which the calculations are carried out is set by the user. The time step has to be chosen with care. An inappropriate time step may produce inaccurate results, e.g. in a very large time step a high water column can be generated within an impact zone, which in its turn leads to the development of alternative flow pathways across the impact zone boundaries that otherwise would not be activated with small gradual water level increase. This may lead to the development of unrealistic inundation patterns and 'chequerboard' oscillations of the water level. Similar argumentation can be applied to the selection of a very small time step.

2.2.3 InfoWorks

The engine used in the fully-dynamic shallow water model InfoWorks RS 2D (MWH Soft / Innovyze) is based on the procedures described in Alcrudo and Mulet-Marti (2005). It uses a conservative formulation of the full shallow water equations and a first-order finite volume explicit scheme. Fluxes at cell interfaces are calculated with Roe's Riemann Solver. The time step is calculated accordingly to the Courant–Friedrichs–Levy condition. This algorithm can be used with both structured and unstructured meshes and is appropriate for representing rapidly varying flows (shock capturing) as well as super-critical and transcritical flows. Detailed description of the model and a model application can be found respectively in Innovyze (2011) and Lhomme et al. (2010).

2.3 Study Area

For the evaluation of both models, a test area adjacent to the river Elbe in Germany was chosen. This reach is part of the middle Elbe and has the characteristics of a lowland river with flat topography and large floodplains. The selected Elbe reach is almost completely protected by dikes.

In Fig. 2-2, the model domain around the gauge at Torgau is shown. It covers an area of 45 km length and width with a total area of 2025 km². The topographical information is derived from a digital elevation model (DEM) provided by the Federal Agency for Cartography and Geodesy in Germany (BKG, 2007). The DEM was constructed from different information sources, such as digitized topographic maps, photogrammetric and laser scanned data. The horizontal grid resolution is 25 m and the vertical accuracy is reported to be in range of ± 1-5 m. The channel and floodplains between dikes were excluded from the modelling domain (displayed in dark blue in Fig. 2-2).

The inundation simulation over the floodplain in the hinterland was simulated after the initial dike breach was initiated (red circle in Fig. 2-2).

Floodplain roughness parameters were derived from ATKIS (Amtliches Topographisch-Kartographisches Informationssystem) and CORINE (COoRdinated INformation on the Environment) land-use data by assigning Manning's values to land-use classes. For the mainly agricultural areas, a constant Manning's value of 0.035 $m^{-1/3}s$ is assumed.

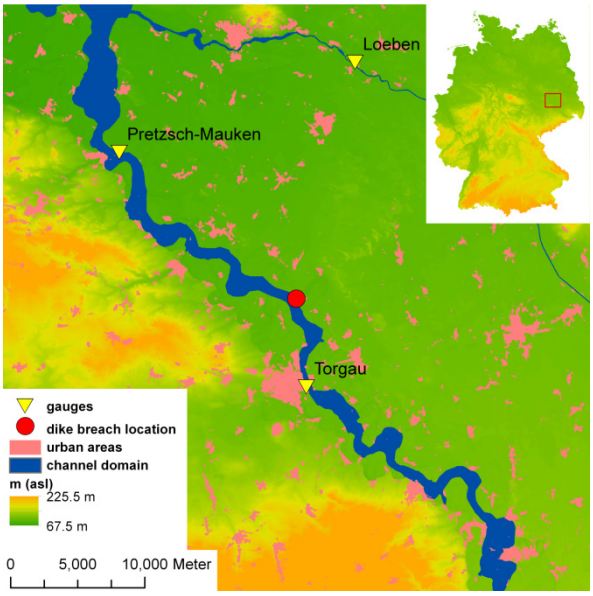

Figure 2-2: Model domain of the study area at the river Elbe.

2.4 Model Testing and Results

For the evaluation of the two models, a hypothetical dike breach scenario along the Elbe reach was implemented. The heavy flood event of August 2002 served as a basis for the calculation of the outflow hydrograph. Water levels within the channel were simulated with a one-dimensional hydraulic model. At the location shown in Fig. 2-2, a dike breach with a breach width of 20 m was enforced. The outflow from the channel to the floodplain was calculated with the weir formula. The total outflow volume calculated was 55×10^6 m³, distributed over an event duration of 7 days with a maximum outflow of 150 m³/s. However, the total simulated duration was taken as 22 days, to ensure that the steady state was reached. No flow from the floodplain back to the river was considered (i.e. wall boundaries).

Results of the model simulations were evaluated in terms of maximum inundation extent and depth in comparison to a benchmark simulation using the following metrics: bias in depth, root mean square difference (RMSD) of maximum depth, bias in inundated area and flood area index (FAI) defined as follows:

$$FAI = \frac{\mathrm{M1D1}}{\mathrm{M1D1} + \mathrm{M1D0} + \mathrm{M0D1}} \quad (5)$$

where, M1D1 is the number of cells simulated as flooded by both models, M1D0 is the number of cells flooded in the prediction and dry in the benchmark simulation and M0D1 the number of cells dry in the prediction, however, indicated as wet in the benchmark simulation.

The benchmark is set up with the fully-dynamic shallow water model InfoWorks RS 2D (MWH Soft / Innovyze). Simulations with the raster model and the Dynamic RFSM were performed on a single core only, with an Intel Core Duo 2.66 GHz processor. The InfoWorks simulation was run on two cores at a Pentium 4, 3 GHz CPU. To keep the run time to an acceptable extent, the model domain for the InfoWorks simulations was cut down to the minimum possible extent of 227 km². The computational mesh is made of 234,184 triangles, which have an area comprised between 500 m^2 and 1500 m^2 (i.e. equivalent to square cells of width between 22 m and 39 m). At the given extent, the overall computational time was 64 hours with a minimum time step of 0.058 s. Due to the smaller model domain used and the automatic parallelization on two cores, a direct comparison of run times to Dynamic RFSM and raster-based inertia model should be avoided. The mass balance error was zero.

To be able to compare the benchmark simulation results based on an irregular computational mesh to the results of Dynamic RFSM and raster-based inertia model on regular grids, the benchmark model results were transformed to a regular raster of 5 m resolution. Accordingly, modelling results of the Dynamic RFSM on 25 m and raster-based inertia model on various grid

sizes were also resampled to a higher resolution of 5 m. The resampling method used was nearest neighbour. With this method only the resolution, not the value, is changed.

2.4.1 Raster-based inertia model

To investigate the impact of grid resolution on run time and model performance, the two-dimensional simulation with the raster model was repeated several times with different resolutions. Simulations with a grid size varying from 25 m to 500 m were run. The α-value has a direct influence on the model time step and the run time. To find the appropriate α-value, where the solution retains stable while the run time is minimum, an extensive sensitivity analysis would be required for each gird resolution. Furthermore, this analysis would only be valid for this particular test case. However, for large scale and long term applications it is necessary that models are stable for most flow conditions. Therefore, a constant and relatively low α-value of 0.2 was chosen, to guarantee the stability of the solution. Nevertheless for a grid size of 25 m, the water volume spread over the grid was still too large for the time step. Thus, water depths below zero were calculated. Accordingly, the α-value had to be lowered to 0.1 for calculations on a 25 m grid.

A summary of simulation results of the raster model on different grid size, compared to the benchmark, is shown in Table 2-1. As a comparison between an unstructured and a structured gird is done, one would always find differences in simulation results. However, the smallest difference from the fully-dynamic model simulation in terms of inundation extent and depths was achieved with the finest resolution of 25 m. This difference gradually increases with the grid resolution. In particular the model accuracy significantly deteriorates at a grid resolution of 200 m. There seems to be a local threshold for model accuracy at which the FAI drops by approximately 10% and RMSD increases by ca. 50%. Almost 90% of the flood extent was correctly predicted with the 25 m resolution. The total inundated area is slightly underestimated at 25 m grid size resolution, for coarser grids the total inundated area is generally overestimated as can be concluded from the bias in inundated area.

To illustrate the spatial variation of differences between the benchmark and the inertia based model, the results of the model run with 100 m resolution are shown in Fig. 2-3. As indicated by the bias and flood area index, the inertia model tends to overestimate the inundation extent as would be expected for coarse resolution, at which topographical boundaries become smoothed. The deviations in depth have been calculated, the absolute error from the reference simulation and the ratio between absolute error and reference depth are shown respectively in Fig. 2-3 (b) and (c). For the vast majority of the cells in the study area, the absolute error is below 20 cm and the relative error in depth less than 20% of the reference depth given by the benchmark model. High errors in absolute depth (more than 1 m) and relative depth (more than 100%) occur mainly at flood extent boundaries, which can be explained by the discrepancy in simulated inundation areas.

Mass balance errors for the raster-based inertia model were calculated at the end of model simulations as a percentage of the input volume. They remained zero for all simulations, which is a good proxy for model accuracy as recently discussed by Neal et al. (2011a).

For the simulation on the 25 m grid, the run time was approximately 20 days and accordingly almost as long as the actual simulated duration. However, the computational time could be reduced remarkably by coarsening the grid resolution. According to Eq. 4, the time step depends on grid size, flow depth between cells and the α-value. For simulations with a grid resolution up to 200 m, where the difference in modelled depth is small, the minimum time step during the simulation increases linearly with coarsening of the grid. However, this is not valid for the simulation on the 25 m grid, due to the fact that a smaller α-value was necessary to achieve numerical stability. In addition to the increase of minimum time step, the run time is even more reduced by coarsening of the grid resolution and the resulting smaller number of computational elements (Table 2-1). It can be expected that for larger grid sizes of 100 m and more, larger α-values could be used, which would result in a further reduction of the run time. However, in order to determine the largest α-value at which the model retains stable, a comprehensive and computationally intensive sensitivity analysis for each grid resolution would be required.

Table 2-1: Influence of grid resolution on maximum simulated inundation extent and depth, as well as on run time, for simulations with the raster-based inertia model.

Grid resolution	Bias in depth (m)	RMSD (m)	Bias in inundated area	Flood area index (%)	Number of computational cells	Minimum occurred time step (s)	Run times (min)
25 m	-0.02	0.14	0.98	89.0	3,097,600	0.4	27,840
50 m	-0.006	0.16	1.02	89.6	774,400	1.6	1,555
100 m	+0.0006	0.21	1.05	86.9	193,600	3.3	154
200 m	+0.01	0.34	1.13	75.7	48,400	6.8	21.6
300 m	+0.02	0.40	1.18	70.8	21,609	7.3	7.3
400 m	+0.006	0.43	1.19	68.9	12,100	9.2	4.5
500 m	+0.004	0.49	1.08	57.0	7,744	12.9	3.4

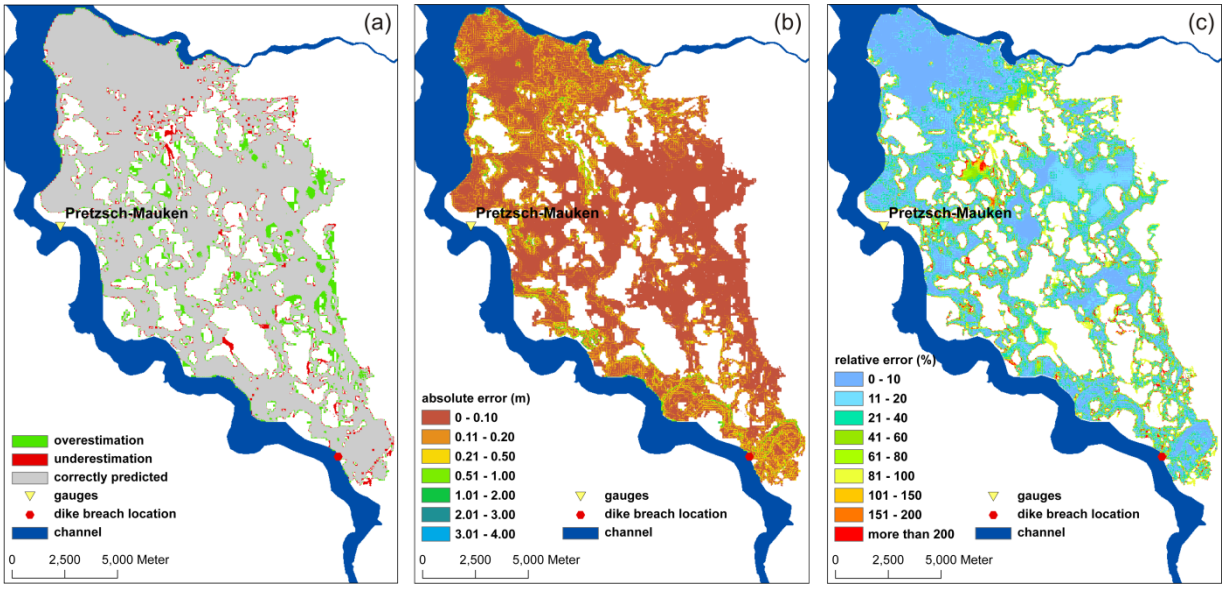

Figure 2-3: Comparison of maximum simulated inundation depths between the raster-based model simulation (at Δx = 100 m) and benchmark. (a) Evaluation of inundation extent, (b) absolute error in depth, (c) ratio between absolute error and reference depth.

2.4.2 Dynamic RFSM

Compared to the regular raster model that runs directly on the DEM, a more extensive pre-processing is needed for the application of the Dynamic RFSM. Firstly, the automatic delineation of impact zones was carried out. The mesh of computational elements was generated from the 25 m resolution digital elevation model (Fig. 2-4). Around 30,000 impact zones were delineated from around 3 million cells of the digital elevation model. Hence the number of computational elements was reduced by factor 100 compared to a regular raster model for the selected representative lowland floodplain. It can be expected that in other areas with more pronounced relief, the reduction factor is lower if more local topographic depressions are detected. The size and shape of the delineated impact zones varies widely. The mesh of impact zones is shown in Fig. 2-4. In the very flat areas, some very

large impact zones were delineated, with characteristic width of 2 km or more.

The time step within the Dynamic RFSM is constant and set by the user. To test the model sensitivity to the time step size, simulations with time steps of 10 s, 20 s, 40 s, 60 s, 80 s and 100 s were performed with the Dynamic RFSM. The volume exchange between the computational elements was calculated with the weir formula.

During the simulation with a large time step of 100 s, 'chequerboard' type instabilities occurred at locations with high exchange volumes (e.g. close to the breach). Within a single large time step, high water volumes flow from one cell to another, creating temporary high water levels. In the next time step, the water is flowing back into the first cell and so forth. As a result, unrealistic high maximum water depths were calculated. For smaller time steps of 60 s and less, no instabilities could be observed. This type of instability can effectively be suppressed by considering the inertia of water mass as was implemented for the raster-based model (Bates et al., 2010). Initial work on the inclusion of the inertial formulation of the momentum equation within the Dynamic RFSM by Jamieson et al. (2012) gives promising results.

The comparison of the six Dynamic RFSM simulations (Δt = 10, 20, 40, 60, 80, 100 s) with the benchmark results are summarized in Table 2-2. Overall, the model underestimates the total inundated area as indicated by the bias in inundated area and additionally supported by the low FAI (Table 2-2). However, the underestimation of maximum inundation depths occurs mainly in areas with very low water depth. As a result, it has a small influence on the RMSD and the depth bias. It appears that, when decreasing the time step the underestimation of inundation extent is increasing. Due to this effect, the decrease of time step from 60 s to 10 s has a negative influence on the RMSD. Although the model runs with 100 and 80 s time steps seem to deliver good results in terms of inundation extent and overall depth bias, the results cannot be used due to the instabilities that occurred during run time producing locally unrealistic high maximum water depth. Therefore, the simulation with a time step of 60 s gives the overall best results in comparison to the fully-dynamic model.

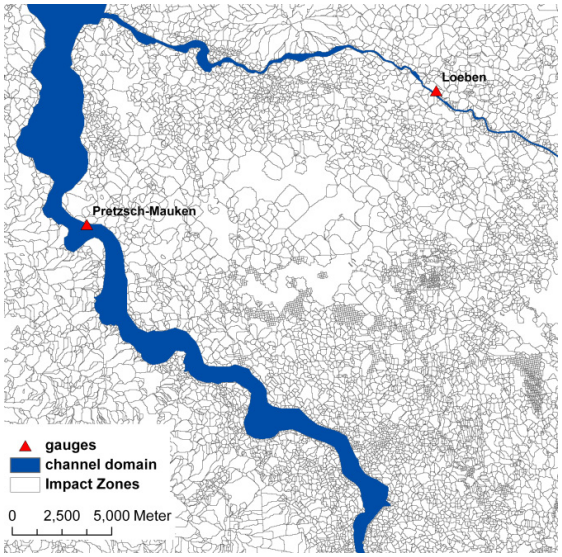

Figure 2-4: Mesh of impact zones within the modelling domain.

In Fig. 2-5 (a), showing the 60 s time step simulation compared to benchmark, the underestimation of flood extent becomes evident. In addition it can be seen that a few 'isolated ponds' of inundation were simulated. The large absolute and relative errors in depth up to 0.5 m or 100% respectively, stretching over extended parts of the model domain, are apparent (Fig. 2-5 (b) and (c)). However, due to the very shallow inundation in these areas, this does not dominate the RMSD value.

For simulations with the Dynamic RFSM, mass balance errors are constrained to zero. This is a result of strict use of discharge limiters implemented. The discharge limiters prevent the total amount of water leaving the cell to be greater than the sum of the initial volume and the volume coming in.

The run times depend roughly linearly on the time step. The simple algorithm, the relatively large time steps and the low number of computational elements enable overall short model run times. However the communications with the SQL database during run time cost a large part of this advantage. The appropriate and structured storage of information is nonetheless indispensable for large-scale applications, where millions of impact zones need to be handled in this framework.

Table 2-2: Influence of time step on maximum simulated inundation extent and depth, as well as on run time, for simulations with the Dynamic RFSM.

Time step size	Bias in depth (m)	RMSD (m)	Bias in inundated area	Flood area index (%)	Run times (min)
10 s	-0.09	0.19	0.76	73.5	558
20 s	-0.08	0.18	0.78	75.0	289
40 s	-0.05	0.17	0.81	76.9	147
60 s	-0.03	0.17	0.83	78.0	102
80 s	-0.01	0.19	0.86	79.0	79
100 s	+0.007	0.22	0.88	79.1	64

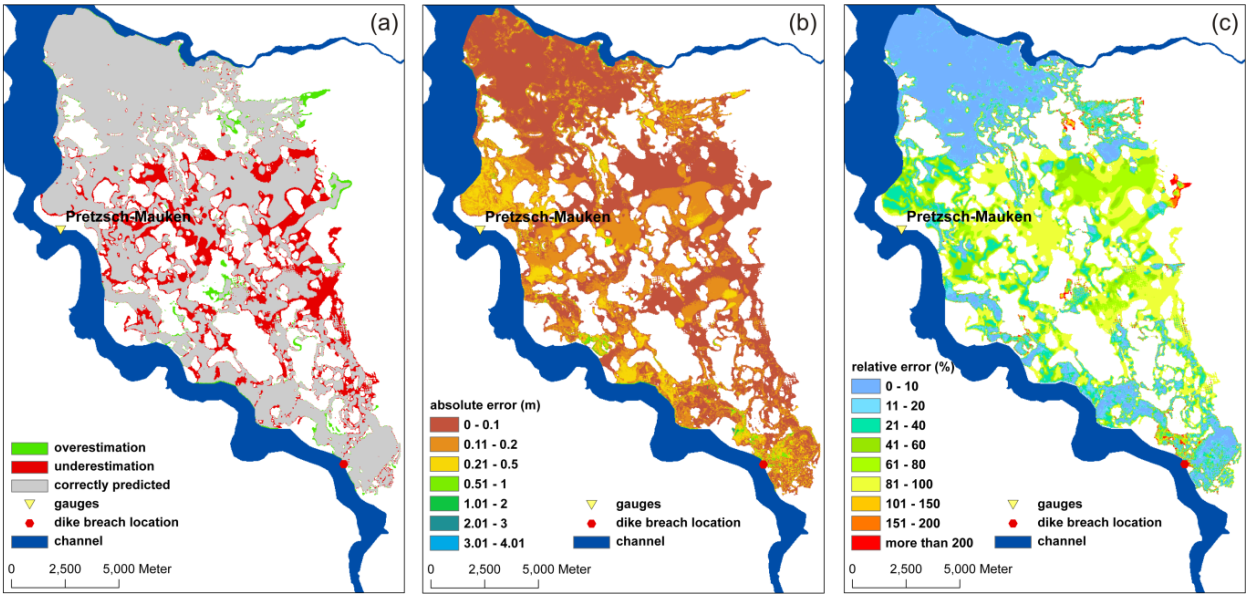

Figure 2-5: Comparison of maximum simulated inundation depths between Dynamic RFSM simulation (with $\Delta t = 60$ s) and benchmark. (a) Evaluation of inundation extent, (b) absolute error in depth, (c) ratio between absolute error and reference depth.

2.5 Discussion and Conclusion

In the previous sections, two simplified hydraulic models, an inertia based raster model and the Dynamic RFSM, were compared to a benchmark scenario. The objective was to investigate their ability to simulate a hypothetical inundation scenario, in comparison to the fully-dynamic InfoWorks model. The accomplished tests included a sensitivity analysis of the raster model to grid size and of the Dynamic RFSM to time step, with respect to model accuracy and run time.

Simulations of inundation processes in the selected lowland study area with wide and flat floodplains were shown to be specifically challenging because of multiple possible flow paths. The simulated scenarios have shown that both simplified models were able to simulate the final inundation extent and depths with a reasonable accuracy.

As was expected, the raster-based model delivered the best results at the finest tested grid resolution of 25 m corresponding to the original DEM resolution used for the benchmark model. However, the total computational time at this resolution becomes intractable in view of the national scale application. Much progress has been made over the past decade with raster-based models to develop simplified and fast hydrodynamic schemes. However they still remain CPU time demanding for large scale problems. Therefore, the strategy of grid coarsening has to be taken into account to cope with computational constraints. It was shown that the model accuracy deteriorates with increasing grid size, as one would have expected, when the topographic constraints become smoothed by interpolation. Indeed, the inertia model tends to overestimate the inundation extent at coarser grids compared to the benchmark result. It is however, evident that doubling the cell size results in a considerable decrease of computational time. Although one must keep the acceptable accuracy level for hydraulic simulations, this does not seem to dominate the risk estimations (Apel et al., 2009), which is especially true for large scale applications, where the local errors can counteract each other in the final risk estimate.

Even with its simplified structure that uses a diffusive-wave approximation on an irregular grid, the Dynamic RFSM was able to simulate the maximum inundation extent and depths in a reasonable manner, although problems occurred with very large impact zones delineated in the flat regions of the case study area. Isolated ponds of inundation were simulated in the study area. This effect is caused by the filling of the impact zones that starts from the lowest point. Whenever an impact zone is not completely filled, the crest between the considered impact zone and its neighbours is not inundated. This effect increases with larger inundation zones and leads to a marked underestimation of inundation extent in the affected areas. However, as indicated by the RMSD, the overall maximum depth is in generally well-reproduced, due to the fact that these effects only occur in areas with very shallow inundation. These problems are likely to be less dominant in areas with a complex topography where generally smaller inundation zones are delineated. Care has to be taken with the choice of time step, as it affects model performance. At large time steps, the level in a given impact zone is likely to rise too high as the exchanged volume was too high. This impact zone will be able to spill towards more neighbours compared to the case where the level is properly estimated. For a too large time step of 100 s 'chequerboard' type of instabilities could be observed. With a shorter time step, the level is likely to rise to a more moderate value and potentially fewer neighbours will be spilt into. A time step of 60 s was optimal in this study area for impact zones of the given size. This type of instability can effectively be suppressed by the implementation of the inertial type approach (Bates et al., 2010). Early exploration of the inclusion of the local acceleration term of the momentum equation within the formulation of the Dynamic RFSM shows considerable promise (Jamieson et al., 2012).

Using a relatively coarse grid resolution of 100 m can reduce the run time of the raster-based model to the run time similar to the computational time of the Dynamic RFSM with a time step of 60 s (Table 2-1 and 2-2). Comparing the results, the raster based model performs better than the Dynamic RFSM in terms of inundation extent, as indicated by FAI and bias in inundated area. On the contrary, the Dynamic RFSM achieved a slightly better RMSD compared to the benchmark simulation. This is an advantage of the Dynamic RFSM over the current version of the inertia model which basically resides in consideration of the sub-grid topographic variability within the impact zones. This characteristic is crucial for representing the inundation depths. On a coarse grid the inertia model uses the averaged topography, whereas Dynamic RFSM retains the detailed topographic information within each impact zone. The advanced model physics in the inertia model cannot fully compensate the reduction in topographic complexity with respect to the simulation of inundation depths.

Thus, overall it can be concluded that with a similar run time, the raster-based model performs slightly better than the Dynamic RFSM in this lowland river case study. Furthermore, there is a potential for reduction of run times of the inertia model by using higher α-values for larger grid sizes. Determination of the highest possible α-value at which the model retains stability requires, however, a computationally intensive sensitivity analysis. An additional advantage of the raster-based model is the easier model set up

which does not require additional pre-processing steps. Nevertheless, it is likely that in areas with more complex topography, the generalization of the DEM has more influence on modelling results. It is possible, that in this case the raster based model might fail to simulate the inundation process correctly on a coarse grid resolution. This problem can however, be relaxed by the implementation of the sub-grid parameterisation schemes aimed at the representation of influences on flow conveyance by small-scale topographical features at a larger scale. This can be realized by deriving a so-called porosity function on a cell basis, which accounts for flow blocking effects by topographic features (e.g. buildings), reduction in floodplain storage and alteration in flow pathways (Defina, 2000; Yu and Lane, 2006b; McMillan and Brasington, 2007; Soares-Frazao et al., 2008). For instance, for the raster cell models, a porosity function can be implemented as a depth dependent percentage of volume of a coarse resolution cell available for storage (Yu and Lane, 2006b; McMillan and Brasington, 2007). In this approach, the sub-grid topographic variability is represented by the volume-depth relationships on a grid-by-grid basis, and is in essence the one used in RFSM models for irregular cells. The porosity models were reported to resemble the hydrodynamics of the high-resolution flow models, however, the improvement obviously comes at the expense of computational time (Yu and Lane, 2006b; McMillan and Brasington, 2007).

Previous application of the Dynamic RFSM model revealed some difficulties in the propagation of high flows (Néelz and Pender, 2010). However this was mainly the result of using too large time steps in order to achieve short run times. This is a common problem with diffusion wave models with no adaptive time stepping (Hunter et al., 2005). This situation has given an impetus to a further development of the Dynamic RFSM model and early work on an adaptation of the inertial form of the momentum equation to the irregular polygon structure shows great potential. This benchmark exercise is, however, particularly focused on the flood characteristics relevant for inundation risk assessment such as maximum inundation extent and depths. With regards to these characteristics, the Dynamic RFSM performed satisfactorily in the present test.

Hence, an application at the national scale appears feasible with both the Dynamic RFSM and the inertia model as they showed reasonable run times and acceptable performance.

Acknowledgements. The work reported in this paper is part of the project “Regional Flood Model for Germany”. We thank the Federal Agency for Cartography and Geodesy in Germany (BKG) for provision of the digital elevation model of Germany (DGM-D) and the two anonymous reviewers for their helpful comments and suggestions.

3 Continuous, large-scale simulation model for flood risk assessments: proof-of-concept

Continuous, large-scale simulation model for flood risk assessments: proof-of-concept

Abstract

In this paper we present the Regional Flood Model (RFM), a process-based model cascade developed for large-scale basins. The objective of this study is to demonstrate that flood risk assessments, based on a continuous simulation approach, including rainfall–runoff, 1D river network, 2D hinterland inundation and damage estimation models, are feasible at the scale of large catchments. RFM is applied to the German part of the Elbe catchment including around 2700 river-km. For this proof-of-concept study, simulations are performed continuously over the period of 1990–2003. Simplification of equations and parallelisation enable the continuous 2D hydrodynamic inundation simulation with reasonable run-times on a relatively high resolution of 100 m. As uncertainties are introduced with each module along the model chain, results are evaluated, where possible, with observed data. Results indicate that uncertainties are significant, especially for hydrodynamic simulations. This is basically a consequence of low data quality and disregarding dike breach effects in the simulations. Reliable information on overbank cross-sections and dikes is expected to considerably improve the results. We conclude that the large scale simulation of catchment processes, inundation and damage, driven by long-term climate data, is viable within a continuous simulation framework. It has the potential to provide a spatially consistent, large-scale picture of flood risk.

Published as:

Falter, D., Dung, N.V., Vorogushyn, S., Schröter, K., Hundecha, Y., Kreibich, H., Apel, H., Theisselmann, F. and Merz, B. (2014), Continuous, large-scale simulation model for flood risk assessments: proof-of-concept. Journal of Flood Risk Management. doi: 10.1111/jfr3.12105

3.1 Introduction

Recent extreme river flooding in June 2013 in Central Europe, affecting large areas of the Danube and Elbe catchments, have once again stimulated the public and scientific controversy in Germany and elsewhere concerning risk oriented flood management. It is widely accepted that there is a need for risk-orientated flood management approaches on a basin-scale, which is also demanded by the European Union Flood Directive (European Commision, 2007). Large scale risk assessments are needed, for example, for national risk policy developments, for large-scale disaster management planning, and in the (re-)insurance industry. However, large-scale risk asessment methods for areas in order of several 10 000 km^2 are still in early stages. Until today only few studies addressed large-scale flood risk assessments, e.g. the RASP project in England and Wales (Hall *et al*., 2003, 2005) or more recently the Taihu Basin Foresight Project in China (Cheng *et al*., 2013).

Speaking of flood risk, we address both the probability of a certain flood at a certain location within a certain period of time (flood hazard) and the associated damage. The limitations of flood risk assessments at large scales are a consequence of the considerable challenges of hazard assessment at these scales; damage assessments are easier to transfer across spatial scales. Bottom-up flood loss approaches start with a detailed damage analysis and the modelling of single elements at risk (e.g. buildings), then an up-scaling procedure for application on basis of land-use units is developed (e.g. Germany-wide: Thieken *et al*., 2008; Kreibich *et al*., 2010). Top-down approaches undertake damage modelling solely on basis of aggregated data (e.g. Europe-wide: Schmidt-Thomé *et al*., 2006; globally: Peduzzi *et al*., 2009; Jongman *et al*., 2012). However, the focus in our literature review is on large-scale approaches for flood hazard assessment. Generally, flood hazard assessments can be subdivided into two steps. First, discharge related to a specific return period (T-year discharge) is estimated. In a second step, discharge is translated to inundation characteristics. The methods used for flood hazard assessment and mapping across Europe are very heterogeneous and restrict currently a spatially consistent view and comparison of flood hazard levels (de Moel *et al*., 2009).

The most common approach of large-scale flood hazard assessment is the reach-wise calculation of T-year discharges for the entire river network assuming a spatially uniform return period. Derived flow peaks (or associated synthetic hydrographs) are used to estimate inundation extent and depths. The estimation of T-year discharges is typically based on extreme value statistics of gauging station data and regionalisation methods. An example is the Rheinatlas (http://www.rheinatlas.de/), providing inundation extent and associated damage along the river Rhine for several return periods. In a similar way, Merz *et al*. (2008) estimated 30-, 100-and 200-year return period flood discharges for 26 000 river-km in Austria. Bradbrook *et al*. (2005) used the regionalised estimations of flood flows with spatially uniform return periods for national scale floodplain mapping in England and Wales. T-year discharges (respectively T-year hydrographs) can also be derived from a continuous hydrological simulation. Alfieri *et al*. (2013) developed a pan-European flood hazard map assuming uniformly a 100-year return period. For each river piece, synthetic hydrographs corresponding to 100-year floods were derived from 21 years of continuous discharge simulation with a hydrological model. Although the assumption of spatially uniform return periods is very valuable for deriving the local hazard, it is of limited use when large-scale patterns are important. The assumption of a T-year flood for the entire river network gives an unrealistic picture and tends to overestimate flood risk on large scales. The probability of a single flood reaching a 100-year period in the entire large-scale river network is much smaller than the annual probability of such a flood at a single site, if this is realistic at all.

The disadvantage of spatially homogeneous return period scenarios is overcome by another group of event-based approaches, where a set of spatially consistent synthetic flood events with heterogeneous local return periods is generated. Rodda (2005) used a judgement-based approach for flood risk assessment in the Czech Republic, where synthetic hydrographs with specific return periods are directly derived from gauging station data of selected historical events. More sophisticated methods generate stochastic flood event

sets with multivariate statistical models from gauging station data, whereas the spatial dependence between gauging stations is considered (Lamb *et al*., 2010; Keef *et al*., 2013). Event-based methods can also be placed higher up in the hydrological cycle by generation of stochastic rainfall events used by hydrological models to simulate the corresponding T-year discharge (e.g. Rodda, 2001; Wicks *et al*., 2013). Depending on the complexity, event-based approaches may suffer from choosing only a bunch of scenarios, generation of unrealistic hydrograph shapes or only providing peak flows. Floods are generated and influenced by a multitude of catchment and river processes that might not be captured adequately by event-based statistical–stochastic methods. For example, Apel *et al*. (2009) demonstrated that upstream dike breaches may influence downstream flood frequency curves. Because dike breaches are rare events, they are not or are only rarely contained in observed time series. Hence, the downstream effects of dike breaches cannot be derived by statistical–stochastic event-based methods. The approaches relying on the estimation of synthetic hydrographs may suffer from their unrealistic shapes if derived statistically even if the peak and volume information are preserved (Grimaldi *et al*., 2013).

An alternative approach is the continuous simulation of rainfall–runoff with hydrological models, driven by continuous synthetic or observed climate data or climate model scenarios. This approach has the advantage that all hydrological processes that influence the runoff are implicitly considered in a consistent way and the complete flood event, including antecedent processes, are modelled throughout the entire catchment. This approach is complemented by including the hydrodynamic simulation of water levels and inundation processes within the continuous simulation. In that way also, physical processes like storage effects, flood attenuation or channel–floodplain interactions can be accounted for. However, large-scale, continuous hydrodynamic simulation requires excessive computational time and brings additional sources of uncertainty into hazard and risk assessment.

On a large scale, detailed hydrodynamic simulations are mainly avoided because of computational constraints and data limitations (e.g. Rheinatlas; Rodda, 2005) or carried out piece-wise in parallel for river reaches in a spatially inconsistent approach (Bradbrook *et al*., 2005; Alfieri *et al*., 2013). Discharge is often transformed to water levels and inundation extent using simple approaches based on rating curves and water surface intersection with topographic data or only 1D hydrodynamic simulations. Representation of dikes and channel–floodplain interactions are often disregarded. Although the channel and its banks might be represented adequately by one-dimensional (1D) hydrodynamic models, inundation processes on extended floodplains need a two-dimensional (2D) representation.

The application of 2D flood inundation models on a large scale is relatively new. Research on simplification of fully hydrodynamic equations and on reduction of model runtime (e.g. parallelising) have only recently encouraged 2D hydrodynamic simulations on a large scale. Current approaches focus on coupled 1D/2D models where the channel flow is simulated one-dimensionally with full shallow water equations or reduced complexity equations like diffusive or kinematic wave. The approaches for 2D floodplain flow simulation range from simple volume conservative storage-filling algorithms to fully dynamic shallow water modelling. Paiva *et al*. (2013) has developed a coupled 1D/2D model for the Amazon catchment with the fully dynamic river network model coupled to a simple floodplain storage model, where the floodplain is represented by discrete storage compartments. More complex handling of floodplain inundation was proposed by applying simplified versions of shallow water equations to regular storage cells as well as to irregular storage cells (Jamieson *et al*., 2012). Besides numerous small-scale applications, regular rasterbased inundation models were applied to the Amazon (Wilson *et al*., 2007), Ob (Biancamaria *et al*., 2009), Pantanal (da Paz *et al*., 2011, 2013) river basins and recently to an 800-km reach of the Niger using a subgrid channel parameterisation (Neal *et al*., 2012). Model run-times and results of raster-based models are promising for the purpose of large-scale flood risk assessments. However, all applications are performed with relatively coarse resolutions (about 0.3–2 km) and on rather natural river systems where representation of dikes is not needed and the interactions between floodplain and channel are easier to represent. With high resolution, however piece-wise

and thus spatially inconsistent, Bradbrook *et al*. (2005) ran a 2D raster-based inundation model for 1-km river reaches in England and Wales. The inundation area estimates were then merged into a single flood inundation pattern. In a similar way, Alfieri *et al*. (2013) applied a raster-based inundation model for pan-European flood hazard mapping. First, they ran the model at 1 × 1 km spatial resolution to define appropriate subdomains, large enough to prevent flood flow crossing domain boundaries. Then, simulations were performed for each subdomain on a higher resolution of 100 × 100 m. Finally, flood extent maps were merged into a single one. Even on a global scale, inundation models are applied now for flood hazard mapping (Yamazaki *et al*., 2011; Pappenberger *et al*., 2012) or flood risk assessments (Winsemius *et al*., 2013). The methods are dominated by simple inundation models and coarse resolutions of 1 × 1 km or more that are appropriate for global scale, however, less suitable for flood risk assessments on large basin scale covering some 10 000 km^2.

Despite the methodological strengths of continuous simulation approaches, hydrological, 1D/2D hydrodynamic and damage assessment models were not combined within a continuous simulation framework for large-scale flood risk assessments because of the computational challenges and data requirements of 2D hydrodynamic flood inundation models. Here, we present a first attempt to apply a full flood risk assessment chain for large-scale basins based on a continuous simulation approach, including rainfall–runoff, 1D river network, 2D hinterland inundation and damage estimation models at a resolution of 100 m. This approach combines different elements of the flood risk chain, from the flood-triggering precipitation to the damage, in a continuous simulation mode which enables a spatially consistent flood hazard and risk assessment. The scope of this publication is a proof-of-concept exercise for large-scale flood risk assessments, carefully discussing the limitations of the proposed methodology. The model chain is applied to one of the largest catchments in Germany, the Elbe. Hydrodynamic simulations include a catchment size of around 66 000 km^2 and a river network of around 2700 km. The simulation period comprises 14 years (1990–2003). Simulation results are presented for each model step and evaluated, as far as possible, against available data.

3.2 Methods

3.2.1 Regional Flood Model

The proposed Regional Flood Model (RFM) consists of four model parts (Figure 3-1): the rainfall–runoff model SWIM, a 1D channel routing model, a 2D hinterland inundation model and the flood loss estimation model for the private sector (FLEMOps+r).

The hydrological model SWIM (Soil and Water Integrated Model, Krysanova *et al*., 1998) computes daily runoff that is routed from sub-basin to sub-basin with the Muskingum hydrological routing method. The routed discharges provide a boundary condition for the 1D hydrodynamic river network model that is based on the diffusive wave equation. In case of a threshold value representing bankfull flow is exceeded, the hydrodynamic model routes the flow exceeding the bankfull discharge downstream along the river network based on simplified cross-sections describing the overbank river geometry and elevation of flood protection dikes. Whenever the water level reaches the dike crest height, the overtopping flow into the hinterland is calculated with the broad-crested weir equation. The propagation of the inundation front in the hinterland is computed with a 2D raster-based hydrodynamic model based on the simplified shallow water equation, neglecting advective acceleration. For each flood event during a continuous simulation, maps of maximum water depths are generated and used as input to the FLEMOps+r damage model (Elmer *et al*., 2010). Further, the recurrence intervals of the flood peaks for each hydrological sub-basin are estimated. Using the information about inundation depth, recurrence intervals as well as exposure and characteristics of the residential building stock, the multifactorial flood damage model FLEMOps+rprovidesan estimate for flood losses. In the following sections, each constituent model of the flood risk chain is described in more detail.

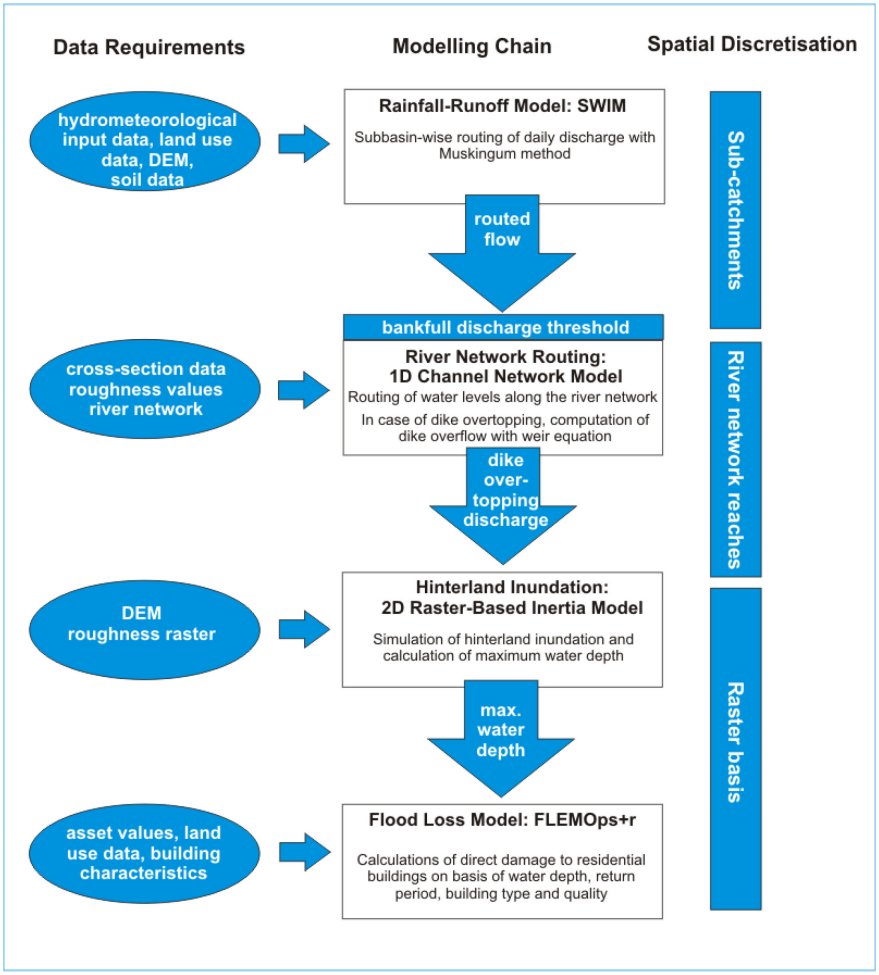

Figure 3-1: Components and data requirements of the Regional Flood Model (RFM). DEM, digital elevation model; FLEMOps+r, Flood Loss Estimation MOdel for the private sector; SWIM, soil and water integrated model.

RFM can be driven with continuously observed or synthetic hydrometeorological data or with output from climate models. Long series of synthetic hydrometeorological data can be generated with a multisite, multivariate weather generator (Hundecha and Merz, 2012) further advanced from Hundecha *et al*. (2009) to provide spatially consistent realisations of meteorological fields for large-scale basins.

3.2.2 Rainfall–runoff model: Soil and Water Integrated Model (SWIM)

The ecohydrological model SWIM (Krysanova *et al*., 1998) simulates the hydrological cycle on a daily time step for river basins. SWIM uses a spatial disaggregation scheme on three levels. The river basin, as primary unit, is subdivided into sub-basins and these are further disaggregated into hydrotopes. A hydrotope is an elementary component with assumed homogenous soil, land use types and average water table depth. Water fluxes are calculated for each hydrotope and aggregated on the sub-basin scale. The surface runoff is computed on the basis of the SCS curve number method.

There are routines integrated for the calculation of snow accumulation and melt, evapotranspiration, percolation, subsurface runoff from the soil column and groundwater runoff. The total runoff is routed

from sub-basin to sub-basin using the Muskingum hydrological routing scheme.

SWIM has been successfully calibrated and applied for several large-scale catchments in Germany focusing on water balance and low-flow events (Hattermann *et al*., 2005; Huang *et al*., 2010, 2013a). Recently, the model has been used for understanding past flood trends (Hundecha and Merz, 2012) and for climate change impact assessment of flood flows in German basins (Huang *et al*., 2013b).

3.2.3 1D hydrodynamic river network model

The hydrological routing method integrated in SWIM routes the flow on a sub-basin scale and does not consider the explicit river channel geometry. However, for the prediction of flood defence overtopping and simulation of inundation processes, it is crucial to obtain water level information along the river network. Therefore, an additional hydrodynamic routing method was implemented to complement the SWIM routing at the areas of interest. Because of missing crosssection data and to minimise the model runtimes, the 1D hydrodynamic river network model simulates only flows exceeding bankfull discharge.

The developed channel routing model solves a 1D representation of the diffusive wave equations with an explicit finite difference solution scheme. The diffusive wave equations are obtained from the continuity (Eqn 1) and the momentum (Eqn 2) of the Saint Venant equations, by neglecting local and advective acceleration terms in the momentum equation:

$$\frac{\partial Q}{\partial x} + \frac{\partial A}{\partial t} = 0 \qquad (1)$$

$$\frac{\partial v}{\partial t} + v\,\frac{\partial v}{\partial x} = -g\frac{\partial h}{\partial x} + gS_f - gS_0 \qquad (2)$$

local and advective acceleration term | pressure term | friction term | bed slope term

where Q is discharge, A is the flow cross-section area, v is velocity, t is time, x is distance, h is water depth, g is gravity, S_f is the friction slope and S_0 is the bed slope.

The runoff information at each subbasin outlet provided by SWIM is used as a boundary condition for the channel routing model. The flow exceeding bankfull discharge is routed downstream subbasin-wise taking the new boundary condition from SWIM at each subbasin outlet into account, in case the bankfull flow threshold value is exceeded.

Whenever a dike crest height is exceeded, outflow into the hinterland is calculated with the broad-crested weir equation:

$$q = C_w H^{3/2} \qquad (3)$$

where, q is the flow per unit width, H is the water depth exceeding the dike crest height and C_w is the broad crest weir discharge coefficient, including the discharge coefficient $C_d = 0.577$:

$$C_w = C_d \frac{2}{3}\sqrt{2g} \qquad (4)$$

3.2.4 2D raster-based inertia model

For the simulation of inundation processes in the hinterland, a two-dimensional raster-based model with an inertia implementation following the approach of Bates et al. (2010) was implemented and tested at the Elbe reach (Falter et al. 2013). The hinterland inundation model solves the simplified Saint-Venant equations (Eq. 1 and 2) with neglected advective acceleration term. The floodplain is discretised into a computational grid of regular interconnected cells. The fluxes across cell boundaries in x and y directions are computed independently of each other. The specific flow per unit width q, is calculated equally for x and y direction from the momentum equation (Eq. 2). Neglecting the advective acceleration term and approximating the hydraulic radius with the flow depth between cells (h_{flow}), the explicit equation for q at time $t+\Delta t$ reads:

$$q_{t+\Delta t} = \frac{q_t - g h_{flow} \Delta t S_f}{(1 + g h_{flow} \Delta t + n^2 |q_t| / h_{flow}^{\frac{10}{3}})} \quad (5)$$

where n is the Manning's roughness coefficient and Δt is the time step.

The water depths in the computational cells are updated at each time step based on the continuity equation given by:

$$\frac{\partial h^{i,j}}{\partial t} = \frac{q_x^{i-1,j} - q_x^{i,j} + q_y^{i-1,j} - q_y^{i,j}}{\Delta x} \quad (6)$$

The numerical scheme is not unconditionally stable. According to the Courant-Friedrichs-Levy criterion, the time step should be constrained as follows:

$$\Delta t_{max} = \alpha \frac{\Delta x}{\sqrt{g h_{flow}}} \quad (7)$$

The α-value was introduced by Bates et al. (2010) as a stability coefficient to reduce the time step. A value ranging between 0.2 – 0.7 was indicated as sufficient for most floodplain situations.

The 2D raster-based model was implemented in the CUDA Fortran programming language to enable the application of the model on highly parallelized NVIDIA Graphical Processor Units (GPU). The model solver was partitioned into single operations on the entire raster which were implemented as kernels in the CUDA environment.

The overtopping flow over dike crest, computed from the 1D model is supplied as a point source to the calculation grid of the 2D model. Additionally, the 1D model passes water level information to the 2D model to provide a boundary condition for the water level in the hinterland. In that way, it is prevented that the water level in the hinterland exceeds the current channel water level.

3.2.5 Flood loss estimation model: FLEMOps+r

The Flood Loss Estimation MOdel for the private sector (FLEMOps+r, Elmer *et al*., 2010, 2012), developed at GFZ Potsdam (German Research Centre for Geosciences, Potsdam, Germany) uses a rule-based multifactorial approach to estimate direct economic damage to residential buildings.

The base model version FLEMOps has been derived on the basis of 1697 empirical damage cases that have been collected through computer-aided telephone interviews after the flood in 2002 in the Elbe and Danube catchments in Germany. FLEMOps calculates the damage ratio for residential buildings using five different classes of inundation depth, three individual building types, two classes of building quality, three classes of contamination and three classes of private precaution (Thieken *et al*., 2008). FLEMOps has been successfully validated on the micro-and meso-scale for the August 2002 flood in Saxony using official damage numbers reported by the Saxonian Relief Bank (Thieken *et al*., 2008). Elmer *et al*. (2010) identified the return period of the inundation at the affected residential building as an important damage factor and included it as an additional parameter in the refined model version FLEMOps+r. Within the RFM framework developed in this paper, FLEMOps+r is applied according to Elmer *et al*. (2012) without taking into account the influence of precautionary measures and contamination.

3.3 Application to the Elbe catchment

The RFM is applied to one of the largest river basins in Germany, the Elbe catchment. For this proof-of-concept application, a simulation period of 14 years was chosen, comprising the years 1990–2003.

3.3.1 Study area

The river Elbe is one of the largest rivers in central Europe with a total catchment area of 148 268 km^2. Around two thirds of the catchment area lies within Germany, where about 18.5 million inhabitants live (IKSE, 2012). The southern German and the Czech Republic parts of the river basin are dominated by mountains, whereas the northern part belongs to the German lowland area. Topographically, the Elbe can

be subdivided into three parts: the Upper Elbe, the Middle Elbe and the Lower Elbe. Large parts of the Upper Elbe lie within the Czech Republic and have a mountainous topography. Downstream of Dresden, the Upper Elbe ends at the entry to the northern lowland area of Germany. The following Middle Elbe part is dominated by low slope and extended floodplains. The final part, the Lower Elbe, forms the Elbe estuary. It starts downstream of the weir Geesthacht and is characterised by the tidal influence of the North Sea. In the German part of the Elbe catchment, 45% of the land is used for cultivating crops, 30% is covered by forest and 14% by grassland. Only 7% of the catchment is covered by settlements, industry and bare soil (IKSE, 2005a). The catchment is located in a temperate zone with transient zone from maritime to more continental climate. Typical for this region is the rain–snow (nival–pluvial) regime with floods occurring predominantly in winter and spring. In the years of 1890–2002, between 70% and 80% of the floods occurred during the hydrological winter at the Upper and Middle Elbe. Accordingly, only 20–30% of floods happened in the time period from May to October. March was the most flood-affected month of the year at 25% (IKSE, 2005b).

Winter floods are mainly caused by snowmelt in combination with rainfall in the Upper Elbe. Besides local flood events in the tributaries, driven by convective events, large-scale floods occurred during the summer months (IKSE, 2012). These floods are caused by long and extensive rain events. The last two disastrous flood events occurred in summer 2002 and 2013. The extensive rainfall that contributed to the flood generation was caused by a low pressure system called ‘Vb’ that is known to produce long-lasting and heavy precipitation over parts of eastern Germany. There occurred, to our knowledge, three flood events that caused inundation in the hinterland during the proposed simulation period of 1990–2003: a spring flood in 1994 and a winter flood in 2003, both mainly affecting the Saale, and in August 2002, a disastrous flood affected the Elbe and Danube catchments causing a damage of around €11.3 billion (IKSE, 2004).

The RFM is applied to the German part of the Elbe catchment. However, SWIM is set up for the entire river basin, including the Czech Republic part (Figure 3-2). This ensures the generation of reliable runoff boundary conditions for the hydrodynamic models. The river network for the 1D hydrodynamic simulations comprises the German part of the Upper Elbe and the Middle Elbe. The Lower Elbe (downstream weir Geesthacht) is excluded from the simulation. Because of the strong tidal influence in this part of the river, the sources of flooding differ from those inland. Additional to the Elbe main channel, relevant tributaries are included depending on the drainage area of a certain reach. On the basis of river network data provided by the Federal Environmental Agency (Umweltbundesamt) and the Joint Research Centre of the European Union (Vogt, 2007), river segments that have a drainage area of 600 km^2 or more were extracted. Upstream parts of the River Havel were excluded because of the extensive river management measures in this region that are not integrated in the hydrodynamic model. The final river network includes 2734 river-km, upon which 560 river-km account for the Elbe main channel and 2174 river-km belong to the following tributaries: Schwarze Elster, Mulde, Saale, Ohre, Havel, Stepenitz, Aland, Elde, Jeetzel and Sude. The 2D model domain for simulation of hinterland inundation envelopes the total selected river network (Figure 3-2). The covered catchment area is around 66 000 km^2 large.

3.3.2 Model set-up

3.3.2.1 Rainfall–runoff model: SWIM

As the hydrological model SWIM is a semi-distributed model, the entire Elbe catchment was subdivided into 2268 subcatchments. The climate input data were then interpolated at the centroid of each subcatchment from the surrounding observation stations. Runoff is computed at homogeneous response units within each subcatchment. The subcatchments were therefore further subdivided into different land-use classes and soil types. A hydrological response unit was defined within a subcatchment for each combination of land-use class and soil type.

The model requires input data of daily precipitation total, maximum and minimum air temperatures, solar radiation and relative humidity, all at the

subcatchment level. Precipitation and temperature, as well as relative humidity, together with sunshine and total cloud cover duration were provided by the German Weather Service (DWD) from all available stations within Germany and from the Czech Hydrometeorological Institute (CHMI) from stations within the Czech Republic. The station data were corrected for inconsistencies and inhomogeneities. Solar radiation was computed using a regression-based approach of sunshine and cloud cover durations,

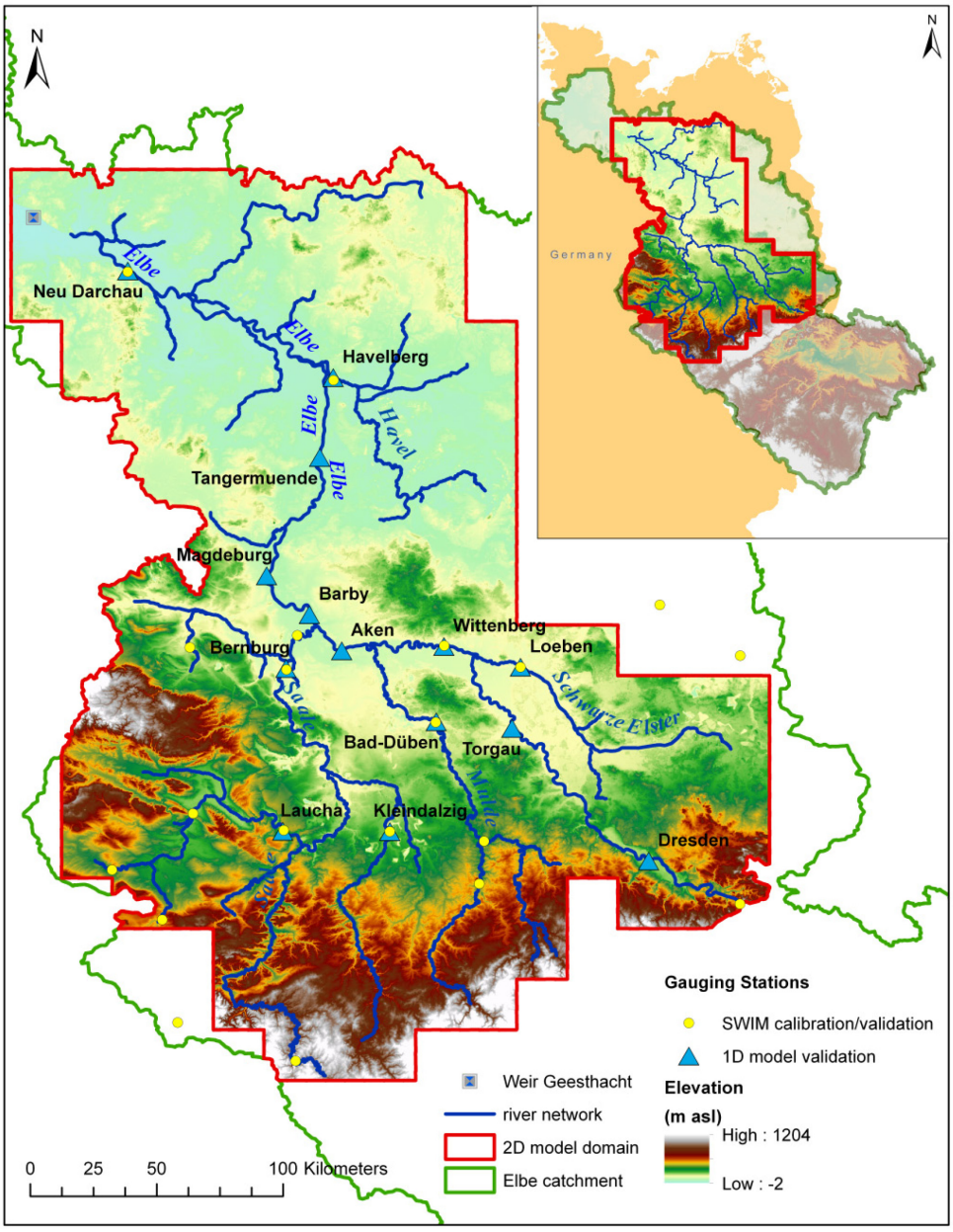

Figure 3-2: Study area and model domains: The hydrological model considers the entire Elbe catchment, including the Czech areas, up to the gauge Geesthacht; the 1D hydrodynamic model is applied to the blue river reaches and the 2D inundation model is confined to the areas inside the red edging. SWIM, soil and water integrated model.

as well as diurnal temperature range and total cloud cover using the method of Oesterle (2001).The station data were interpolated to the centroids of the subcatchments from the nearby stations using a kriging technique. Daily stream flow data were also obtained for a number of gauging stations from different water authorities in charge of the data. Because the data are part of the hydrometric observation network of the water authorities in Germany, the observations are regularly checked and can be assumed to be of good reliability. The observation period varies for the different stations.

In addition to the hydrometeorogical data, a number of digital data were acquired from different sources. A detailed soil map for entire Germany (BÜK 1000 N2.3) was obtained from Bundesanstalt für Geowissenschaften und Rohstoffe (BGR). A European Soil Database map for entire Europe was also obtained from the European Commission's Land Management and Natural Hazards unit. The CORINE (COoRdinated INformation on the Environment) land cover map and the Shuttle Radar Topography Mission digital elevation maps were also used in the study.

The model was run as a continuous daily water balance model using daily input data. Model calibration was performed from 1981 to 1989. A nested calibration technique was employed in which parameter estimation was carried out progressively from upstream to downstream subcatchments. An automatic calibration technique was used in this work by employing the SCE-UA algorithm (Duan *et al.*, 1992). A normalised weighted sum of the square of the differences between the observed and simulated discharges (NS) was employed as objective function. The weight at each time step was set to the observed discharge to give more emphasis to higher flows. The resulting objective function is similar to the well known Nash–Sutcliffe efficiency measure (Nash and Sutcliffe, 1970) except for the weights (Hundecha and Bárdossy, 2004):

$$NS = 1 - \frac{\sum_{i=1}^{N} w(\cdot)(Q_c(t_i) - Q_0(t_i))^2}{\sum_{i=1}^{N} w(\cdot)(Q_0(t_i) - \bar{Q}_0)^2} \quad (8)$$

where $Q_c(t_i)$ and $Q_0(t_i)$ are the simulated and observed discharges, respectively, at time t_i and Q_0 is the mean observed discharge over the simulation period (N days), $w(\cdot)$ is a weight, which is equal to the observed discharge $Q_0(t_i)$.

Seven parameters, which were found to be generally sensitive, were calibrated: two parameters of the Muskingum channel routing, two parameters of the degree-day snowmelt process, two parameters controlling the subsurface flow contribution to the stream flow and a parameter to fine-tune the saturated hydraulic conductivity of the soil layer that was read from the soil database.

3.3.2.2 1D hydrodynamic river network model

For the 1D hydrodynamic simulation of water levels along the generated river network, overbank cross-section profiles including dike information, Manning's roughness values and boundary conditions are required (Figure 3-1). The acquisition of overbank cross-section profiles including dike location and elevation along the river network is difficult. Neither a uniform dike database nor channel profiles throughout the Elbe catchment are available in a homogeneous form. This is especially true for the smaller Elbe tributaries. Contrary to large river basins elsewhere, the flood flows in German rivers are heavily controlled by flood defences.

To generate the river network description, we developed an automated procedure in the form of ArcMap Add-In tools, where we extract and merge all data sources available. The profiles are generalised to trapezoid-like shapes, consequently we only need channel location and width, ground elevation (bankfull depth), dike location, bottom height of the dike and dike crest height. Because the cross-section profiles were generated from the available digital elevation models (DEM) which do not include the full channel geometry, cross-sections were assumed to represent the section above the bankfull depth. In total more than 5000 profiles were derived at 500 m spacing for the simulation of the river network. We derived the bottom elevation (bankfull depth) of the channel from a DEM with resolution of 25 m (BKG, 2007). Channel width

information is extracted from the digital basic landscape model (Base DLM). Data related to dike information is attributed with a reliability level to enable the use of preferred data sources:

Reliability level 1: location and/or height of dikes provided by authorities

Reliability level 2: location of dikes extracted from Base DLM

Reliability level 3: location and height derived from DEM.

The most reliable dike data comes from German authorities (State Reservoir Administration of Saxony and Federal Institute of Hydrology). However, we could obtain only few such data. Therefore, we used the Base DLM as secondary data base for dike locations. Finally, we extracted dike locations and height from DEM 25 with a topographical search algorithm including a breaking-up condition, in case no topographical restrictions were found.

Additionally, the bankfull flow threshold values are needed, as only flow exceeding the bankfull flow is represented. We assume that bankfull flow is equivalent to a 2-year flood event (HQ2). The same or similar assumptions were made in previous works (e.g., Bradbrook *et al*., 2005; Rodda, 2005) and are based on the theories regarding the magnitude and frequency of channel forming flow (Dury, 1976). HQ2 is computed as the median annual maximum flow at each subcatchment outlet. Therefore, we fitted a Generalized Extreme Value distribution to the simulated annual maximum flows over the period of 1951–2003 and estimated the median value of the fitted distribution.

Moreover, because of the relatively coarse resolution of the DEM and the few available data with high reliability level, the quality of the automatic derived river profiles had deficits. Therefore, manual adjustments of channel width and dike height were necessary. Additionally, the bottom elevation profile had to be smoothed to avoid negative or strongly changing slopes to ensure model stability.

The cross-sections are connected to the corresponding SWIM sub-basins by location. This enables the assignment of runoff-boundary conditions provided by SWIM. According to the assumption that only the profile above bankfull flow is represented, the bankfull flow is subtracted from the runoff. The Manning's value was assumed to be $n = 0.03$ for the whole river network and dike overtopping length was assumed to be 20 m. Finally, the 1D river network model passes the computed overtopping flow and water levels with corresponding coordinates, in hourly resolution, as boundary condition to the 2D hinterland inundation model.

3.3.2.3 2D raster-based inertia model

The set-up of the 2D raster-based inertia model is less demanding, compared with the river network model. The data requirements for the hinterland inundation model comprise a computational grid in the form of a digital elevation model, a roughness grid and boundary conditions (Figure 3-1).

The computational grid is derived from a recently available DEM with 10-m horizontal resolution, provided by the Federal Agency for Cartography and Geodesy in Germany (BKG). The vertical accuracy is reported to be in the range of ± 0.5–2 m. The 2D hydrodynamic model was lately benchmarked against a 2D fully dynamic shallow water model, regarding sensitivity of model performance and run-times to grid resolution (Falter *et al*., 2013). The study concluded that the resolution of 100 m offers the best compromise between the model performance and computational time in the lowland parts of the Elbe catchment. Hence, the DEM 10 was resampled to a resolution of 100 m. The channel and river banks embedded between dikes (1D model domain) were excluded from the 2D modelling domain. In such a way, the computationally intensive 2D modelling is only carried out in the hinterland areas behind the dikes in case of their overtopping. Especially for continuous long-term simulation, this results in immense savings of CPU times.

The roughness grid was generated from CORINE land use maps by assigning roughness values from literature (Chow, 1959; Bollrich, 2000) to land-use classes (Table 3-1).

The boundary conditions are derived from the 1D hydrodynamic channel network model in form of dike

crest overtopping flow and corresponding channel water levels. Given the dike overtopping location, the overtopping flow is assigned to the corresponding cell of the 2D calculation grid. The α-value of 0.4 was found to deliver stable numerical solutions (see Eqn 7).

Table 3-1: Summary of CORINE (COoRdinated INformation on the Environment) land cover classes and the associated Manning's values

CORINE land cover class	Manning's *n*
Urban areas	0.11
Pastures and natural grassland	0.033
Sands, dunes, beaches	0.033
Sparsely vegetated areas	0.03
Green urban and recreation areas	0.06
Roads, ports and airports	0.013
Forests	0.11
Fruit trees and berry plantations	0.11
Vineyards	0.06
Water bodies	0.03
Moors, marshes, peat bogs and transitional woodland shrub	0.05
Agricultural areas	0.035

3.3.2.4 Flood loss estimation model: FLEMOps+r

The application of the FLEMOps+r model to the Elbe catchment for estimating flood damage to residential buildings required spatially detailed information about asset values, building qualities and building types to quantify exposure. Further, inundation depths and return periods of peak flows have been used to differentiate susceptibility and to evaluate the flood impact. All data were prepared at the consistent spatial resolution used for flood inundation modelling of 100 m.

Asset values of the regional stock of residential buildings were defined on the basis of standard construction costs (BMVBS, 2005), i.e. quantifying the market price of the construction works for restoring a damaged building (Kleist *et al*., 2006). These values were spatially distributed to the CORINE land cover classes, 111 (continuous urban fabric) and 112 (discontinuous urban fabric), which describe residential areas (EEA, 2005) using a binary disaggregation scheme (Wünsch *et al*., 2009).

The characteristics of the municipal building stock were derived from the INFAS Geodaten dataset (Infas Geodaten GmbH, 2009). The composition of building types in each municipality is described using a cluster centre approach. In total, five clusters were defined differentiating the share of single-family houses, semi-detached/detached and multifamily houses (Thieken *et al*., 2008). Further, average building quality is aggregated to two classes: high-quality and medium/low-quality (Thieken *et al*., 2008).

The spatial distribution of inundation depths is provided by the 2D raster-based inertia model. Maximum inundation depths (h) for different flood events are classified according to the classes defined in the FLEMOps+r model (0 m < $h \leq$ 0.2m; 0.2m < $h \leq$ 0.6m; 0.6m < $h \leq$ 1.0 m; 1.0 m < $h \leq$ 1.5m; 1.5m < h). Return periods of flood discharge peaks were estimated within each SWIM sub-basin on the basis of an extreme value statistics derived from an annual maximum discharge series generated through a long-term (53 years) continuous SWIM simulation of the Elbe catchment.

The simulation period of 14 years which was analyzed in this paper required the alignment of the exposure data to account for changes in land use, asset values and building characteristics with the aim to approximate the given situation at the time of a flood event. For this purpose, we followed the approach proposed by Elmer *et al*. (2012) to adjust disaggregated asset values and stock of building types to the specific points of time of the flood events considered. In detail, the building values in terms of reconstruction costs for the reference year 2000 were time-adjusted using official indexed construction prices (Baupreisindex, DESTATIS, 2013).

Changes in the composition of the municipal building stock in terms of building types were derived in terms of a trend in official statistics about increase and decrease of residential buildings for each building type at the district level in the period from 1995 to 2004 (DESTATIS, 2010). Accordingly, changes in the building type composition within each municipality were determined by extending this trend back-ward to 1990. The assignment of the resulting building stock to the five cluster centres was revised and adjusted.

Concerning building quality, the vast majority of municipalities in Germany are classified from medium to low average building quality. Therefore, we assumed that the class affiliation of the municipalities remained unchanged for all points in time.

The estimation of flood losses comprised the determination of the damage ratio to residential buildings given the inundation depths and return periods as well as the information about building quality and building type clusters in each location affected by flooding. Flood losses were calculated as the product of relative building damage and location-dependent asset values.

3.4 Results and discussion

3.4.1 Rainfall–runoff model results

The rainfall–runoff model SWIM was calibrated and validated at 20 gauging stations distributed throughout the catchment (Figure 3-2). The calibration was performed over the period 1981–1989, validation results relate to the RFM simulation period of 1990–2003. Along the Elbe main channel, Mulde and Schwarze Elster, the achieved NS efficiencies (see Eqn 8) with values above 0.76 for the calibration and the validation period indicate a reasonable reproduction of discharges. Discharge simulations along the Saale and Havel/Spree catchment are less reliable. Whereas in the downstream part of the Saale catchment discharges are reasonably represented with NS above 0.7, at upstream parts of the Saale and its tributaries partly only rather poor NS values down to 0.342 (NS calibration: 0.247) could be achieved. Havel and Spree are dominated by extensive river management measures not represented in the hydrologic model setup which resulted in low NS efficiencies, between−0.093 and 0.637 (NS calibration: between −0.239 and 0.456).

Additional information, i.e. conventional NS and peak error, is given for selected gauging stations in Table 3-2. The peak error is the ratio (%) of the sum of peak flow errors that exceed the bankfull flow threshold value and the sum of corresponding observed peak flows. For the purpose of flood inundation calculations, reliable peak flow simulations are important. Peak flows were over-and underestimated, likewise, throughout the catchment and are in the range of ± 5% along Elbe, Mulde and Schwarze Elster. Particular at the Saale, peak flow errors are high with values exceeding 40%. SWIM does not provide a reliable basis for the subsequent water level calculations in this part of the catchment.

3.4.2 1D hydrodynamic model results

The performance of the 1D hydrodynamic model at 14 gauging stations along the Elbe main channel and its tributaries is summarised in Table 3-2. Performance measures are given for discharge calculation from SWIM and 1D river network model, as well as for peak water level calculation. As SWIM was validated and calibrated only at two of the listed Elbe gauging stations, values of the SWIM validation are not given for six stations in this table.

The 1D river network model basically reproduces the SWIM discharge simulation; NS and peak errors are in the same range. For the validation of the water level, root mean square error (RMSE) and mean bias of the peak flows are given in absolute values. Both measures include only peak flows that were actually modelled and disregard those flood peaks that were completely missed in the model results. In the last column of Table 3-2, the number of peak flows above bankfull depth and the number of peaks matching with water level simulations (matched peaks) are given. At almost all gauging stations, the number of observed flood peaks exceeding the bankfull depth threshold is much higher than actually simulated flood peaks.To understand this difference, Figures 3-3 and 3-4 show simulated and observed discharges and water levels at four sample gauging stations along the Elbe main channel, includeing the corresponding threshold values for bankfull depth and flow as horizontal lines. Keeping in mind that the 1D hydrodynamic river network model simulates only water levels for peak flows exceeding bankfull flow, it can be seen that relatively often peak flows were not included in water level simulations (Figure 3-4), as they did not exceed the bankfull discharge threshold value (Figure 3-3). One reason is the underestimation of discharge by the hydrological model and, as consequence, the disregard of

Table 3-2: Summary of model validation of SWIM and 1D river network model at selected gauging stations.

		SWIM			1D river network model					
					discharge			peak water level		
River	Gauge	NS	conventional NS	Peak Error (%)	NS	conventional NS	Peak Error (%)	RMSE (m)	mean Bias (m)	Peaks > bankfull depth (matched peaks)
Elbe	Dresden	-	-	-	0.849	0.653	8.35	1.13	1.08	12 (9)
	Torgau	-	-	-	0.888	0.708	-3.10	0.81	0.57	14 (10)
	Wittenberg	0.838	0.642	-5.81	0.822	0.638	-0.72	0.63	0.15	57 (10)
	Aken	-	-	-	0.808	0.667	2.29	1.24	-1.24	50 (10)
	Barby	-	-	-	0.849	0.750	-2.53	0.92	-0.67	63 (11)
	Magdeburg	-	-	-	0.816	0.727	8.37	0.43	-0.40	39 (12)
	Tangermünde	-	-	-	0.884	0.773	-5.14	0.41	-0.39	42 (10)
	Neu Darchau	0.846	0.779	4.90	0.852	0.782	3.53	1.25	-1.08	70 (14)
Schwarze Elster	Loeben	0.822	0.628	5.00	0.799	0.587	6.50	0.21	0.13	12(6)
Mulde	Bad-Düben	0.842	0.801	-4.47	0.830	0.792	-2.74	1.91	-1.91	38(8)
Saale	Laucha	0.639	0.581	-42.89	0.527	0.540	-47.93	0.81	-0.81	62(14)
	Kleindalzig	0.733	0.585	21.12	0.660	0.486	28.81	0.33	-0.16	35(8)
	Bernburg	0.736	0.658	14.96	0.551	0.516	30.94	0.42	-0.40	20(7)
Havel	Havelberg	0.637	0.561	7.45	0.636	0.560	8.62	0.83	-0.61	86(8)

flood peaks. Another reason is the mismatch of threshold values. The threshold value for bankfull flow does not always match with the corresponding bankfull depth. The bankfull depth elevation is basically taken from the DEM 25, which do not seem appropriate in all cases. For the majority of the given gauging stations, the bankfull depth is underestimated, leading to an underestimation of water levels. However, the problem of mismatching threshold values is very variable and site-specific and no general conclusion can be drawn. In other parts of the catchment, we observe overestimation of bankfull depth by taking the level from DEM 25.

The general picture of the discharge validation is not repeated in the water level validation. The errors made in discharge simulation are overlaid with errors in water level simulation. Along the Elbe main channel, the RMSE of water level peaks ranges between 0.4 and 1.25 m. Gauge Bad Düben (Mulde), which showed reasonable performance during the discharge simulation, has errors of almost 2 m. The average bias of peak flows shows an overestimation up to Wittenberg, then peak flows are underestimated. At tributaries, only for Loeben (Schwarze Elster) a slight overestimation can be seen. SWIM gave reasonable results for discharge simulations, except for Saale and Havel catchments. Over- and underestimations of water levels in other parts of the catchment can mainly be attributed to uncertainties from cross-section and bankfull depth threshold values.

3.4.3 2D raster-based inertia model results

During the period 1990–2003, the 1D hydrodynamic river network model simulated five events that lead to dike overtopping and inundation of the hinterland: April 1994, August 2002, November 2002, December 2002 and January 2003. A group of locally distinct and short-termed flood events, simulated by the 1D hydrodynamic model, were disregarded as they had no relevance for flood inundation simulation and damage

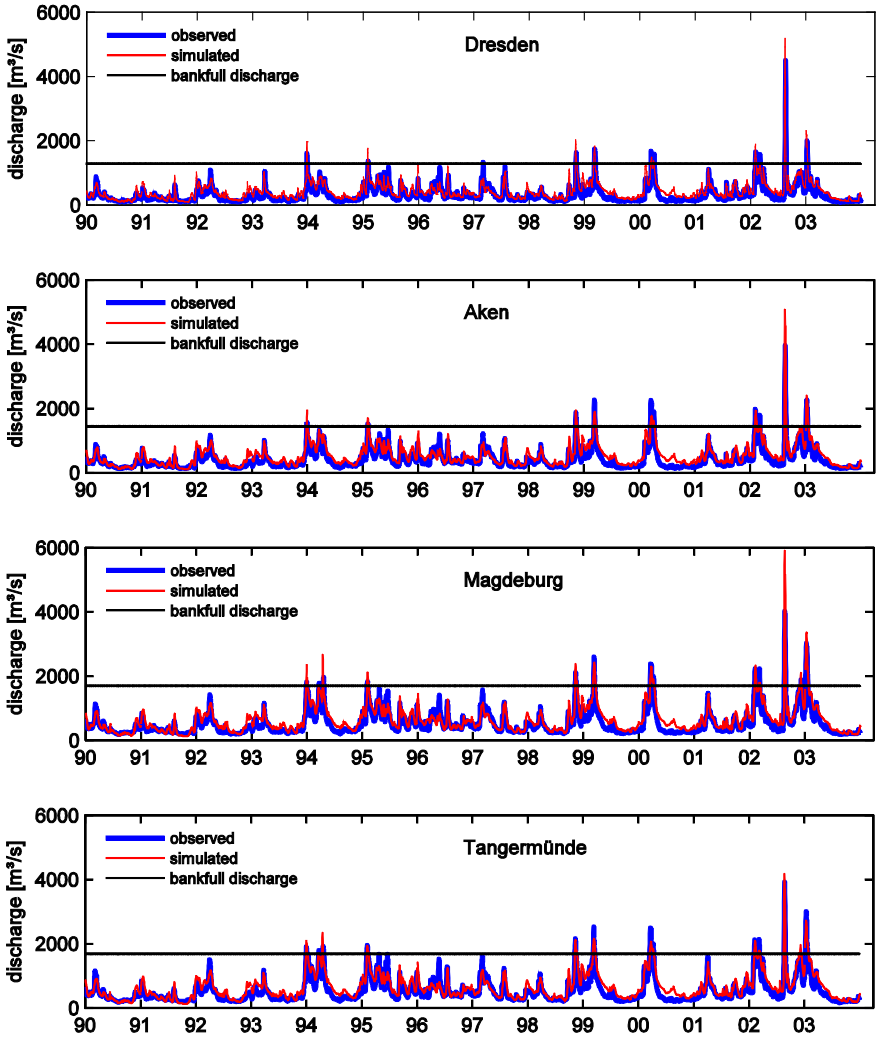

Figure 3-3: Observed (blue) and simulated discharge (red) at four gauging stations along the Elbe for the simulation period of 1990–2003. Additionally, threshold values for bankfull flows are given as horizontal lines.

assessment. The simulated flood events in April 1994, January 2003, November and December 2002 mainly caused hinterland inundation along the Saale, whereas the simulated flood event in August 2002 affected the Elbe main reach and the Mulde.

It is known that the flood events in April 1994, August 2002 and January 2003 led to hinterland inundation; however, only for the flood in August 2002 inundation extents are documented. The simulation of two small flood events in November and December 2002 at the Saale is a consequence of an overestimation of peak flows by the hydrological model SWIM. The observed runoff time series show only moderate water level raises in this period that in all likelihood have not led to hinterland inundation. This stresses once again how difficult flood hazard and risk assessments are in heavily urbanised catchments with river courses protected by flood defences. In this case, threshold processes of dike overtopping and/or breaching decisively control inundation patterns and resulting damages. These threshold processes appear to be sensitive to in-channel water elevation in the centimetre range.

To the authors' knowledge, no other flood event occurred throughout the Elbe catchment in the period

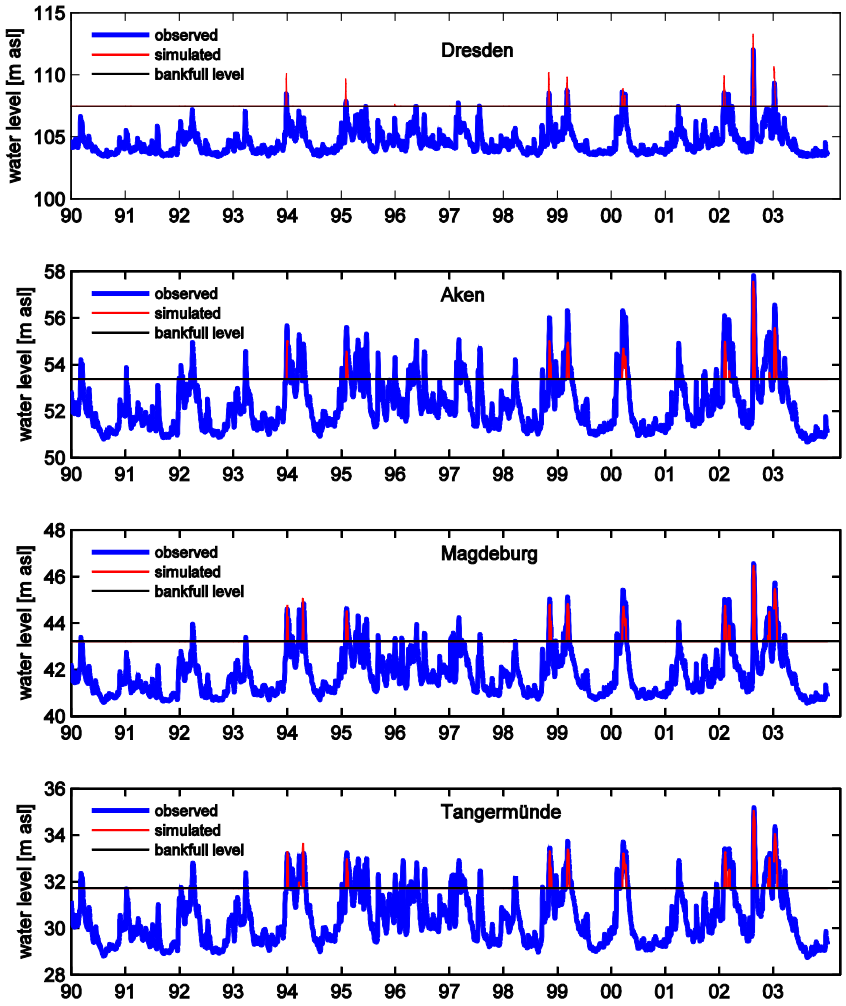

Figure 3-4: Observed (blue) and simulated water levels (red) at four gauging stations along the Elbe for the simulation period of 1990–2003. Additionally, threshold values for bankfull depth are given as horizontal lines.

1990–2003 that led to hinterland inundation and damage. Accordingly, we can conclude that the hydrodynamic models were able to capture all floods that were associated with hinterland inundation. However, because of discharge overestimation, two additional hinterland inundation events were simulated.

3.4.3.1 Inundation extent

The validation of the hinterland inundation is more difficult than validation of discharge and water level in the main channel. There is only very few remote sensing data on inundation extent available and no information on inundation depths. Only for the disastrous flood in August 2002, there is a flood mask available provided by the National Aeronautics and Space Research Centre of the Federal Republic of Germany (DLR). However, comparison of observed and modelled inundation extent has to be handled with care. It is not possible to actually remodel an observed flood scenario at this scale, especially if dike breaches occurred. To correctly simulate inundation extent and maximum water depth as consequence of dike breaches, the location, timing and characteristics of breaches

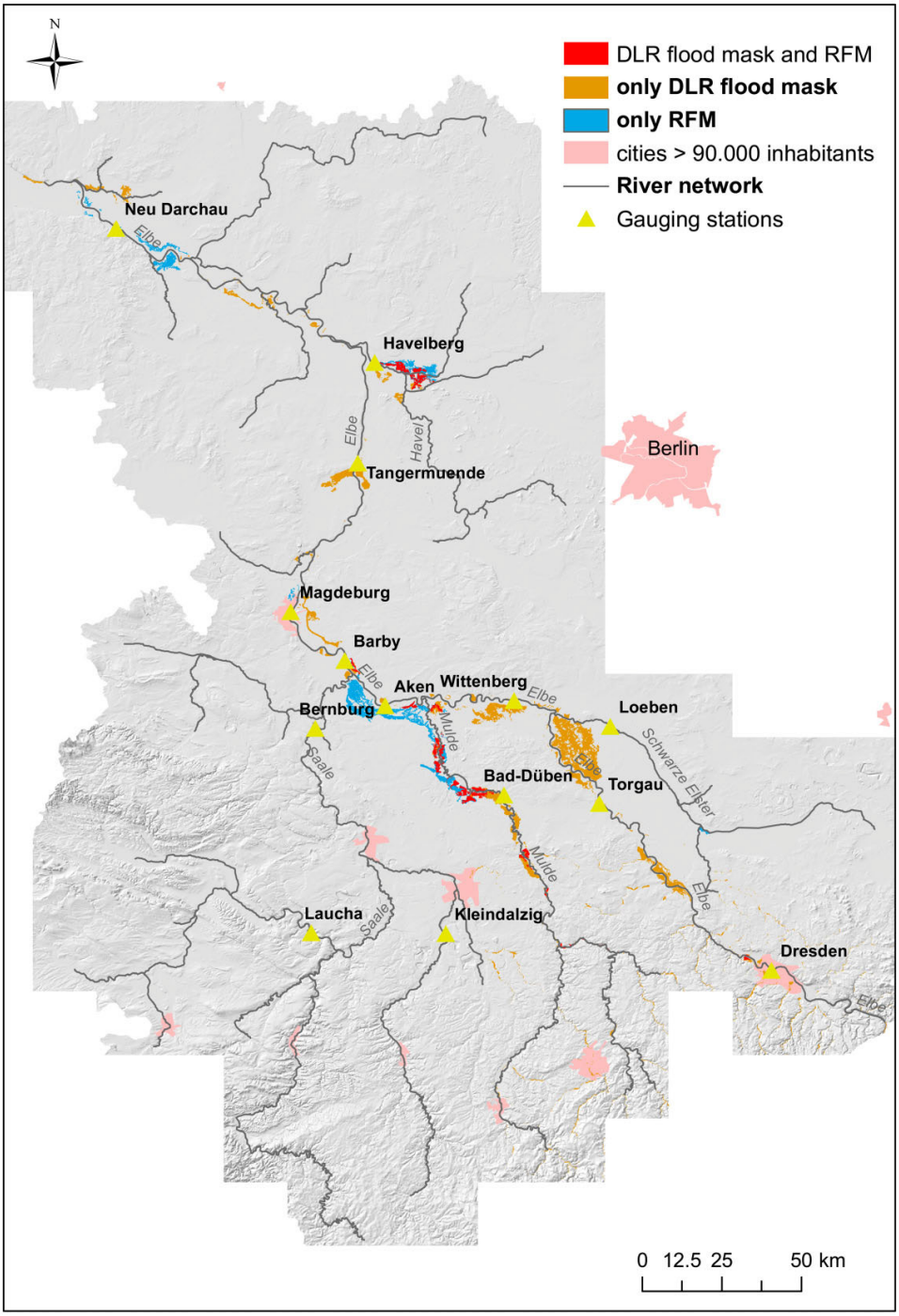

Figure 3-5: Comparison of inundation extents of the August 2002 flood. DLR, National Aeronautics and Space Research Centre of the Federal Republic of Germany; RFM, Regional Flood Model.

have to be known. This information could be provided ex-post, but cannot be estimated ex-ante, unless the investigated river and dike reach is very well known. Hence, flood risk assessments for diked river reaches frequently use probabilistic approaches which provide a probability estimate of dike breaching given certain

flooding conditions (Vorogushyn *et al.*, 2009, 2010). Therefore, we abstain from computing the performance measures for the flood inundation simulation (e.g. flood area index). Nevertheless, a comparison of observed and simulated flood inundation areas for the flood in August 2002 is given in Figure 3-5 for a qualitative, visual evaluation. Generally, an underestimation of the flood extent can be seen, in particular, along the Elbe main channel (downstream Dresden until the confluence with the Mulde). This underestimation can be attributed to the effect that only dike overtopping but not dike breaching were included in the simulation.

3.4.3.2 Computation time

The 2D raster-based inertia model was implemented in the CUDA Fortran programming language to enable the application of the model on highly parallelised NVIDIA GPUs. The 2D hydrodynamic simulation of all five flood events took around 19 h for an overall simulation period of almost three months' run on a NVIDIA Tesla C1060 GPU card containing 240 processor cores. For the period of 14 years the 1D hydraulic simulations, run at an Intel Xenon 2.27 GHz processor (Intel, Santa Clara, CA, USA), took around 1 h. In total, the 1D/2D hydrodynamic simulation took around 20 h for 14 years, which can be regarded as applicable for large-scale and long-term simulations. The calibrated hydrological model SWIM runs relatively faster. Using an MPI implementation on four processors of a high performance cluster, it took 17 min to simulate 53 years of daily runoff for the entire Elbe basin.

3.4.4 Flood loss estimation model results

The highest direct damage to residential buildings is estimated for the August 2002 flood amounting to €237 million in the German part of the Elbe basin. The flood of April 1994, which affected mainly the Saale river, yields residential building damage of €42 million. For the 2003 flood and for the events in November and December of 2002, estimated damage add up to €8.8 million, €3.9 million and €1.9 million, respectively.

For the evaluation of model results, damage estimates were only available for the April 1994 flood and the major flood in August 2002 from the international disaster database EM-DAT (http://www.emdat.be) and (Munich Re, 1999) for the whole of Germany. These data sources provide estimates of total flood damage per event. Detailed data that discerns damage to different economic sectors, types of damage and regions is rather an exception but is available for the very well-documented extreme flood in August 2002. For instance, the Saxonian Relief Bank (SAB, personal communication, 2004) and Saxony-Anhalt (personal communication, 19 September 2002) provided information about damage to residential buildings on the municipality level. The Staatskanzlei Freistaat Sachsen (2003) reported that a proportion of approximately 30% of total damage in Saxony was due to losses to residential buildings during the August 2002 flood. Even though a transfer of this proportion to other flood events seems problematic, because this share is expected to vary from region to region and from event to event, it offers a rough estimate of this damage share. Accordingly, we apply this proportion available from flood damage data in Saxony in August 2002 (Staatskanzlei Freistaat Sachsen, 2003) to the other damage estimates from Em-DAT (http:// www.emdat.be/), Munich Re (1999) and IKSE 2004 (Table 3-3).

Table 3-3 summarises the flood loss model results and the comparison with damage data from different sources along with an estimate of damage to residential buildings. For the April 1994 flood, the loss estimate obtained from RFM is comparable with the damage estimates provided by EM-DAT (http://www.emdat.be) and Munich Re (1999). Since the April 1994 flood affected mainly the Saale catchment, large differences between the estimates for the whole of Germany and for the Elbe catchment are not expected. In contrast, the loss estimated by RFM in the German part of the Elbe catchment for the August 2002 flood is significantly lower than flood damage indicated by other sources (http:// www.emdat.be, Munich Re, 1999, IKSE, 2004). This is not surprising given the significant differences between the inundated areas obtained from the RFM model chain and

Table 3-3: Comparison of flood loss model results with other damage estimates in € millions for April 1994 and August 2002 floods.

Event	Area	FLEMOps+r	other damage estimates		
		Res. building damage (€ millions)	total damage (€ millions)	Res. building damage (€ millions)	Source
Apr. 94	Germany	-	161	48*	EM-DAT 2012
		-	153	46*	Munich Re
	Elbe catchment in Germany	42	-	-	
Aug. 2002	Germany	-	8,923	2,677*	EM-DAT 2012
		-	11,800	3,540*	Munich Re
	Elbe catchment in Germany	237	8,900	2,670*	IKSE 2004
	Saxony	-	6,196	1,706	Staatskanzlei Freistaat Sachsen 2003

* estimated as a share of 30% from total damage based on Staatskanzlei Freistaat Sachsen 2003

documented by remote sensing data (Figure 3-5), e.g. at the confluences of the Schwarze Elster, Mulde and Saale rivers. Further, the city of Dresden has been a focal area of flood damage during the August 2002 flood. However, this area is only marginally inundated in the model simulation. In addition, smaller rivers, e.g. Weisseritz which have caused considerable damage in the 2002 flood, are not included in the RFM river network.

3.4.5 Limitations

From the results shown in the previous paragraphs it becomes apparent that with each model step, uncertainties are introduced. Although SWIM was calibrated carefully, it still shows deficits in discharge simulations, e.g. at upstream parts of the Saale. Subsequent calculation of water levels with the 1D river network model depend on highly simplified overbank cross-sections and definition of bankfull flow threshold values that are not always appropriate. This leads to partly large errors of water level simulations (e.g. gauge Bad-Düben with RMSE of 1.91 m). Hinterland inundation extent and depth depend on previously simulated water levels and uncertain dike heights, as well as on the resolution and quality of topographical data. Finally, the flood loss estimation is highly sensitive to the actually flooded area and its assets, e.g. urban areas or grasslands. Results indicate that more investigation should be invested, especially in the 1D hydraulic model set-up. Better representation of overbank cross-sections and bankfull depth by using high-resolution DEMs and additional data from authorities have high potential to reduce the current uncertainties in 1D hydrodynamic simulations. However, RFM was designed to provide a large-scale picture of flood risk assessments at a regional scale. Correct simulation of small scale or detailed inundation patterns is not the scope of the framework presented.

Another limitation is caused by not considering dike breaches in the modelling framework. This resulted in an underestimation of inundation extent of the August 2002 flood event. Simulation of dike breaches requires knowledge on the location, timing and characteristics of breaches. However, the investigated river and dike reach needs to be known very well to estimate these variables. An alternative approach would be to provide a probability estimate of dike breaching given

certain flooding conditions. This probabilistic approach would, however, necessitate a large number of flood event simulations to represent probabilities adequately.

Additionally, the 1D hydrodynamic river network model is directly connected to SWIM sub-basins, performing the routing only sub-basin-wise. The influence of dike overtopping and subsequent attenuation of the flood wave is limited to the current sub-basin and currently cannot be given further downstream. However, this approach has the advantage that errors in channel water level calculations do not accumulate over the entire river network. Additionally, possible mass balance inconsistencies in the 1D river network model, introduced by the one-way coupling of 1D and 2D hydrodynamic simulation models, do not add up.

Of course, flood damage modelling is also associated with uncertainties. Novel multifactorial flood loss estimation models like FLEMOps+r significantly improve damage estimates in comparison with traditional stage-damage functions; however, errors in exposure and susceptibility estimation are still high (e.g. Wünsch *et al*., 2009; Elmer *et al*., 2010; Seifert *et al*., 2010). For instance, the mean relative error of the damage estimates for five municipalities affected by the 2002 flood event amounted to 24% for FLEMOps (Thieken *et al*., 2008).

3.5 Conclusions

This paper presented the RFM, a process-based model cascade, developed for large-scale flood risk assessments. The objective of this study was to prove that the concept of flood risk assessments, based on the model chain 'meteorological input – hydrological model – hydrodynamic river network model – hydrodynamic hinterland inundation model – damage estimation model', is feasible at the scale of large catchments within a continuous simulation framework. RFM was applied to a large river basin in Germany, the Elbe catchment, comprising an area of about 66 000 km^2 and a river network of 2700 km. RFM was continuously run for the period of 1990–2003.

The continuous and coupled simulation of rainfall–runoff processes, 1D hydrodynamic river network simulation including representation of the dike system, 2D hydrodynamic simulation of hinterland inundation and flood loss estimation at relatively high spatial resolution at the large-catchment scale is unique. In contrast to large-scale applications that use a reach-wise approach, assuming a spatially uniform return period for the entire river network, the holistic approach used in RFM can potentially provide a realistic large-scale picture of flood risk. Because of the continuous simulation approach, also no limitation on event sets is necessary as it is proposed by other studies. Additionally, the creation of hydrographs that might be unrealistic in their shapes is not needed. The relatively high resolution of 100 m has the potential to provide adequate inundation depths and extents for detailed flood loss estimations. Because each module of the model chain introduces uncertainties, simulation results were validated against observed data where possible. Discharge was found to be generally simulated adequately with SWIM in comparison with observed data, although simulations are not reliable for tributaries under heavy human intervention. The quality of water level simulation varies and depends on the representation of overbank cross-sections and on the definition of bankfull flow thresholds. Better data on cross-sections and better definition of threshold values have high potential to improve current simulation results. Hinterland inundation extents are difficult to validate. To our knowledge, there occurred three floods during the simulated period causing hinterland inundation and flood loss: April 1994, August 2002 and January 2003. However, only for the disastrous flood event in August 2002, inundation extents are documented. It was not expected that the simulated and observed flood extents match, as the inundation areas of 2002 depended strongly on the location, timing and characteristics of the numerous cases of dike overtopping and dike breaching. A qualitative comparison indicated an underestimation of inundation extents. This can be attributed to missing dike breach representation within the RFM framework. Flood loss estimates were available only for two out of three documented flood events. Whereas calculated flood loss estimates of the flood in April 1994 are at the same order of magnitude as the available estimates,

the damage of August 2002 is underestimated in accordance to the underestimation of inundation extent.

The runtime of the 2D hydrodynamic hinterland inundation model was optimised by implementation for highly parallelised GPUs. For a simulation period of 14 years, the 1D and 2D hydrodynamic models needed around 20-h run-time. This enables the application of 1D and 2D hydrodynamic models, in terms of runtime, for long-term simulations of several decades and longer. Errors are significant in the current application of RFM. This is, besides the neglect of dike breach processes, mainly a consequence of low data quality. Better information on dike location and height and overbank cross-sections will significantly improve the hydrodynamic simulation results and the damage estimation. We conclude that the concept of RFM should be applicable for large-scale flood risk assessment. Results and run-time are adequate for the purpose of continuous simulation at the large-catchment scale, driven by long-term observed or generated climate data or climate change scenarios. RFM, first applied to the Elbe catchment, can be transferred to other large basins in Germany and elsewhere, and has the potential to provide flood risk statements for national planning, re-insurance aspects or other questions where spatially consistent, large-scale assessments are required.

Acknowledgements. The work reported in this paper is part of the project ‘Regional Flood Model for Germany’. We thank the Federal Agency for Cartography and Geodesy in Germany (BKG) for provision of the digital elevation model of Germany (DGMD), the German weather Service (DWD) for providing meteorological data and the authorities that provided gauging station data. Furthermore, we thank the State Reservoir Administration of Saxony (LTV) and the Federal Institute of Hydrology (BfG) for data related to the dike system.

4 Spatially coherent flood risk assessment based on long-term continuous simulation with a coupled model chain

Spatially coherent flood risk assessment based on long-term cotinuous simulation with a coupled model chain

Abstract

A novel approach for assessing flood risk in river catchments in a spatially consistent way is presented. The approach is based on a set of coupled models representing the complete flood risk chain, including a multisite, multivariate weather generator, a hydrological model, a coupled 1D–2D hydrodynamic model and a flood loss model. The approach is exemplarily developed for the meso-scale Mulde catchment in Germany. 10,000 years of meteorological fields at daily resolution are generated and used as input to the subsequent models, yielding 10,000 years of spatially consistent river discharge series, inundation patterns and damage values. This allows estimating flood risk directly from the simulated damage. The benefits of the presented approach are: (1) in contrast to traditional flood risk assessments, where homogenous return periods are assumed for the entire catchment, the approach delivers spatially heterogeneous patterns of precipitation, discharge, inundation and damage patterns which respect the spatial correlations of the different processes and their spatial interactions. (2) Catchment and floodplain processes are represented in a holistic way, since the complete chain of flood processes is represented by the coupled models. For instance, the effects of spatially varying antecedent catchment conditions on flood hydrographs are implicitly taken into account. (3) Flood risk is directly derived from damage yielding a more realistic representation of flood risk. Traditionally, the probability of discharge is used as proxy for the probability of damage. However, non-linearities and threshold behaviour along the flood risk chain contribute to substantial variability between damage probabilities and corresponding discharge probabilities.

Published as:

Falter, D., Schröter, K., Nguyen, D., Vorogushyn, S., Kreibich, H., Hundecha, Y., Apel, H., Merz, B. (2015): Spatially coherent flood risk assessment based on long-term continuous simulation with a coupled model chain. - Journal of Hydrology, 524, p. 182-193. doi.org/10.1016/j.jhydrol.2015.02.021

4.1 Introduction

River flooding is increasingly seen from the risk perspective which considers not only the flood hazard, e.g. discharge and inundation extent, but also the vulnerability and adaptive capacity of the flood-prone regions (Merz et al., 2010). This shift in perspective is visible, for instance, by the development of flood risk maps demanded by the European Flood Directive on the Assessment and Management of Flood Risks (European Commission, 2007). These maps are now widely available throughout Europe and are important for risk communication and integrated flood risk management. Alfieri et al. (2014) argued, however, that these maps are generated with inconsistent methods on different spatial scales, using different data bases, and are therefore not comparable on the European scale. Even within European member states, methods might not be consistent, as it is the case for Germany where different federal states adopted different approaches for deriving and presenting flood maps (see e.g. BfG (2014) for an overview). To enable comparisons, Alfieri et al. (2014) proposed the development of a pan-European flood hazard map with a spatial consistent methodology based on the assessment of uniform 100-year flood flows for all river stretches and piece-wise hydraulic modelling of corresponding flood areas.

This proposal alleviates the problem of method and data inconsistency, but it does not overcome the problem of assuming spatially uniform return periods for flood scenarios. This traditional approach in flood risk assessment derives scenarios with a constant T-year return period (e.g. T = 100) for flood peaks within the entire catchment. The assumption of spatially uniform return periods is valuable for local hazard and risk assessments, however, it is of limited use for large-scale assessments, for example, for national risk policy developments, for large-scale disaster management planning, and in the (re-)insurance industry. The assumption of a T-year flood peak for the entire river network gives an unrealistic large-scale picture. It is not realistic that a single flood reaches a 100-year return period in the entire large-scale river network. Flood risk would be overestimated, as the probability of a single flood reaching a 100-year return period throughout the catchment is much smaller than the probability of a 100-year flood at a single site. The overestimation of flood risk, derived with the traditional approach, was recently shown by Thieken et al. (in press) for the river Rhine in Germany.

There are different possibilities for generating flood events that respect the spatial variability of occurrence probability at the catchment scale. One approach that has recently gained attention is the application of multivariate distribution functions to represent the joint probability of flood peaks at multiple sites (e.g. Lamb et al., 2010, Ghizzoni et al., 2012 and Keef et al., 2013). A multivariate distribution function, considering the spatial dependence between gauging stations, is fitted to observed flood peaks at multiple gauges and can be used to generate spatial fields of flood peaks. A disadvantage of this method is that only flood peaks are provided. It is not obvious how such an event set could be used as input into unsteady inundation models, because hydraulic models require the entire hydrographs conserving flood volume in order to simulate the temporal evolution of flood waves within the river system. This problem can be bypassed when the event generation starts with the precipitation event. Rodda (2001) developed a stochastic model generating rainfall events for the UK. These events were used as input into a hydrological model to simulate the spatial distribution of the T-year discharge. A disadvantage of the event based simulation approach is the assumption that the return period of flood discharge equals the return period of rainfall. This is usually not given, since storm characteristics, such as the rainfall time pattern, or the initial catchment state influence the relationship between rainfall probability and flood probability (Haberlandt and Radtke, 2014).

This simplifying assumption can be avoided by continuous hydrological simulation (e.g. Boughton and Droop, 2003 and Viviroli et al., 2009; Grimaldi et al., 2013 and Haberlandt and Radtke, 2014). This increasingly popular concept consists of generating long synthetic meteorological time series and using them as input into a continuous hydrological model. Flood probabilities can then be derived from the simulated synthetic discharge time series. This ‘derived flood

frequency approach based on continuous simulation' has the advantage that the complete flood event, including antecedent processes, are modelled throughout the entire catchment in a consistent way. The importance of initial catchment conditions for the flood development was recently investigated by Nied et al. (2013) and also could be observed from the disastrous flood event in 2013 in Central Europe, where the interplay of event precipitation and very wet initial catchments played a dominant role for the exceptional event severity (Schröter et al., 2015). Grimaldi et al. (2013) demonstrated the effect of a continuous hydrologic-hydraulic simulation on floodplain inundation patterns compared to an event-based approach for a small-scale basin.

In this paper we extend the 'derived flood frequency approach based on continuous simulation' and propose a novel concept for assessing flood risks: the 'derived flood risk approach based on continuous simulation' Thereby we use the synthetic discharge time series as input into flood impact models and derive flood risk directly from the resulting synthetic damage time series. In this way, the processes, and their space–time interactions, underlying the flood risk in a catchment are represented in a consistent way. For instance, the hydrodynamic simulation of floodplain processes, such as storage effects or channel-floodplain interactions, allows considering the effects of floodplain processes on flood damage patterns.

A further advantage is that flood risk can be directly derived from the synthetic damage time series. The return period of damages is thus based on the empirical distribution constructed from long-term simulation. Ideally, risk is estimated as (probability × damage), whereas probability is the probability of damage. Thieken et al. (in press) used this approach by generating a stochastic flood event set from discharge station data, combining it with a flood impact model and fitting an extreme value distribution directly to the synthetic damage data. This attempt to derive flood risk directly from the probability of damage is a rare exception in the flood risk literature. The usual way is to use the probability of discharge or the probability of precipitation as proxy for the probability of damage. However, the probability for the different phenomena (precipitation–discharge–inundation–damage) may change along the flood risk chain. For example, two events with the same flood peak discharge may lead to very different inundation and damage patterns.

In this paper, we explore the idea 'derived flood risk approach based on continuous simulation'. The Mulde catchment, a meso-scale catchment in East Germany, is selected as example. A multisite, multivariate weather generator is linked to the Regional Flood Model (RFM). RFM is a coupled model chain, consisting of a continuous hydrological model, 1D/2D hydrodynamic models and a flood loss model. It has been recently developed for risk assessments in large-scale river catchments and took part in a proof-of-concept study, driven by observed meteorological time series for a period of 14 years (Falter et al., in press). For the first time, RFM is driven by synthetic meteorological data, generated by a multisite, multivariate weather generator, providing 100 realisations of 100 years of data. This virtual period of 10,000 years is simulated continuously, providing a sample of more than 2000 flood events with detailed information on inundation depth, extent and damage on a resolution of 100 m. On basis of this unique data set, we present a flood risk analysis directly on damage values. Additionally, this allows us to examine the assumption that probability of peak discharge is a suitable proxy for probability of damage. Derived damage probabilities are compared to corresponding flood peak probabilities to discuss problems that may arise from transformations of flood peak probabilities to damage probabilities.

4.2 Methods

4.2.1 Weather generator

The meteorological input data for the model chain is provided by a multisite, multivariate weather generator (Hundecha and Merz, 2012), further advanced from Hundecha et al. (2009). It provides spatially consistent realisations of meteorological fields for large-scale basins. The model generates synthetic daily meteorological forcing in two stages. In the first stage, precipitation series are generated at multiple sites by respecting the spatial and temporal correlations of the observed daily precipitation amounts on

monthly basis. At each station, daily precipitation is sampled from a parametric distribution, which is estimated from the observed daily precipitation series as a mixture of Gamma and Generalized Pareto distributions. The mixing weight varies dynamically with respect to the precipitation intensity. The second stage of the model simulates daily maximum, minimum and average temperatures and solar radiation by keeping the correlations between the variables as well as their inter-site correlation and the autocorrelation of each variable. Temperature values are sampled from Gaussian distributions fitted to the corresponding observations, whilst for solar radiation a square root transformation was used prior to fitting a Gaussian distribution. Both temperature and solar radiation are conditioned on the state of precipitation. A multivariate autoregressive model is implemented to simulate the time series of all the daily forcing variables (precipitation, temperature and radiation). Details of the model are presented in Hundecha et al. (2009) and Hundecha and Merz (2012).

4.2.2 Regional Flood Model (RFM)

The Regional Flood Model (RFM) is a process-based model cascade developed for flood risk assessments of large-scale basins (Falter et al., in press). It has been developed for basin areas in the order of several 10,000 km^2. RFM consists of four coupled models: the rainfall-runoff model SWIM, a 1D channel routing model, a 2D hinterland inundation model and the flood loss estimation model for residential buildings FLEMOps+r (Fig. 4-1). We briefly describe the model chain and each model part here, for detailed information the reader is referred to Falter et al. (in press).

4.2.2.1 Rainfall-runoff model SWIM

The eco-hydrological model SWIM (Soil and Water Integrated Model, Krysanova et al., 1998) is a conceptual, semi-distributed model that simulates the hydrological cycle on a daily basis. The model is spatially disaggregated on three levels: the primary unit is the river basin that is subdivided into subbasins and these are further disaggregated into hydrotopes. Water fluxes are computed for each hydrotope and aggregated on the subbasin scale. Computed daily runoff is routed from subbasin to subbasin using the Muskingum hydrological routing scheme. The routed discharges provide a boundary condition for the 1D hydrodynamic river network model.

4.2.2.2 Hydrodynamic models

The hydrological routing method integrated in SWIM routes the flow on a subbasin scale without considering explicitly the river channel geometry. However, for the prediction of flood defence overtopping and simulation of inundation processes in the hinterland, it is crucial to obtain water level information along the river network. Therefore, a 1D hydrodynamic channel routing model was developed to complement the SWIM routing. Additionally, a 2D hydrodynamic inundation model was implemented to simulate floodplain inundation processes. Both models are two-way coupled and exchange water level information during runtime.

The developed channel routing model solves a 1D representation of the diffusive wave equation with an explicit finite difference solution scheme. The diffusive wave equation is derived from the full dynamic shallow water equation by neglecting the local and advective acceleration terms. Due to the lack of precise information on the full cross-section geometry and in order to reduce the model run-times, the 1D hydrodynamic river network model only simulates flows exceeding bankfull discharge. The latter is assumed to be equivalent to a 2-year flood derived from the discharge series from the hydrological model at subbasin scale. Runoff time series at each SWIM subbasin outlet are used as boundary condition for the channel routing model. In case the bankfull flow threshold is exceeded within a subbasin, the excess flow is routed downstream subbasin-wise taking the new boundary condition from SWIM at each subbasin outlet into account. The cross-sections representing channel geometry are considered to cover the entire floodplain between flood protection dikes stretching from crest to crest. Whenever a dike crest height is

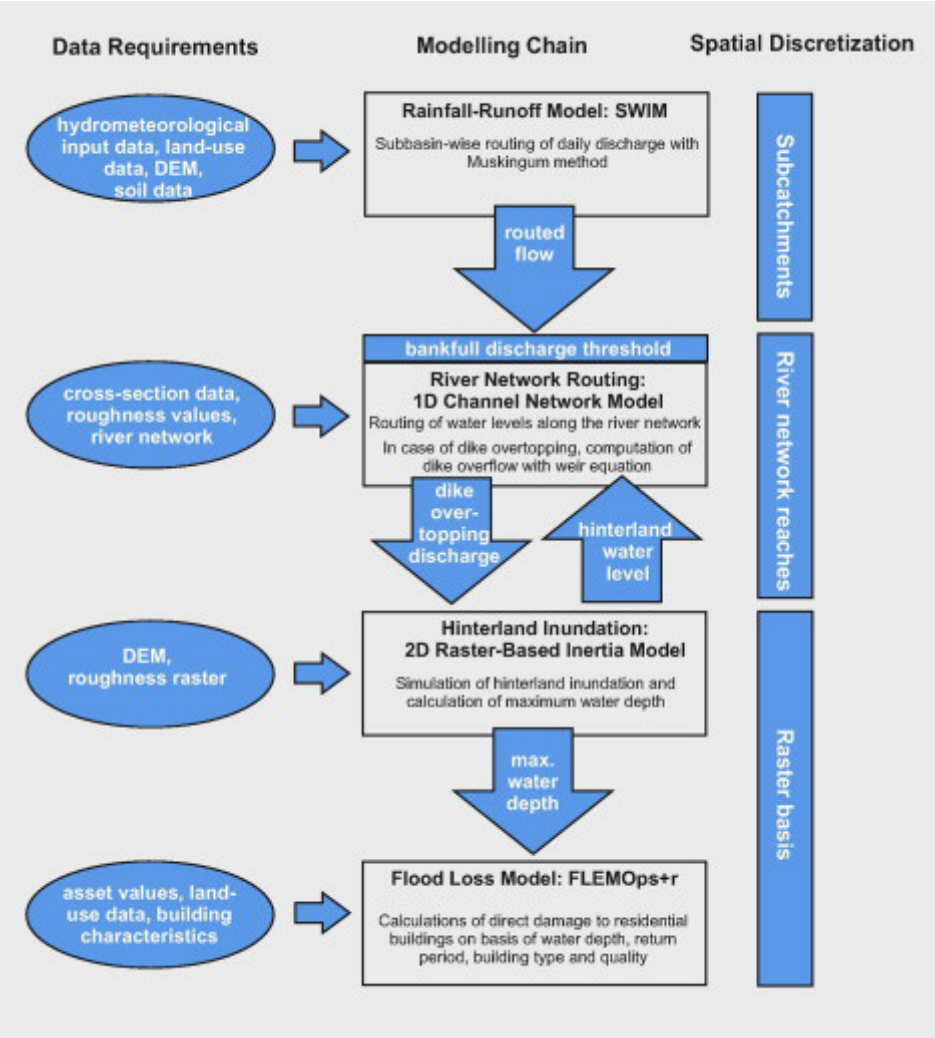

Figure 4-1: Components and data requirements of the Regional Flood Model (RFM). DEM, digital elevation model; FLEMOps + r, Flood Loss Estimation MOdel for the private sector; SWIM, Soil and Water Integrated Model.

exceeded, outflow into the hinterland is calculated with the broad-crested weir equation.

The dike overtopping discharge is treated as a point source boundary condition for the 2D floodplain model. The outflow of the 1D model is additionally controlled by the feedback of the 2D model. In case the water level in the hinterland is equal to the channel water level, the outflow into the hinterland is stopped. In that way, the uncontrolled water flux out of the 1D model domain is prevented in case the water level in the hinterland exceeds the channel water level.

The 2D inundation model uses a raster-based inertia formulation (Bates et al., 2010) implemented in the CUDA Fortran environment (PGI, Lake Oswego, Oregon, USA) which enables the application on the highly parallelised NVIDIA Graphical Processor Units (GPU; NVIDIA, Santa Clara, California, USA) with a strong performance gain compared to a CPU-based version. The model was benchmarked against a 2D fully dynamic shallow water model, regarding sensitivity of model performance and run-times to grid resolution (Falter et al., 2013).

For each flood event, where dike overtopping discharge and hinterland inundation occurred, grids of maximum water levels at each cell are extracted and used for calculation of flood loss with a multi-

parametric damage model. A flood event starts as soon as bankfull discharge is exceeded anywhere along the river network and ends as soon as discharge drops below bankfull discharge along the whole river.

4.2.2.3 Flood loss model FLEMOps + r

From the maximum water level grids, damage to residential buildings is calculated for each flood event with the Flood Loss Estimation MOdel for the private sector (FLEMOps + r, Elmer et al., 2010 and Elmer et al., 2012), developed at the German Research Centre for Geosciences (GFZ), Potsdam. It uses a rule-based multifactorial approach to estimate direct economic damage to residential buildings. The base model version FLEMOps calculates the damage ratio for residential buildings using five different classes of inundation depth, three individual building types, two classes of building quality, three classes of contamination and three classes of private precaution (Thieken et al., 2008). The advanced model version FLEMOps + r additionally considers the return period of the inundation at the affected residential building as an important damage influencing factor (Elmer et al., 2010). Within the RFM framework, FLEMOps + r is applied according to Elmer et al. (2012) without taking into account the influence of precautionary measures and contamination.

4.3 Application to the Mulde catchment

4.3.1 Study area

The Mulde catchment comprises the Vereinigte Mulde – a sinistral tributary to the Elbe River, and its main frontal flows Zwickauer Mulde, Freiburger Mulde and Zschopau (Fig. 4-2). The total catchment area is approximately 7400 km^2 (IKSE, 2005). About 70% of the catchment is dominated by mountain areas that drain a large part of the Ore Mountains, 30% of the catchment are lowland areas. The elevation ranges from 52 m to 1213 m a.s.l. The mean annual precipitation is about 770 mm, ranging from 1000 mm in the mountains to 550 mm in the lowlands.

The catchment was affected by several severe flood events during the last 100 years: 1954, 1958, 2002 (Petrow et al., 2007) and most recent in June 2013. The floods in July 1954, August 2002 and June 2013 were caused by intense and widespread precipitation. The flood in 2013 was additionally triggered by extraordinary initial wetness within the affected basins (Schröter et al., 2015). The August flood in 2002, mainly affecting the Elbe and Danube catchments, was the most expensive natural hazard that occurred in Germany so far and caused damage of around €15 billion in Germany alone (in values of 2013, Merz et al., 2014). The exceptional flood in June 2013 caused about €8.8 billion (Bundestag, 2013 and GDV, 2013), although it was more severe in hydrological sense, i.e. with the highest degree of affected river network (Schröter et al., 2015).

For this study, we selected river reaches of the Mulde catchment that have a drainage area larger than 600 km^2. The final study area comprises about 6000 km^2 catchment area and about 380 river kilometres (Fig. 4-2).

4.3.2 Model set-up

The recent proof-of-concept study by Falter et al. (in press) applied the RFM model chain to the Elbe catchment (Germany) and demonstrated that flood risk assessment based on a continuous simulation approach, including rainfall-runoff, hydrodynamic and damage estimation models is feasible for large catchments. The study revealed however significant uncertainties especially associated with the 1D hydrodynamic model resulting from channel geometries. Therefore, an advanced set-up of the hydrodynamic models was implemented for the Mulde catchment based on high-resolution topography data.

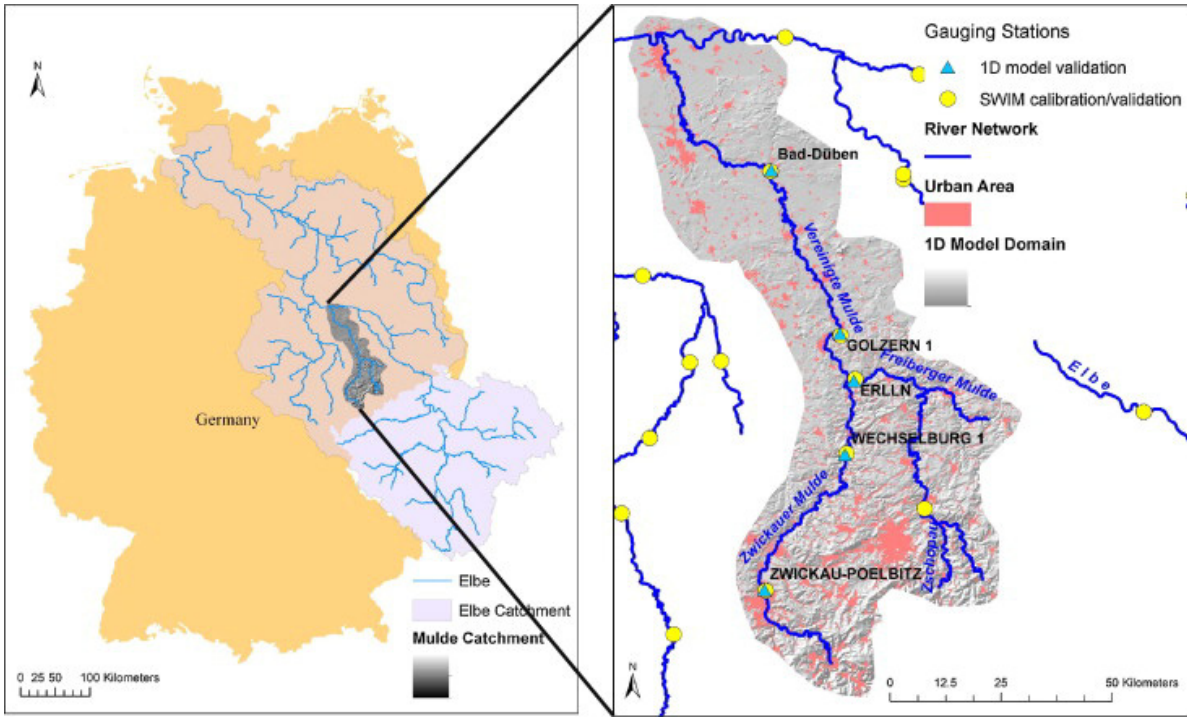

Figure 4-2: Study area, left panel: overview of the entire Elbe catchment including Czech areas; right panel: study area including the simulated river network, the 2D model domain and locations used for model calibration and validation.

Daily meteorological input data for 10,000 years were provided by the weather generator for the entire Elbe catchment. The long-term simulation of meteorological fields reflects the climatology from 1951 until 2003 and is assumed to provide a basis for estimating the current flood risk. Likewise, rainfall-runoff simulations with SWIM were performed for the entire Elbe catchment including parts belonging to the Czech Republic. Hydrodynamic models and the flood loss model FLEMOps + r were run only for the proposed study area of the Mulde catchment and were based on the most recent data on river system, dike geometry, topography, land use and building characteristics thus reflecting the present level of flood risk. Data used for flood damage estimation reflects the state as of 2010.

4.3.2.1 Rainfall-runoff model SWIM

For setting-up the semi-distributed model SWIM, the Elbe catchment was subdivided into 2268 subcatchments based on the SRTM digital elevation data. The historical hydrometerological input data for SWIM calibration/validation and for parameterisation of the weather generator were provided by the German Weather Service (DWD) from all available stations within Germany and from the Czech Hydrometeorological Institute (CHMI) from stations within the Czech Republic. In addition to the hydrometeorological data, soil and land-use data were derived from the soil map for Germany (BÜK 1000 N2.3), obtained from Bundesanstalt für Geowissenschaften und Rohstoffe (BGR) and the European Soil Database map, obtained from the European Commission's Land Management and Natural Hazards unit and the CORINE (COoRdinated INformation on the Environment) land cover map. SWIM was run with historical daily input data and calibrated over the period from 1981 to 1989. A nested and automatic calibration technique was used in this work by employing the SCE-UA algorithm (Duan et al., 1992). A modified Nash–Sutcliffe efficiency (mNS) presented as normalised weighted sum of the squared differences between the observed and simulated discharges was employed

as an objective function (Hundecha and Bárdossy, 2004) giving more emphasis to higher flows:

$$mNS = 1 - \frac{\sum_{i=1}^{N} w(\cdot)(Q_c(t_i) - Q_0(t_i))^2}{\sum_{i=1}^{N} w(\cdot)(Q_0(t_i) - \bar{Q}_0)^2} \quad (1)$$

where $Q_c(t_i)$ and $Q_0(t_i)$ are the simulated and observed discharges at time t_i, respectively, and Q_0 is the mean observed discharge over the simulation period (N days), $w(\cdot)$ is a weight which is equal to the observed discharge $Q_0(t_i)$.

4.3.2.2 Hydrodynamic models

To simulate water levels along the selected river network with the 1D hydrodynamic river network model, the following input data is needed: river cross-section profiles, dike location and height information, Manning's roughness values and boundary conditions (Fig. 4-1). The main data source for the acquisition of river cross-section profiles including dike location and elevation along the river network was a digital elevation model (DEM) with 10-m horizontal resolution, provided by the Federal Agency for Cartography and Geodesy in Germany (BKG), with a vertical accuracy of ±0.5–2 m. Additional information on dike location and channel width were taken from the digital basic landscape model (Base DLM) also provided by the BKG. Profiles were manually extracted in 500 m distance, perpendicular to the flow direction, with the GIS integrated tool Hec-GeoRas 10 for ArcGIS 10 (US Army Corps of Engineers, May 2012). Since only overbank flow above threshold was routed by the 1D model, cross-section profiles were corrected to represent only active floodplain without river channel. Cross-sections were further simplified to trapezoid-shape, by an algorithm that extracted the necessary parameters (channel location and width, dike location, bottom height of the dike, dike crest height and ground elevation, respectively bankfull depth) whilst conserving the original cross-section area. Dike heights are not well resolved by the DEM 10. Therefore a minimum dike height of 1.8 m was assumed at dike locations provided by the base DLM. The threshold for bankfull flow was assumed to be equivalent to a 2-year flood (Bradbrook et al., 2005 and Rodda, 2005) and computed from simulated discharge series at each subbasin outlet. The runoff-boundary condition from SWIM assigned to the corresponding cross-section in the 1D hydrodynamic model is corrected by subtracting bankfull flow from the total runoff. The Manning's value (n = 0.03) was assumed to be homogenous for the whole river network. In case of dike overtopping, the width of overtopping flow was assumed to be 20 m. The 1D river network model is two-way coupled with the 2D hinterland inundation model and provides computed overtopping flow as boundary condition to the 2D model, whilst receiving hinterland water levels controlling the channel water level and overtopping flow.

The 2D raster-based inertia model was based on the computational grid of 100 m resampled from the DEM 10 to reduce model run-times. The 100 m resolution was selected based on the previous benchmark study by Falter et al. (2013) investigating the model sensitivity to grid resolution in terms of simulation of inundation depth and extent and computational time. The resolution of 100 m was found to offer a good compromise between model performance and computational time. The computationally intensive 2D modelling was performed only for the hinterland, and the channel and river banks embedded between dikes (1D model domain) were excluded from the 2D modelling domain. This simplification reduced run-time requirements considerably and seems justified for risk assessment studies along diked river stretches in Germany where assets in floodplains between dikes are minor compared to those on protected floodplains. Roughness grid was generated from CORINE land use maps by assigning roughness values from literature (Chow, 1959 and Bollrich, 2000) to different land-use classes. The boundary conditions derived from the 1D hydrodynamic channel network model in form of dike crest overtopping flow are assigned to the corresponding cell of the 2D calculation grid by location.

4.3.2.3. FLEMOps + r

The estimation of flood damage to residential buildings using FLEMOps + r requires spatially detailed information about asset values, building quality and building type. Inundation depths and return period of

peak flows are used as impact variables to evaluate flood loss ratio. All input data in grid format were scaled to a spatial resolution of 100 m to comply with the 2D hydrodynamic modelling output.

Asset values of the regional stock of residential buildings are defined on the basis of standard construction costs (BMVBS, 2005), i.e. quantifying the market price of the construction works for restoring a damaged building (Kleist et al., 2006). The values used reflect the state of 2010. The asset values were disaggregated to the digital basic landscape model (Basic DLM) of the German ATKIS (Authoritative Topographic Cartographic Information System; BKG GEODATENZENTRUM, 2009) using the binary disaggregation scheme proposed by Wünsch et al. (2009). Within this procedure the ATKIS objects of the 'residential areas' (ATKIS code 2111) and 'areas of mixed use' (ATKIS code 2113) are used to determine residential areas.

The characteristics of the municipal building stock are derived from the INFAS Geodaten data set (Infas Geodaten GmbH, 2009). The composition of building types in each municipality is described using a cluster centre approach. In total, five clusters are defined differentiating the share of single-family houses, semi-detached/detached and multifamily houses (Thieken et al., 2008). Average building quality is aggregated to two classes; high quality and medium/low quality (Thieken et al., 2008).

The spatial distribution of inundation depths is provided by the 2D raster-based inertia model. Maximum inundation depths (h) for different flood events are classified according to the classes defined in the FLEMOps + r model (0 m < h $\leqslant$ 0.2 m; 0.2 m < h $\leqslant$ 0.6 m; 0.6 m < h $\leqslant$ 1.0 m; 1.0 m < h $\leqslant$ 1.5 m; 1.5 m < h). Return periods of flood discharge peaks are estimated within each SWIM subbasin on the basis of extreme value statistics (GEV) derived from annual maximum discharge series generated through the long-term (10,000 years) continuous SWIM simulation of the Elbe catchment.

The estimation of flood losses comprises the determination of the damage ratio to residential buildings given the inundation depths and return periods, as well as the information about building quality and building type clusters in each location affected by flooding. Absolute flood losses in Euros are calculated as the product of damage ratio and location-dependent asset value per raster cell.

4.4 Results and discussion

4.4.1 RFM model performance evaluation

The performance of the coupled model chain was evaluated on the period of 1951–2003 where possible with observed data.

4.4.1.1. Runoff validation

The hydrological model SWIM was calibrated and validated on 20 gauging stations in the entire Elbe catchment, whereas 3 gauging stations were located within the Mulde catchment (Fig. 4-2). The validation was performed for the period 1951–2003 with observed discharge data, excluding the calibration period of 1981–1989. Results indicate a reasonable simulation, especially of high discharges, for the Mulde catchment with mNS larger than 0.8. Additionally, the conventional Nash–Sutcliffe (NS) values are displayed in Table 4-1 for reference. The results indicate that SWIM is particularly tuned to adequately simulate high flows relevant for flood risk assessment.

4.4.1.2 Water level evaluation

Water levels simulated by the 1D hydrodynamic model were validated at 5 gauging stations throughout the catchment (Fig. 4-2) with observed water level data for the period of 1951–2003. Peak errors are in the range of 0.18–0.56 m (Table 4-2) and are in the range of uncertainty associated with dike crest heights controlling overtopping flow. As indicated by the bias, both an overall water level under- and overestimation occur likewise. Although dike overtopping is a threshold process sensitive to water level height, we consider the simulation acceptable for large-scale

purposes aiming at providing the large-scale picture but not at representing local details.

Table 4-1: Validation of SWIM at three gauging stations in the Mulde catchment.

Gauging Station	NS	conventional NS
Bad Dueben	0.842	0.801
Erlln	0.866	0.808
Wechselburg	0.818	0.692

Table 4-2: Water level evaluation in the Mulde catchment.

Gauging station	Peak Error (m)	Bias (m)
Wechselburg 1	0.565	0.239
Zwickau-Poelbitz	0.304	0.212
Bad-Dueben	0.391	-0.255
Golzern 1	0.341	0.342
Erlln	0.184	-0.014

4.4.1.3 Inundation extent evaluation

Evaluation of inundation extent simulations of past floods is difficult, as availability of inundation extents, e.g. from satellite data, is limited. Particularly, in non-natural urbanised floodplains protected by dikes widespread inundations are exceptional and strongly controlled by performance of flood protection structures. In our case only for the flood in August 2002 inundation extents are documented by the National Aeronautics and Space Research Centre of the Federal Republic of Germany (DLR). A comparison of observed and simulated inundation extents is shown in Fig. 4-3. For the Freiberger Mulde, inundated areas match quite well as partly constricted by topographic barriers. For the other parts of the catchment, over- and underestimation of inundated areas are present. Especially for the low-land part of the Vereinigte Mulde inundation patterns are widespread but were not exactly represented by the model resulting in a Flood Area Index (FAI) of 0.49. FAI is defined as follows:

$$FAI = \frac{M1D1}{M1D1+M1D0+M0D1} \quad (2)$$

where M1D1 is the number of cells correctly predicted as flooded, M1D0 is the number of cells flooded in the prediction and observed dry and M0D1 the number of cells dry in the prediction, however, observed wet. Only about 50% of the flood extent was correctly predicted by the simulation. Flood events at this scale are complex particularly when occurring dike breaches strongly shape inundation extent as was the case in the Mulde catchment in 2002. Within the current version of the hydrodynamic model dike breach processes are not implemented and no detailed information on the time and dynamics of breaching process was available. For large-scale applications, we consider the model to give a reasonable estimate on the dimension of the inundation extent and the severity of the event. Although, a general underestimation of inundation extents is to be expected by disregarding dike breach processes.

4.4.1.4. Damage estimation evaluation

Official damage estimates for the August 2002 flood are available for all 19 affected communities in the Federal State of Saxony in Germany which can be used to evaluate the results of the FLEMOps + r model. For these communities the sum of damage to residential buildings officially reported for the August 2002 flood (Staatskanzlei Freistaat Sachsen, 2003; SAB, personal communication 2004) amounts to €240 million. The results obtained from the model chain in these communities amount to €67 million, which are about 30% of the reported numbers.

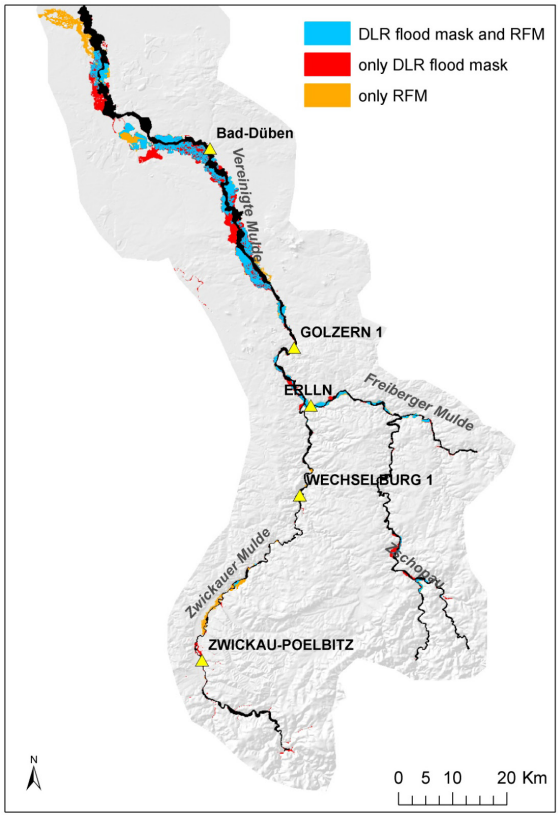

Figure 4-3: Comparison of simulated and observed inundation extents for the August 2002 flood.

Mainly two factors presumably contribute to this underestimation. First, the differences in inundated areas between the DLR flood footprint and hydraulic model results (FAI = 0.49) translates into differences in affected residential areas. According to the DLR flood footprint, 9.9 km^2 of residential areas have been affected in August 2002 in the study region. The hydraulic model estimated 7.9 km^2 affected residential areas which amounts about 80%. In addition, the simulated and observed inundation patterns are not exactly matching. The Flood Area Index computed only for residential areas (FAIres), compare Eq. (2), for the hydraulic simulation is 0.29. Hence, the simulation correctly predicts about 30% of the affected residential areas. Accordingly, the areas where damage was actually caused by the 2002 flood differ considerably from the simulation. Therefore, the comparison of the damage values should be interpreted with caution. Second, former applications of FLEMOps + r on the meso-scale indicate a tendency to underestimate damage, e.g. (Wünsch et al., 2009 and Jongman et al., 2012). In this light, the systematic underestimation of reported damage may be also due to uncertainty in asset values and their spatial distribution and/or to the uncertainty of the damage model.

4.4.2 Long-term simulation results: flood risk in the Mulde catchment

For the continuous and long-term simulation, RFM was driven by meteorological input data, generated by the weather generator. The weather generator was set up to generate synthetic weather variables based on observed meteorological data for the years 1951–2003. Consequently, the weather generator reproduces the climate conditions of this time period. In total, 100 realisations of 100 years of daily weather variables were generated at 528 stations within Germany and neighbouring upstream countries. The virtual period of 10,000 years of meteorological data served as input for the rainfall-runoff model SWIM. The subsequent 1D/2D hydrodynamic simulations were run on a NVIDIA Tesla C1060 GPU server, containing four devices with each having 240 processor cores. The simulation of the virtual period of 10,000 years for the Mulde catchment took about 10 days run time. In total 2016 flood events, where hinterland inundation has occurred, were simulated. For each event, damage to residential buildings was calculated with the model FLEMOps + r. This resulted in a unique data set of about 2000 flood loss events including spatially detailed information on inundation depths and damage to residential buildings that served as basis for the subsequent flood risk analysis.

In Fig.4-4 we present the total count of flooding events for each computational cell of 100 m resolution. The frequency of flooding is unevenly distributed in space. There are areas that are flooded up to 1326 times in 10,000 years and others are never affected by inundation. Patterns like that are to be expected, as there are always areas that are more flood prone than others for several reasons. Remarkably, there are no areas inundated in all of the 2016 flood events.

This illustrates that the model chain provides different spatial patterns of flood generation and alternating

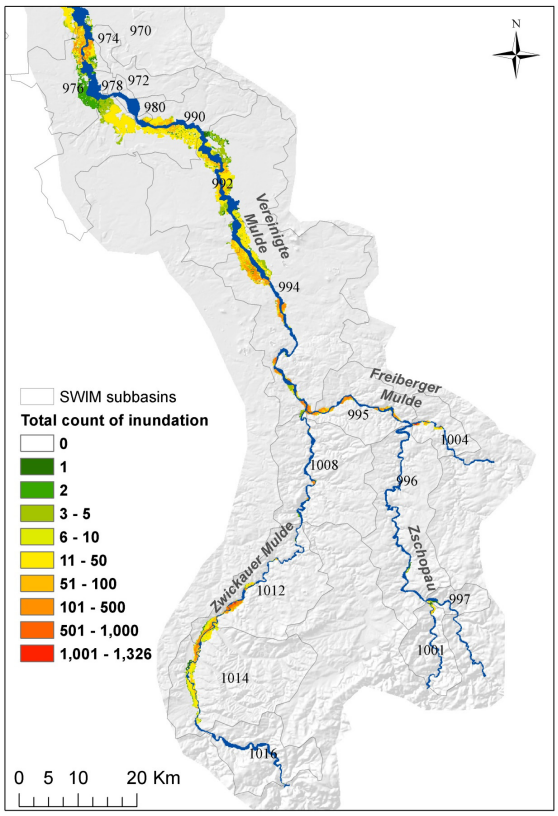

Figure 4-4: Inundation frequency in 10,000 years of simulation for each computational cell.

inundation pathways within the Mulde catchment. As both tributaries Zwickauer and Freiberger Mulde seem to be affected nearly equally often, this suggests an alternating centre of flood impact between those tributaries.

4.4.2.1 Flood frequency estimation

The combined performance of the weather generator and SWIM was evaluated by comparing the flood frequency curve derived by simulation with the flood quantiles based directly on observed discharge. Fig.4-5 shows this comparison for gauge Bad Düben, the most downstream gauge of the Mulde catchment (see Fig. 4-2). For this gauge daily flow was available for the 43-year period 1951–2003. The plotting positions were calculated according to Weibull. The derived flood frequency curve was estimated using the following resampling approach: annual maximum discharge values were extracted from the 10,000 years continuous simulation. 1000 random samples of length 43 were drawn with replacement from these 10,000 values, and the Generalised Extreme Value distribution was fitted to each sample. Parameters were estimated via L-moments (Hosking and Wallis, 1997). The median and the 50% and 95% confidence intervals are derived from the 1000 flood frequency curves.

Fig. 4-5 shows that the derived flood quantiles agree reasonably well with the observation based plotting positions. Two events are clearly outside the 95% sampling uncertainty, namely the floods in 1974 and 2002. These two largest events need to be put in perspective. They resulted from unusually high precipitation amounts in the Ore Mountains, the headwater areas of the Mulde catchment. A total of 312 mm within 24 h was recorded on 12 and 13 August 2002 at Zinnwald. This is the highest amount of rainfall that has ever been measured in Germany (Ulbrich et al., 2003). Given that the rainfall generator has been set up for the much larger Elbe catchment, thereby ignoring some of the local rainfall variability, and the extreme nature of these two events in the Mulde headwater catchments, Fig. 4-5 shows a good agreement between observations and derived flood quantiles.

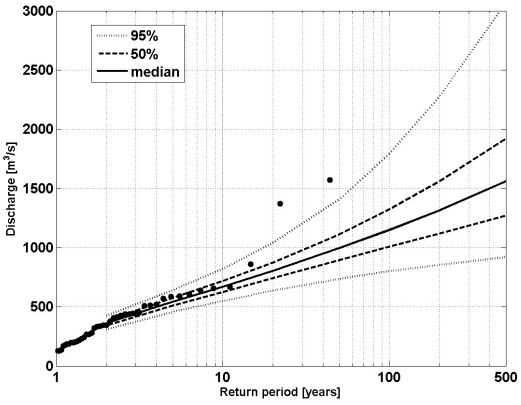

Figure 4-5: Comparison of derived flood frequency curve and plotting positions for gauge Bad Düben. Dots are the observations; the solid line is the median of the derived frequency curves; the dashed and dotted lines show the 50% and 95% confidence interval, respectively.

4.4.2.2 Flood risk curves

Usually, it is not possible to estimate flood loss probabilities directly from damage data, as information on flood loss is sparse or the number of synthetic event sets is not large enough to draw robust statistics. Here, the number of loss events derived from more than 2000 simulated floods within different subbasins ranges between 0 and 774. Apparently not every flood caused damage in each subbasin. This unique data set allowed for the first time to estimate the probabilities directly from damage data. Flood risk curves were derived for all 19 Mulde subbasins based on the aggregated damage values. However, the estimates for 7 subbasins were excluded from the analysis, as the number of damage events was too small (below 30).

In Fig. 4-6, the histograms of damage values, aggregated to the subbasin level, and the risk curve are displayed for an example subbasin. The step in the risk curve visible for p = 0.99 (100-years return period) results from loss estimates of the FLEMOps + r model. FLEMOps + r uses the recurrence interval of the peak discharge as an explanatory variable on an ordinal scale which defines three different classes (below 10 years, above 10 years and below 100 years, above 100 years). As a consequence, loss estimates increase stepwise at 10 and 100 years causing also shifts in the loss estimate. This threshold behaviour implicitly reflects increasing damage propensity in areas which have been affected by low probability events only. This in turn is related to lower flood experiences, lower preparedness and lower resistance, and hence, higher damage (Elmer et al., 2010).

Fig. 4-6a illustrates that the distribution of flood loss is strongly skewed. For the example subbasin, there were 646 loss events during the 10,000 years simulation period. Damage was smaller than 4 million € in 85% (551 events) and smaller than 1 million € in 48% (313 events), however, there were also a few very large loss events with more than 30 million € damage.

To illustrate the advantage of our approach, we compared the risk curves based on our approach and on the traditional approach. In our approach, the probability of a loss event is directly derived from the sample of the damage data (empirical cumulative distribution function CDF in Fig. 4-6b). In contrast, the traditional approach uses the probability of peak discharge as a proxy for damage probability, by fitting a Generalized Extreme Value (GEV) distribution to the simulated annual maximum flows of the 10,000 years period (GEV-based proxy in Fig. 4-6b). Probabilities of peak flows scatter in varying degree around the loss probabilities (note the log scale of the y-axis). This highlights the strong variability in the relationship between probability of peak runoff and probability of damage.

4.4.2.3 Is probability of peak runoff a suitable proxy for probability of damage?

As discussed before, the probability of damage is commonly approximated by the probability of peak runoff as information on flood loss is rare. This approximation is based on the assumption that there is an unambiguous transformation between these probabilities. This assumption holds on average for individual subbasins, however, Fig. 4-6b illustrates that there is significant variability around the mean behaviour, and that the return period of runoff peaks does not necessarily increase with increasing damage. For example, events in the range of 800 years return period may cause damage between 1.5 and 2.5 million €. Similarly, a loss event of 1.2 million € may be caused by events with return periods between 120 and 400 years.

To illustrate this observation, we selected two flood events with the same peak runoff but different damage. One simulation caused 122,058 € damage within the subbasin 995, whereas another one almost the double loss of 236,935 €. The return period of the corresponding peak flow was about T = 50 years. Although the peak runoff is the same, the shape of the hydrographs is different. The second flood featured a larger volume. When dikes are overtopped, this caused a larger volume of water flowing into the hinterland and, hence, higher inundation depth with differences up to 2.7 m (Fig. 4-7) and higher damages. Of course, there are also examples where floods with different runoff peaks result in the same damage. For example, two simulations resulted in a damage of 2,791,450 €

within subbasin 1012, whilst the peak runoffs corresponded to T = 86 years and T = 51 years, respectively.

A flood loss event is the outcome of complex interactions along the flood risk chain, from the flood-triggering rainfall event through the processes in the catchment and river system, the behaviour of flood defences, the spatial patterns of inundation processes, the superposition of inundation areas with exposure and flood damaging mechanisms. Hence, the common assumption that peak runoff corresponds proportionally to damage is not necessarily valid. The presented long-term, continuous simulation of the complete flood risk chain proved to be capable of partly representing these process interactions. Not represented by our current model setup, however, are dike breach processes and subsequent flood attenuation and storage effects. In case of a dike breach, the relationship between peak runoff and damage is all the more questionable. This is the case for the dike breach location, but also for the downstream part of the river. In case dike breach effects are represented it is to expect that differences in discharge probabilities and loss probabilities increase.

Our results show the discrepancy in traditional flood risk estimates, whereas risk is based on the probability of peak discharge, and the more comprehensive approach, where risk is based on the probability of damage. Relying on return periods of maximum flows may result in both under- and overestimation of risk values.

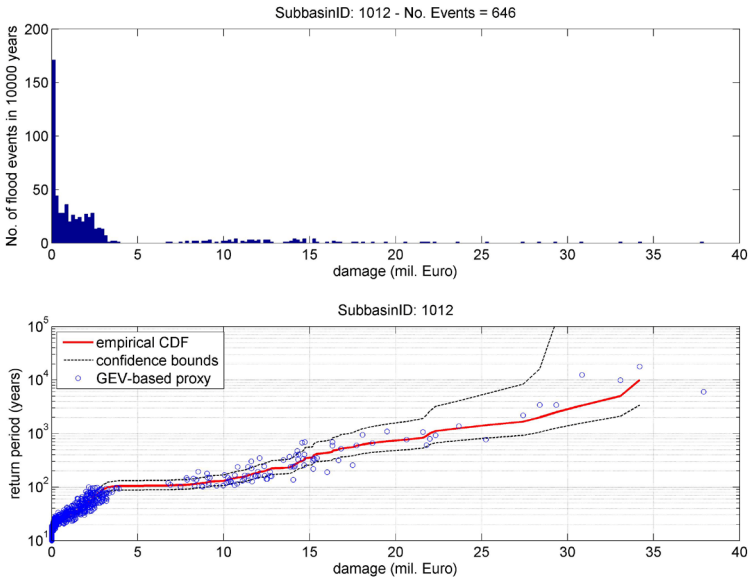

Figure 4-6: (a) Histogram of damage events and (b) comparison of traditional and simulation-based risk curves for an exemplarily subbasin.

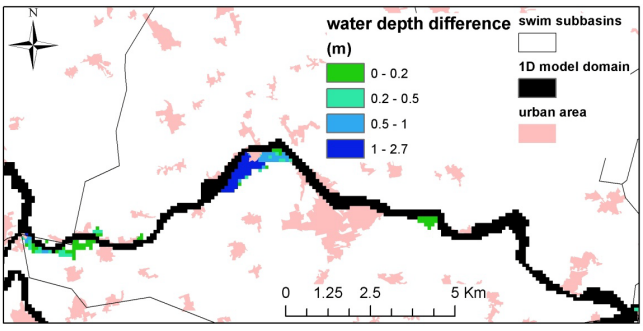

Figure 4-7: Differences in inundation depth for two flood events with the same flood peak in subbasin 995.

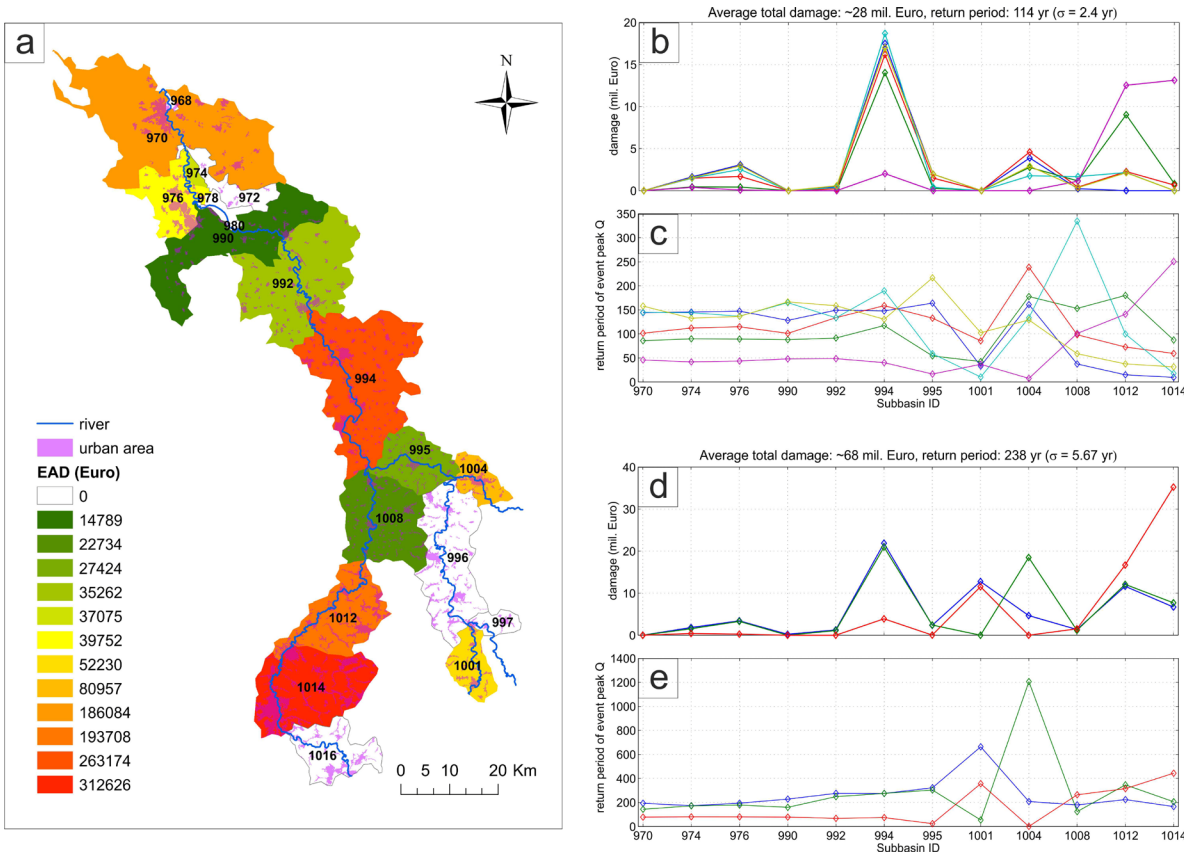

Figure 4-8: (a) Distribution of expected annual damage to residential buildings in the Mulde catchment at the subbasin scale. (b)–(e) Comparison of total damage (b, d) and discharge return period (c, e) spatial distributions amongst subbasins (*x*-axis) and different flood events (coloured lines) for two different levels of total catchment damage.

4.4.2.4 Spatial flood risk patterns and their variability

The presented coupled model chain allows deriving spatially consistent flood risk estimates at any scale – from the local scale to the catchment scale. Fig. 4-8a shows, for example, the distribution of the expected annual damage (EAD) as risk indicator at the subbasin scale. The EAD values differ between subbasins, highlighting the spatial variability in both flood hazard (discharge, inundation extent and depth) and vulnerability (exposure, susceptibility).

Fig. 4-8b–e compares the spatial distribution of discharge return periods and flood damage for two exemplary sets of flood events in the Mulde catchment with approximately 28 and 68 million Euro damage, respectively. Single flood events exhibit a strong variability of discharge return periods (more than two orders of magnitude) across different subbasins opposed to the steady values of damage return period of 114 years (standard deviation of damage return periods: σ = 2.4 years) and 238 years (σ = 5.67 years). This highlights the importance of explicitly considering the spatial variability of flood hazard contrary to the assumption of homogeneous return periods for large-scale basins.

The results further point out the presence of non-linear or threshold processes in the relationship between discharge return period and damage. For instance in subbasin 994 (Fig. 4-8b–e), the damage value increases disproportionally above the return period of about 50 years. This can be a result of the dike overtopping process and/or jump in the affected assets. Furthermore, the order of flood events according to the discharge return period does not necessarily translates

into the order of damage values as shown for subbasin 1012 (Fig. 4-8b–e). This highlights the importance of different inundation pathways affecting spatially distributed assets in various manners with increasing flood hazard. These pathways can be shaped by both the flood generation processes, reflected in the flood wave form, and by river and floodplain processes such as dike overtopping and inundation front propagation patterns. Once again, the return period of discharge attached to an entire subbasin is not capable of fully explaining the variability of damage and serving as a robust proxy for damage probability. This advocates our spatially distributed and continuous simulation approach to obtain spatially consistent distributed risk values. Assuming a homogeneous discharge return period across all subbasins as in the traditional risk assessment approach would also lead to a spatially distributed pattern of EAD values. Those would be, however, conditioned only by the spatial variability in vulnerability and neglect the spatial variability of hazard.

4.5 Conclusions

This paper presents a novel approach for assessing flood risk in river catchments in a spatially consistent way. The derived flood risk approach is based on a set of coupled models representing the complete flood risk chain, including a large-scale multisite, multivariate weather generator, a hydrological model, a coupled 1D–2D hydrodynamic model and a flood loss estimation model. Long time series of spatially consistent meteorological fields are generated and transformed, through the subsequent models, into long time series of flood damage. This allows deriving flood risk estimates directly from the simulated damage.

The approach is exemplarily developed for the mesoscale catchment Mulde, located in east of Germany. 10,000 years of spatially consistent meteorological time series are generated and used as input to the model chain, yielding 10,000 years of spatially consistent river discharge series, inundation patterns and damage values. This results in a unique data set of more than 2000 flood events, including detailed spatial information on inundation depth and damage at a resolution of 100 m. On this basis flood risk curves and risk indicators, such as expected annual damage, can be derived for any scale, from the grid cell scale to the catchment scale. The derived flood risk approach is per se transferable to other river basins without methodological limitations. The selection of models to simulate flood risk chain processes and case-specific hydro-meteorological and topographic data will certainly affect the accuracy of resulting risk estimates.

To the authors' knowledge, this is the first study which extends the derived flood frequency approach based on long-term continuous simulation and computes flood damage and associated risk. We foresee a number of advantages for this approach compared to the traditional flood risk assessments:

(1) Spatially coherent patterns of catchment meteorology, hydrology and floodplain processes:

In contrast to traditional flood risk assessments, where homogenous return periods are assumed for the entire catchment, the presented approach delivers spatially heterogeneous patterns which respect the spatial correlations of the different processes and their spatial interactions. For example, the spatial correlation structure of rainfall is modelled by the weather generator resulting in consistent event fields. Further, the superposition of flood waves at river confluences as function of rainfall characteristics and initial catchment state is implicitly considered. This advantage is particularly valuable for large-scale assessments, where it cannot be assumed that the catchment is uniformly affected by a single flood event.

(2) Holistic representation of flood processes:

Catchment and floodplain processes are represented in a holistic way, since the complete chain of flood processes is represented by the coupled model approach. For instance, the effects of spatially varying antecedent catchment conditions on the flood hydrographs are implicitly taken into account. Another exam-

ple is the damage-reducing effect immediately downstream of a river reach where large water volumes overtop the dike. Running the coupled model in the continuous modes implicitly considers such effects. Contrary to the traditional event based approach, it is not necessary to define representative events based on flood frequency analysis and synthetic hydrographs.

(3) More realistic representation of damage probability, and hence, flood risk:

Traditional flood risk assessments use the probability of discharge as proxy for the probability of damage. Our approach of simulating the complete flood risk chain for long periods, e.g. 10,000 years, enables us to derive flood risk directly from damage data and their empirical frequency distribution. Problems associated with translating the probabilities of rainfall or peak runoff to probabilities of damage are bypassed. A comparison of damage probabilities and corresponding discharge probabilities shows a substantial variability in this relationship at the subbasin scale. Non-linearities and threshold behaviour along the flood risk chain contribute to this variability. For example, flood damage depends not only on the flood peak but on the hydrograph shape or floodplain hydraulics including dike overtopping and inundation pathways. Differences between traditional and derived flood risk approach in discharge and damage probabilities are expected to further increase, when dike breach processes are accounted for in the hydrodynamic modelling.

Acknowledgements. The work reported in this paper is part of the project ‘Regional Flood Model for Germany’ undertaken at the GFZ German Research Centre for Geosciences. We thank the Federal Agency for Cartography and Geodesy in Germany (BKG) for provision of the digital elevation model of Germany (DGM-D), the German Weather Service (DWD) for providing meteorological data and the authorities that provided gauging station data.

5 Discussion, Conclusions and Outlook

Discussion, Conclusion and Outlook

5.1 Summary of achievements

The objective of this work was the development and application of a flood risk framework, appropriated for the large scale and based on long term and continuous simulation. It aimed to overcome several discussed challenges of large scale flood risk assessments as: method and data inconsistency, spatial variability of occurrence probability and transformation of probability. The novel approach of 'derived flood risk approach based on continuous simulations' was introduced. Gradually this aim was realized. Firstly, fast and simplified hydraulic approaches were chosen, and then all model parts were linked together and applied on the large scale. Finally, a flood risk assessment was performed based on a long-term simulation. Each step of the work was accompanied by one research question:

1. **What kind of hydraulic model is suitable for the large-scale and long term application?**
   From the range of existing methods, two fast and simplified storage cell models were selected and evaluated to find an appropriate method for the large-scale application. The Dynamic Rapid Flood Spreading Model (Dynamic RFSM) based on irregular storage cells, and a raster-based model with inertia formulation were compared. As reference served the fully dynamic shallow water model InfoWorks RS 2D. The hydraulic models were applied to a test area within the Elbe catchment. The area was characterized by a very flat topography, as it is typical for the northern lowland area in Germany. The outflow through a hypothetical dike breach served as benchmark scenario. Simulations with the raster model were carried out with different grid sizes, to investigate the impact of the grid resolution on run time and model performance. Furthermore, the sensitivity of the Dynamic RFSM to the choice of time step was investigated. Coarsening the grid resolution reduced the run time of the raster-based model considerably and was found to be a promising strategy to constrain the computational efforts for a large-scale application, although the model accuracy gradually deteriorated. The best compromise between run-time and model accuracy was achieved with a resolution of 100 m. Both models were found to be generally suitable for the large-scale application. They were able to reproduce inundation extents and depth with reasonable accuracy and acceptable run-times, although, DynamicRFSM showed some weaknesses in the reproduction of inundation extents over flat areas. The raster-based model performed little better in terms of inundation extent prediction with similar run time. Therefore and for practical reasons we chose the raster-based approach to be used within the flood risk chain approach with a relative high resolution of 100 m and in combination with a fast 1D channel routing model.

2. **Is the continuous simulation of the entire flood risk chain a suitable approach on the large-scale?**
   To investigate the suitability of the continuous simulation of a full flood risk chain for the large scale, firstly all model parts were integrated into a new framework, the Regional Flood Model (RFM). RFM consists of the hydrological model SWIM, a 1D hydrodynamic river network model, a 2D raster based inundation model and the flood loss model FELMOps+r. Subsequently, the model chain was applied to the Elbe catchment, one of the largest catchments in Germany. For the proof-of-concept, a continuous simulation of rainfall-runoff processes, 1D hydrodynamic river network simulations, 2D hydrodynamic simulation of hinterland inundation

with a relatively high resolution of 100 m and flood loss estimation were performed for the period of 1990-2003. To minimize runtimes, the 2D hydrodynamic hinterland inundation model was optimized by implementation for highly parallelised graphics processing units. Results were validated, respectively evaluated as far as possible with available observed data in this period. Especially for hydrodynamic simulations, errors were significant. This originates basically from low data quality and disregarding dike breach effects in the simulations. Reliable information on overbank cross-sections and dikes will considerably improve the results. Although each model part introduced its own uncertainties, results and run-time were generally found to be adequate for the purpose of continuous simulation at the large catchment scale. The concept of RFM should be applicable for large-scale flood risk assessments. In contrast to large-scale applications that use a reach-wise approach, assuming a spatially uniform return period for the entire river network, the unique and holistic approach used in RFM can potentially provide a realistic large-scale picture of flood risk. The advantage of the continuous simulation approach is that no definition of event sets is necessary and no hydrographs that might be unrealistic in their shapes are necessary.

3. **What are the advantages of flood risk assessments with the 'derived flood risk approach based on continuous and long-term simulations'? What are the differences to traditional flood risk assessments?**

In the previous section we have investigated the concept of continuous simulation of the entire flood risk chain on basis of 14 years simulation. For flood risk assessments, however, long term simulations are needed. Therefore, RFM was driven by long term synthetic meteorological input data generated by a multisite, multivariate weather generator. Thereby the statistical properties of the period 1951-2003 were resampled and a virtual time series of climate data of 10,000 years were generated. This served as input in RFM providing subsequent 10,000 years of spatially consistent river discharge series, inundation patterns and damage values. The long-term application was exemplarily applied for the meso-scale catchment Mulde, located in the east of Germany. The long-term and continuous application of RFM resulted in a unique data set of about 2,000 flood events, including detailed spatial information on inundation depth and damage at a resolution of 100 m. On this basis flood risk curves and expected annual damage, could be derived directly from damage data on a subbasin scale, presenting a large-scale picture of flood risk. For the first time, a flood risk assessment could be performed with the novel approach of 'derived flood risk assessment based on continuous simulations'. It has several advantages compared to traditional flood risk assessments. In contrast to traditional flood risk maps, where homogenous return periods are assumed for the entire basin, the presented approach provides a coherent large-scale picture of flood risk. The spatial variability of occurrence probability is respected. Additionally, data and methods are consistent. Catchment and floodplain processes are represented in a holistic way and not restricted to selected 'representative' events. Antecedent catchment conditions are implicitly taken into account, as well as physical processes like storage effects, flood attenuation or channel–floodplain interactions and related damage influencing effects. Finally, the simulation of a virtual period of 10,000 years and consequently large data set on flood loss events allowed the calculation of flood risk directly from damage distributions. Problems associated with the transfer of probabilities in rainfall or peak runoff to

probabilities in damage, as often used in traditional approaches, are bypassed and the damage probability and hence flood risk is more realistically represented. A comparison of probabilities in damage and probabilities in corresponding peak runoff showed the variability of the relationship between peak runoff and damage. Direct and proportional correlation between peak runoff and damage cannot be assumed to be generally valid. Damage also depends on the hydrograph shape and associated hydraulic effects, the actually inundated area or initial catchment conditions.

5.2 Discussion and future research questions

The objectives to develop and apply a full flood risk model chain could be realized with the framework RFM. Continuous simulations on a large catchment scale and a flood risk assessment based on long term simulations were successfully carried out. However, methods and models are partly new and detailed investigation of provided simulation results is necessary. Within a complex model framework like RFM, additionally driven by a weather generator, each part of the model brings its own uncertainty into the chain. Errors might add up within the chain or overlay each other and sometimes the sources for errors are not easy to identify. As far as possible each part of the model was validated, respectively evaluated. It would be advisable to apply the model chain beyond this study, to further investigate simulation results and the methods used. For example, discharge was found to be generally simulated adequately with SWIM in comparison with observed data. However, simulations were less reliable for tributaries under heavy human intervention and some upstream river parts. The quality of water level simulation depends strongly on the quality of data, e.g. cross-section geometries. Hinterland inundation simulations depend on previously simulated water levels and uncertain dike heights, as well as on the resolution and quality of topographical data. Finally, damage estimations are highly sensitive to the actual flooded area and its assets, e.g. urban areas or grasslands.

Besides this, an underestimation of flood risk is to be expected with the current model chain, due to missing dike breach representation und subsequent underestimation in flood extent and damage by the flood loss model. A reasonable future advancement would be to include dike breaches processes, but in order to represent dike breaches, knowledge on the location, timing and characteristics of breaches is required. For the estimation of these variables, investigated river and dike reaches need to be known very well. An alternative approach would be to provide estimates of dike breach probabilities, given certain flooding conditions. This probabilistic approach would, however, require a large number of simulations to represent probabilities adequately.

Dike breaches play a dominant role for the expected damage. Differences between traditional flood risk assessments that used probabilities of peak discharge as proxy for probability of damage and the ‘derived flood risk approach based on continuous simulation’ are expected to become more dominant by the inclusion of dike breach processes in the model framework.

The presented coupled model chain allows deriving spatially consistent flood risk estimates at any scale – from the local scale to the catchment scale. In this study flood risk is estimated solely on a subbasin level. The investigation of the dependency of flood risk on spatial aggregation levels underlying the statistical analysis of flood damage will be subject of future research.

5.3 Concluding remarks

The developed fast 1D/2D hydrodynamic models were additionally optimized by the implementation for highly parallelised graphics processing units. On a relatively high resolution of 100 m detailed simulations of inundation extent and depth are possible even for long term simulations. With the newly set-up RFM framework spatial coherent and continuous simulation of the full flood risk chain,

from rainfall to damage, are possible. In combination with an available weather generator, providing long term synthetic meteorological input data, flood risk assessments are feasible that are directly based on damage data. RFM and the 'derived flood risk approach based on continuous simulations' are per se transferable to other river basins without methodological limitations. The approach has the potential to provide flood risk statements for national planning, re-insurance aspects or other questions where spatially consistent, large-scale assessments are required.

References

Alcrudo F, Mulet-Marti J. (2005). Urban inundation models based upon the shallow water equations. Numerical and practical issues. In Proceedings of finite volumes for complex applications IV. Problems and perspectives, Benkhaldoun F,Ouazar D, Raghay S (eds).Hermes Science: London; 1–12.

Alfieri, L., Salamon, P., Bianchi, A., Neal, J., Bates, P., & Feyen, L. (2014). Advances in pan-European flood hazard mapping. *Hydrological Processes*, *28*(13), 4067–4077. doi:10.1002/hyp.9947

Apel, H., Merz, B., & Thieken, a. H. (2009). Influence of dike breaches on flood frequency estimation. *Computers & Geosciences*, *35*(5), 907–923. doi:10.1016/j.cageo.2007.11.003

Aureli F, Maranzoni A, Mignosa P, Ziveri C. 2005. Flood hazard mapping by means of fully-2D and quasi-2D numerical modelling: a case study. In Floods, from defence to management, Alphen V, van Beek T (eds). Taylor & Francis Group: London; 41–51.

Barredo, J. I. (2009). Normalised flood losses in Europe: 1970–2006. *Natural Hazards and Earth System Science*, *9*(1), 97–104. doi:10.5194/nhess-9-97-2009

Bates, P. D., & De Roo, A. P. J. (2000). A simple raster-based model for flood inundation simulation. *Journal of Hydrology*, *236*(1-2), 54–77. doi:10.1016/S0022-1694(00)00278-X

Bates, P. D., Horritt, M. S., & Fewtrell, T. J. (2010). A simple inertial formulation of the shallow water equations for efficient two-dimensional flood inundation modelling. *Journal of Hydrology*, *387*(1-2), 33–45. doi:10.1016/j.jhydrol.2010.03.027

BfG. (2014). Geoportal. Retrieved from http://geoportal.bafg.de/mapapps/resources/apps/HWRMRL-DE/index.html?lang=de

Biancamaria, S., Bates, P. D., Boone, A., & Mognard, N. M. (2009). Large-scale coupled hydrologic and hydraulic modelling of the Ob river in Siberia. *Journal of Hydrology*, *379*(1-2), 136–150. doi:10.1016/j.jhydrol.2009.09.054

BKG. (2007). *Digitales Geländemodell für Deutschland DGM-D, technical report*. Frankfurt am Main, Germany. Retrieved from http://www.geodatenzentrum.de/docpdf/dgm-d.pdf

BKG GEODATENZENTRUM. (2009). ATKIS-Basis-DLM.

BMVBS. (2005). *Normalherstellungskosten 2005 (NHK 2005)*. Berlin: Bundesministerium für Verkehr, Bau und Stadtentwicklung.

Bollrich, G. (2000). *Technische Hydromechanik*. Berlin: Verlag Bauwesen.

Boughton, W., Droop, O., (2003). Continuous simulation for design flood estimation – a review. *Environ. Modell. Software* 18 (49), 309–318.

Bradbrook, K., Waller, S., & Morris, D. (2005). National floodplain mapping: datasets and methods–160,000 km in 12 months. *Natural Hazards*, 103–123. Retrieved from http://link.springer.com/article/10.1007/s11069-004-4544-9

Bundestag, D. (2013). *Bericht zur Flutkatastrophe 2013: Katastrophenhilfe, Entschädigung, Wiederaufbau*. Berlin.

Castellarin, A., Domeneghetti, A., & Brath, A. (2011). Identifying robust large-scale flood risk mitigation strategies: A quasi-2D hydraulic model as a tool for the Po river. *Physics and Chemistry of the Earth, Parts A/B/C*, *36*(7-8), 299–308. doi:10.1016/j.pce.2011.02.008

Cheng, X. T., Evans, E. P., Wu, H. Y., Thorne, C. R., Han, S., Simm, J. D., & Hall, J. W. (2013). A framework for long-term scenario analysis in the Taihu Basin, China. *Journal of Flood Risk Management*, *6*(1), 3–13. doi:10.1111/jfr3.12024

Chow, V. T. (1959). *Open channel Hydraulics*. New York, USA: McGraw-Hill.

Cunge JA. (1975). Two-dimensional modeling of flood plains. *Water Resources Publications*, Ch. 17: 705–762.

Defina A. (2000). Two-dimensional shallow flow equations for partially dry areas. *Water Resources Research* 36: 3251–3264.

DESTATIS. (2010). Baufertigstellungen: Errichtung neuer Wohngebäude.

DESTATIS. (2013). *Preisindizes für die Bauwirtschaft* (No. 4). Wiesbaden: Statistisches Bundesamt.

Dottori, F., & Todini, E. (2011). Developments of a flood inundation model based on the cellular automata approach: Testing different methods to improve model performance. *Physics and Chemistry of the Earth, Parts A/B/C*, *36*(7-8), 266–280. doi:10.1016/j.pce.2011.02.004

Duan, Q., Sorooshian, S., & Gupta, V. (1992). Effective and efficient global optimization for conceptual rainfall-runoff models. *Water Resources Research*, *28*(4), 1015–1031. Retrieved from http://onlinelibrary.wiley.com/doi/10.1029/91WR02985/abstract

Dury, G. (1976). Discharge prediction, present and former, from channel dimensions. *Journal of Hydrology*, *30*, 219–245. Retrieved from http://www.sciencedirect.com/science/article/pii/0022169476901025

EEA. (2005). *COoRdinate INformation on the Environment (Corine) - Land Cover*. European Environment Agency.

Elmer, F., Hoymann, J., Düthmann, D., Vorogushyn, S., & Kreibich, H. (2012). Drivers of flood risk change in residential areas. *Natural Hazards and Earth System Science*, *12*(5), 1641–1657. doi:10.5194/nhess-12-1641-2012

Elmer, F., Thieken, a. H., Pech, I., & Kreibich, H. (2010). Influence of flood frequency on residential building losses. *Natural Hazards and Earth System Science*, *10*(10), 2145–2159. doi:10.5194/nhess-10-2145-2010

European Commision (2007). Directive 2007/60/EC of the European Parliament and of the Council of 23 October 2007 on the assessment and management of flood risks. *Off J Eur Communities 2007a*, (2455), 27–34.

Falter, D., Dung, N. V., Vorogushyn, S., Schröter, K., Hundecha, Y., Kreibich, H., Apel, H., Theisselmann, F., Merz, B. (2014). Continuous, large-scale simulation model for flood risk assessments: proof-of-concept. *Journal of Flood Risk Management*, n/a–n/a. doi:10.1111/jfr3.12105. (in press)

Falter, D., Vorogushyn, S., Lhomme, J., Apel, H., Gouldby, B., & Merz, B. (2013). Hydraulic model evaluation for large-scale flood risk assessments. *Hydrological Processes*, *27*(9), 1331 – 1340. doi:10.1002/hyp.9553

Fewtrell, T. J., Bates, P. D., Horritt, M., & Hunter, N. M. (2008). Evaluating the effect of scale in flood inundation modelling in urban environments, *5118*(November), 5107–5118. doi:10.1002/hyp

FLORIS. (2005). Flood Risks and Safety in the Netherlands (Floris). Floris study - Full report,Ministerie vanVerkeer enWaterstaat,DWW-2006-014. ISBN 90-369-5604-9.

GDV. (2013). *Erste Schadenbilanz: Hochwasser 2013 verursacht 180.000 versicherte Schäden in Höhe von fast 2Milliarden Euro*. Retrieved from http://www.presseportal.de/pm/39279/2505807/erste-schadenbilanz-hochwasser-2013-verursacht-180-000-versicherte-schaeden-in-hoehe-von-fast-2

Ghizzoni, T., Roth, G., Rudari, R., (2012). Multisite flooding hazard assessment in the Upper Mississippi River. J. Hydrol. 412–413, 101–113. http://dx.doi.org/10.1016/j.jhydrol.2011.06.004.

Gouldby B, Sayers P, Mulet-Marti J, Hassan M, Benwell D. 2008. A methodology for regional-scale flood risk assessment. *Proceedings of the Institution of Civil*

Engineers - Water Management 161: 169–182.

Grimaldi, S., Petroselli, A., Arcangeletti, E., & Nardi, F. (2013). Flood mapping in ungauged basins using fully continuous hydrologic–hydraulic modeling. *Journal of Hydrology*, *487*, 39–47. doi:10.1016/j.jhydrol.2013.02.023

Haberlandt, U., Radtke, I., (2014). Hydrological model calibration for derived flood frequency analysis using stochastic rainfall and probability distributions of peak flows. Hydrol. Earth Syst. Sci. 18, 353–365. http://dx.doi.org/10.5194/hess-18- 353-2014.

Hosking, J.R.M., Wallis, J.R., (1997). Regional Frequency Analysis: An Approach Based on L-Moments. Cambridge University Press, Cambridge, UK, p. 224.

Hall, J., Dawson, R., & Sayers, P. (2003). A methodology for national-scale flood risk assessment. *Proceedings of the Institution of Civil Engineers*, Water & Maritime Engineering (WM3), 235–247. Retrieved from http://www.icevirtuallibrary.com/content/article/10.1680/wame.2003.156.3.235

Hall, J. W., Sayers, P. B., & Dawson, R. J. (2005). National-scale Assessment of Current and Future Flood Risk in England and Wales. *Natural Hazards*, *36*(1-2), 147–164. doi:10.1007/s11069-004-4546-7

Hattermann, F. F., Wattenbach, M., Krysanova, V., & Wechsung, F. (2005). Runoff simulations on the macroscale with the ecohydrological model SWIM in the Elbe catchment-validation and uncertainty analysis. *Hydrological Processes*, *19*(3), 693–714. doi:10.1002/hyp.5625

Horritt MS, Bates PD. (2001a). Effects of spatial resolution on a raster based model of floodplain flow. Journal of Hydrology 253: 239–249.

Horritt, M. S., & Bates, P. D. (2001b). Predicting floodplain inundation: raster-based modelling versus the finite-element approach. *Hydrological Processes*, *15*(5), 825–842. doi:10.1002/hyp.188

Horritt, M. S., & Bates, P. D. (2002). Evaluation of 1D and 2D numerical models for predicting river flood inundation. *Journal of Hydrology*, *268*(1-4), 87–99. doi:10.1016/S0022-1694(02)00121-X

Huang, S., Hattermann, F. F., Krysanova, V., & Bronstert, A. (2013). Projections of climate change impacts on river flood conditions in Germany by combining three different RCMs with a regional eco-hydrological model. *Climatic Change*, *116*(3-4), 631–663. doi:10.1007/s10584-012-0586-2

Huang, S., Krysanova, V., & Hattermann, F. F. (2013). Projection of low flow conditions in Germany under climate change by combining three RCMs and a regional hydrological model. *Acta Geophysica*, *61*(1), 151–193. doi:10.2478/s11600-012-0065-1

Huang, S., Krysanova, V., Österle, H., & Hattermann, F. F. (2010). Simulation of spatiotemporal dynamics of water fluxes in Germany under climate change. *Hydrological Processes*, *24*(23), 3289–3306. doi:10.1002/hyp.7753

Hundecha, Y., & Bárdossy, A. (2004). Modeling of the effect of land use changes on the runoff generation of a river basin through parameter regionalization of a watershed model. *Journal of Hydrology*, *292*(1-4), 281–295. doi:10.1016/j.jhydrol.2004.01.002

Hundecha, Y., & Merz, B. (2012). Exploring the relationship between changes in climate and floods using a model-based analysis. *Water Resources Research*, *48*(4), W04512. doi:10.1029/2011WR010527

Hundecha, Y., Pahlow, M., & Schumann, A. (2009). Modeling of daily precipitation at multiple locations using a mixture of distributions to characterize the extremes.

Water Resources Research, *45*(12), n/a–n/a. doi:10.1029/2008WR007453

Hunter, N., Horritt, M., & Bates, P. (2005). An adaptive time step solution for raster-based storage cell modelling of floodplain inundation. *Advances in Water …*. Retrieved from http://www.sciencedirect.com/science/article/pii/S0309170805000850

Infas Geodaten GmbH. Das DataWherehouse. Bonn, INFAS GEOdaten GmbH. (2009). Available from: http://www.infas - geodaten.de.

International Commission for the Protection of the Elbe (IKSE 2004). Dokumentation des Hochwassers vom August 2002 im Einzuggebiet der Elbe, report, Magdeburg, Germany.

International Commission for the Protection of the Elbe (IKSE 2005a). Internationale Flussgebietseinheit Elbe, report, Dresden, Germany.

International Commission for the Protection of the Elbe (IKSE 2005b). Die Elbe und ihre Einzugsgebiete, report, Magdeburg, Germany.

International Commission for the Protection of the Elbe (IKSE 2012). Abschlussbericht über die Erfüllung des 'Aktionsplans Hochwasserschutz Elbe' 2003–2011, report,Magdeburg, Germany.

Innovyze. (2011). Infoworks 11.5 RS Help. Innovyze: Wallingford.

Jamieson, S. R., Wright, G., Lhomme, J., & Gouldby, B. P. (2012). Validation of a Computationally Efficient 2D Inundation Model on Multiple Scales. In *Flood Risk*. Rotterdam: Taylor & Francis Group.

Jongman, B., Kreibich, H., Apel, H., Barredo, J. I., Bates, P. D., Feyen, L., … Ward, P. J. (2012). Comparative flood damage model assessment: towards a European approach. *Natural Hazards and Earth System Science*, *12*(12), 3733–3752. doi:10.5194/nhess-12-3733-2012

Jongman, B., Ward, P. J., & Aerts, J. C. J. H. (2012). Global exposure to river and coastal flooding: Long term trends and changes. *Global Environmental Change*, *22*(4), 823–835. doi:10.1016/j.gloenvcha.2012.07.004

Keef, C., Tawn, J. a., & Lamb, R. (2013). Estimating the probability of widespread flood events. *Environmetrics*, *24*(1), 13–21. doi:10.1002/env.2190

Kleist, L., & Thieken, A. (2006). Estimation of the regional stock of residential buildings as a basis for a comparative risk assessment in Germany. *Natural Hazards …*, *6*(4), 541–552. doi:10.5194/nhess-6-541-2006

Kreibich, H., Seifert, I., Merz, B., & Thieken, A. H. (2010). Development of FLEMOcs – a new model for the estimation of flood losses in the commercial sector. *Hydrological Sciences Journal*, *55*(8), 1302–1314. doi:10.1080/02626667.2010.529815

Krysanova, V., Müller-Wohlfeil, D., & Becker, A. (1998). Development and test of a spatially distributed hydrological/water quality model for mesoscale watersheds. *Ecological Modelling*, *106*, 261–289. Retrieved from http://www.sciencedirect.com/science/article/pii/S0304380097002044

Lamb, R., Keef, ;, CTawn, J., Laeger, S., Meadowcroft, I., Surendran, S., … Batstone, C. (2010). A new method to assess the risk of local and widespread flooding on rivers and coasts. *Journal of Flood Risk Management*, *3*(4), 323–336.

Lhomme J, Sayers P, Gouldby B, Samuels P, Wills M. (2008). Recent development and application of a rapid flood spreading method. In Flood risk management: research and practice, Samuels P, Huntington S, Allsop W, Harrop J (eds.). Taylor & Francis Group: London, UK.

Lhomme J, Gutierrez-Andres J, Weisgerber A, Davison M, Mulet-Marti J, Cooper A, Gouldby B. (2010). Testing a new two-dimensional flood modelling system: analytical tests and application to a flood event. *Journal of Flood Risk Management*, 3:33–51.

McMillan, H. K., & Brasington, J. (2007). Reduced complexity strategies for modelling urban floodplain inundation. *Geomorphology*, *90*(3-4), 226–243. doi:10.1016/j.geomorph.2006.10.031

Merz, B., Hall, J., Disse, M., Schumann, A., (2010). Fluvial flood risk management in a changing world. Nat. Hazard. Earth Syst. Sci. 10, 509–527. http://dx.doi.org/ 10.5194/nhess-10-509-2010.

Merz, B., Elmer, F., Kunz, M., Mühr, B., Schröter, K., & Uhlemann-Elmer, S. (2014). The extreme flood in June 2013 in Germany. *La Houille Blanche*, *1*(1), 5–10. doi:10.1051/lhb/2014001

Merz, R., Blöschl, G., & Humer, G. (2008). National flood discharge mapping in Austria. *Natural Hazards*, *46*(1), 53–72. doi:10.1007/s11069-007-9181-7

De Moel, H., van Alphen, J., & Aerts, J. C. J. H. (2009). Flood maps in Europe – methods, availability and use. *Natural Hazards and Earth System Science*, *9*(2), 289–301. doi:10.5194/nhess-9-289-2009

Moussa, R., & Bocquillon, C. (2009). On the use of the diffusive wave for modelling extreme flood events with overbank flow in the floodplain. *Journal of Hydrology*, *374*(1-2), 116–135. doi:10.1016/j.jhydrol.2009.06.006

Munich Re. (1999). *Naturkatastrophen in Deutschland Schadenerfahrungen und Schadenpotentiale*. Munich.

Munich Re. (2014). *Natural Catastrophes 2013 Analyses, Assessments, Positions*. Munich.

Nash, J., & Sutcliffe, J. (1970). River flow forecasting through conceptual models part I—A discussion of principles. *Journal of Hydrology*, *10*, 282–290. Retrieved from http://www.sciencedirect.com/science/article/pii/0022169470902556

Neal, J., Schumann, G., & Bates, P. (2012). A subgrid channel model for simulating river hydraulics and floodplain inundation over large and data sparse areas. *Water Resources Research*, *48*(11), W11506. doi:10.1029/2012WR012514

Neal, J., Schumann, G., Fewtrell, T., Budimir, M., Bates, P., & Mason, D. (2010). EVALUATING A NEW LISFLOOD-FP FORMULATION WITH DATA FROM THE SUMMER 2007 FLOODS IN TEWKESBURY , UK Environmental Systems Science Centre , University of Reading , Reading . RG6 6AL ., (2008).

Neal, J., Villanueva, I., & Wright, N. (2012). How much physical complexity is needed to model flood inundation? *Hydrological Processes*, *26*(15), 2264–2282. doi:10.1002/hyp

Néelz S, Pender G. (2010). Benchmarking of 2D hydraulic modelling packages. Environment Agency: Bristol, UK.

Nied, M., Hundecha, Y., & Merz, B. (2013). Flood-initiating catchment conditions: a spatio-temporal analysis of large-scale soil moisture patterns in the Elbe river basin. *Hydrology and Earth System Science*, *17*(4), 1401-1414.

Oesterle, H. (2001). Reconstruction of daily global radiation for past years for use in agricultural models. *Physics and Chemistry of the Earth, Part B: Hydrology, …*, *26*(3), 253–256. Retrieved from http://www.sciencedirect.com/science/article/pii/S1464190900002483

Paiva, R. C. D., Buarque, D. C., Collischonn, W., Bonnet, M.-P., Frappart, F., Calmant, S., & Bulhões Mendes, C. A. (2013). Large-scale hydrologic and hydrodynamic modeling of the Amazon River basin. *Water Resources Research*, *49*(3), 1226–1243. doi:10.1002/wrcr.20067

Pappenberger, F., Dutra, E., Wetterhall, F., & Cloke, H. L. (2012). Deriving global flood hazard maps of fluvial floods through a physical model cascade. *Hydrology and Earth System Sciences*, *16*(11), 4143–4156. doi:10.5194/hess-16-4143-2012

Da Paz, A. R., Collischonn, W., Bravo, J. M., Bates, P. D., & Baugh, C. (2013). The influence of vertical water balance on modelling Pantanal (Brazil) spatio-temporal inundation dynamics. *Hydrological Processes*, n/a–n/a. doi:10.1002/hyp.9897

Da Paz, A. R., Collischonn, W., Tucci, C. E. M., & Padovani, C. R. (2011). Large-scale modelling of channel flow and floodplain inundation dynamics and its application to the Pantanal (Brazil). *Hydrological Processes*, *25*(9), 1498–1516. doi:10.1002/hyp.7926

Peduzzi, P., Dao, H., Herold, C., & Mouton, F. (2009). Assessing global exposure and vulnerability towards natural hazards: the Disaster Risk Index. *Natural Hazards and Earth System Science*, *9*(4), 1149–1159. doi:10.5194/nhess-9-1149-2009

Petrow, T., & Merz, B. (2009). Trends in flood magnitude, frequency and seasonality in Germany in the period 1951–2002. *Journal of Hydrology*, *371*(1-4), 129–141. doi:10.1016/j.jhydrol.2009.03.024

Petrow, T., Merz, B., Lindenschmidt, K.-E., & Thieken, a. H. (2007). Aspects of seasonality and flood generating circulation patterns in a mountainous catchment in south-eastern Germany. *Hydrology and Earth System Sciences Discussions*, *4*(2), 589–625. doi:10.5194/hessd-4-589-2007

Soares-Frazao S, Lhomme J, Guinot V, Zech Y. (2008). Two-dimensional shallow water models with porosity for urban flood modelling. Journal of Hydraulic Research 46:45–64.

Rodda, H. J. E. (2001). The Development of A Stochastic Rainfall Model for UK Flood Modelling. In P. Krahe & D. Herpertz (Eds.), *Gerneration of Hydrometeorological Reference Conditions for Assessment of Flood Hazard in large River Basins*. Koblenz.

Rodda, H. J. E. (2005). The Development and Application of a Flood Risk Model for the Czech Republic. *Natural Hazards*, *36*(1-2), 207–220. doi:10.1007/s11069-004-4549-4

Schmidt-Thomé, P., Greiving, S., Kallio, H., Fleischhauer, M., & Jarva, J. (2006). Economic risk maps of floods and earthquakes for European regions. *Quaternary International*, *150*(1), 103–112. doi:10.1016/j.quaint.2006.01.024

Schröter, K., Kunz, M., Elmer, F., Mühr, B., & Merz, B. (2015). What made the June 2013 flood in Germany an exceptional event? A hydro-meteorological evaluation. *Hydrology and Earth System Sciences*, *19*, 309–327. doi:10.5194/hessd-11-8125-2014

Seifert, I., Kreibich, H., Merz, B., & Thieken, A. H. (2010). Application and validation of FLEMOcs – a flood-loss estimation model for the commercial sector. *Hydrological Sciences Journal*, *55*(8), 1315–1324. doi:10.1080/02626667.2010.536440

Staatskanzlei Freistaat Sachsen. (2003). *Schadensausgleich und Wiederaufbau im Freistaat Sachsen*. Dresden: Leitstelle Wiederaufbau.

Thieken, a. H., Apel, H., & Merz, B. (2014). Assessing the probability of large-scale flood loss events: a case study for the river Rhine, Germany. *Journal of Flood Risk Management*, *000*, n/a–n/a. doi:10.1111/jfr3.12091

Thieken, A. H., Olschewski, A., Kreibich, H., Kobsch, S., & Merz, B. (2008). Development and evaluation of FLEMOps – a new F lood L oss E stimation MO del for the p rivate s ector. In E. Proverbs, D., Brebbia, C. A., Penning-Rowsell (Ed.), *Flood Recovery, Innovation and Response* (Vol. I, pp. 315–324). Southampton, UK: WIT Press. doi:10.2495/FRIAR080301

Trigg, M. a., Wilson, M. D., Bates, P. D., Horritt, M. S., Alsdorf, D. E., Forsberg, B. R., & Vega, M. C. (2009). Amazon flood wave hydraulics. *Journal of Hydrology*, *374*(1-2), 92–105. doi:10.1016/j.jhydrol.2009.06.004

Ulbrich, U., Brücher, T., Fink, A.H., Leckebusch, G.C., Krüger, A., Pinto, J.G., 2003. The central European floods in August 2002. Part I: Rainfall periods and flood development. Weather 58 (10), 371–377.

Villarini, G., Smith, J. a., Serinaldi, F., & Ntelekos, A. a. (2011). Analyses of seasonal and annual maximum daily discharge records for central Europe. *Journal of Hydrology*, *399*(3-4), 299–312. doi:10.1016/j.jhydrol.2011.01.007

Viviroli, D., Zappa, M., Schwanbeck, J., Gurtz, J., Weingartner, R., 2009. Continuous simulation for flood estimation in ungauged mesoscale catchments of Switzerland – Part I: Modelling framework and calibration results. J. Hydrol. 377 (1–2), 191–207. http://dx.doi.org/10.1016/j.jhydrol.2009.08.023.

Vogt, J. (2007). *A pan-European river and catchment database*. Luxembourg: Joint Research Center of the European Commission. doi:10.2788/35907

Vorogushyn, S., Merz, B., & Apel, H. (2009). Development of dike fragility curves for piping and micro-instability breach mechanisms. *Natural Hazards and Earth System Science*, *9*(4), 1383–1401. doi:10.5194/nhess-9-1383-2009

Vorogushyn, S., Merz, B., Lindenschmidt, K.-E., & Apel, H. (2010). A new methodology for flood hazard assessment considering dike breaches. *Water Resources Research*, *46*(8), W08541. doi:10.1029/2009WR008475

Wicks, J. M., Hu, C., Scott, M., Chen, L., & Cheng, X. (2013). A broad scale model for flood simulation in the Taihu Basin, China. *Journal of Flood Risk Management*, *6*(1), 33–41. doi:10.1111/j.1753-318X.2012.01169.x

Wilby, R. L., Beven, K. J., & Reynard, N. S. (2008). Climate change and fluvial flood risk in the :UKmore of the same ?, *2523*(December 2007), 2511–2523. doi:10.1002/hyp

Wilson, M., Bates, P., Alsdorf, D., Forsberg, B., Horritt, M., Melack, J., … Famiglietti, J. (2007). Modeling large-scale inundation of Amazonian seasonally flooded wetlands. *Geophysical Research Letters*, *34*(15), L15404. doi:10.1029/2007GL030156

Winsemius, H. C., Van Beek, L. P. H., Jongman, B., Ward, P. J., & Bouwman, A. (2013). A framework for global river flood risk assessments. *Hydrology and Earth System Sciences Discussions*, *17*(5), 1871–1892. doi:10.5194/hessd-9-9611-2012

Wünsch, A., & Herrmann, U. (2009). The role of disaggregation of asset values in flood loss estimation: a comparison of different modeling approaches at the Mulde River, Germany. *Environmental Management*, *44*(3), 524–541. doi:10.1007/s00267-009-9335-3

Yamazaki, D., Kanae, S., Kim, H., & Oki, T. (2011). A physically based description of floodplain inundation dynamics in a global river routing model. *Water Resources Research*, *47*(4), W04501. doi:10.1029/2010WR009726

Yu, D., & Lane, S. N. (2006a). Urban fluvial flood modelling using a two-dimensional diffusion-wave treatment, part 1: mesh resolution effects. *Hydrological Processes*, *20*(7), 1541–1565. doi:10.1002/hyp.5935

Yu, D., & Lane, S. N. (2006b). Urban fluvial flood modelling using a two-dimensional diffusion-wave treatment, part 2: development of a sub-grid-scale treatment. *Hydrological Processes*, *20*(7), 1567–1583. doi:10.1002/hyp.5936

Author's declaration

I prepared this dissertation without illegal assistance. The work is original except where indicated by special reference in the text and no part of the dissertation has been submitted for any other degree. This dissertation has not been presented to any other University for examination, neither in Germany nor in another country.

Daniela Falter

Potsdam, November 2015